Aus dem Institut für kardiovaskuläre Computer-assistierte Medizin
der Medizinischen Fakultät Charité – Universitätsmedizin Berlin

DISSERTATION

Nicht-invasive MRT-Diagnostik von Gefäßwand- und Gewebeeigenschaften in zwei Risikopopulationen mit arterieller Hypertonie

zur Erlangung des akademischen Grades
Doctor medicinae (Dr. med.)

vorgelegt der Medizinischen Fakultät
Charité – Universitätsmedizin Berlin

von Niky Ghorbani
aus Hamburg

Datum der Promotion: 04. Juni 2021

Inhaltsverzeichnis

Abkürzungsverzeichnis

AoA	Aorta ascendens
AoD	Aorta descendens
AVS	Acquired voxel size (Voxelgröße)
BMI	Body Mass Index
CC	Korrelationskoeffizient
CI	Konfidenzintervall
Cine	Cinematographisch
CMR	Kardiovaskuläre Magnetresonanztomographie
DHZB	Deutsches Herzzentrum Berlin
FA	Flip angle (Flipwinkel)
GRE	Gradient Echo
ICC	Intra-Klassen-Korrelationskoeffizient
IQR	Interquartilsabstand (Q1-Q3)
ISTA	Aortenisthmusstenose
MMP	Matrix-Metalloproteinasen
MRT	Magnetresonanztomographie
NSA	Number of signal average (Anzahl der Signalmittelungen)
OR	Odds Ratio
PWV	Pulswellengeschwindigkeit
ROI	Regions of interest
SE	Spin Echo
SSFP	Steady state free precession
TA	Time of acquisition (Aufnahmezeit)
TE	Echo time (Echozeit)
TI	Inversion time (Inversionszeit)
TR	Repetition time (Repetitionszeit)
TGFß-1	Transforming growth factor beta-1

Zusammenfassung der Publikationspromotion

Einführung: Die elastische Dehnbarkeit der arteriellen Gefäßwände hat sich als ein relevanter Marker zur Verlaufsbeurteilung der arteriellen Hypertonie herausgestellt. Die elastischen Eigenschaften der Arterien können durch die Distensibilität beschrieben werden, welche als die relative Änderung der Querschnittsfläche bezogen auf eine gegebene Druckänderung definiert ist. Dabei sind eine langjährig bestehende arterielle Hypertonie sowie eine erhöhte Natriumaufnahme mit einer verringerten Distensibilität der großen arteriellen Gefäße assoziiert, die langfristig die kardiovaskuläre Morbidität und Mortalität erhöht. Ziel der vorliegenden Dissertation war die Untersuchung der Distensibilität der Aorta beziehungsweise die Messung des Gewebenatriums in zwei kardiovaskulär gefährdeten Patient*innenpopulationen mit begleitender arterieller Hypertonie anhand nicht-invasiver MRT-Methoden, die in die klinische Routine integriert werden könnten.

Methodik: Für die Untersuchung der Messmethodik zur Erhebung der Distensibilität der Aorta anhand nicht-invasiver kardiovaskulärer MRT erfolgte zunächst eine systematische Analyse der Reproduzierbarkeit (Inter- und Intraobserver-Reliabilität) (Publikation 1). An einer Kohorte von 121 Patient*innen mit Aortenisthmusstenose wurde mittels der MRT-Methodik die Auswirkung der arteriellen Hypertonie auf die Lokalisation und den Schweregrad einer Einschränkung der aortalen Distensibilität untersucht (Publikation 2). Die Querschnittsdurchmesser der Aorta ascendens und Aorta descendens wurden in der axialen Schnittebene erhoben, um die Distensibilität der Aorta zu berechnen. Die Ergebnisse wurden mit altersspezifischen Referenzwerten verglichen. Die Messung des Gewebenatriums wurde an einer Kohorte von 32 Jugendlichen, bestehend aus normotensiv- und hypertensiv-adipösen Patient*innen und altersgleichen normalgewichtigen Kontrollen, mittels ^{23}Na-MRT durchgeführt (Publikation 3).

Ergebnisse: Hinsichtlich der Methodik zur Messung der aortalen Distensibilität zeigte sich eine hohe Inter- und Intraobserver-Reliabilität (mittlerer ICC = 0,92 und 0,95). Patient*innen mit einer Aortenisthmusstenose (>10 Jahre) wiesen bei bestehender arterieller Hypertonie signifikant niedrigere Distensibilitätswerte der Aorta descendens als normotensive Patient*innen (p=0,020) auf. Eine antihypertensive Behandlung war mit einer verbesserten Distensibilität der Aorta assoziiert. Weiterhin konnte gezeigt werden, dass adipöse Jugendliche mit arterieller Hypertonie einen niedrigeren Natriumgehalt des Musculus triceps surae und einen niedrigeren Gesamtquerschnittsgehalt an Natrium aufwiesen als diejenigen ohne Hypertonie (p=0,043 und 0,045) oder normotensive Kontrollen (p=0,012 und 0,005).

Schlussfolgerung: Die angewandte Methodik zur Messung der Distensibilität bietet eine reproduzierbare, nicht-invasive Möglichkeit zur Erhebung elastischer Eigenschaften der Aorta und kann mit wenig Aufwand in die klinische Routine integriert werden. Die arterielle Hypertonie geht schon ab der frühen Adoleszenz mit einer Beeinträchtigung der aortalen Distensibilität und einer veränderten Natrium-Homöostase und -Speicherung einher. Die Erhebung der Distensibilität großer arterieller Gefäße und des Gewebenatriums anhand der durchgeführten MRT-Methoden bietet eine nicht-invasive Möglichkeit zur Verlaufsbeurteilung einer arteriellen Hypertonie und Identifizierung von kardiovaskulären Risikopatient*innen.

Abstract

Background: The elasticity of arterial vessel walls has become a relevant marker for assessing the course of arterial hypertension. Elastic properties of the arteries can be described by the distensibility, which is defined as the relative change in cross-sectional area for a given change in pressure. Long-standing arterial hypertension and increased sodium intake are associated with reduced distensibility of the large arterial vessels, increasing cardiovascular morbidity and mortality in the long term. The aim of the present dissertation was to investigate the distensibility of the aorta, respectively tissue sodium content in two patient populations with increased cardiovascular risk and concomitant arterial hypertension using non-invasive MRI-methods that could be integrated into clinical routine.

Methods: To investigate the measurement methodology for determining the distensibility of the aorta by non-invasive cardiovascular MRI, a systematic analysis of the reproducibility (inter- and intraobserver reliability) was performed (publication 1). In a cohort of 121 patients with aortic coarctation, effects of arterial hypertension on the location and severity of aortic distensibility impairment were investigated using the MRI-method (publication 2). The cross-sectional diameters of the ascending and descending aorta were assessed in the axial plane to calculate distensibility of the aorta. The results were compared with age-specific reference values. Tissue sodium content was determined in a cohort of 32 adolescents, consisting of normotensive and hypertensive obese patients and age-matched normal-weight controls by means of ^{23}Na-MRI (publication 3).

Results: The measurement of aortic distensibility using cardiac MRI showed high inter- and intraobserver reliability (mean ICC=0.92 and 0.95). Aortic coarctation patients (>10 years) with arterial hypertension showed significantly lower distensibility values of the descending aorta than normotensive patients (p=0.020). Antihypertensive treatment was associated with improved distensibility of the aortic vessel wall. Furthermore, obese adolescents with arterial hypertension

had lower sodium content of the triceps surae muscle and lower total cross-sectional sodium content than those without hypertension (p=0.043 and 0.045) or normotensive controls (p=0.012 and 0.005).

Conclusion: The applied methodology for measuring the distensibility offers a reproducible, non-invasive way to assess elastic properties of the aorta and can easily be integrated into clinical routine. Arterial hypertension is associated with impairment of aortic distensibility and altered tissue sodium homeostasis and storage from early adolescence onwards. The assessment of the distensibility of large arterial vessels and tissue sodium using the performed MRI-methods offers a non-invasive possibility to evaluate the course of arterial hypertension and to identify patients at cardiovascular risk.

1. Einführung

1.1. Bedeutung der Dehnbarkeit arterieller Gefäßwände

In den letzten Jahren hat sich die elastische Dehnbarkeit der arteriellen Gefäßwände als ein relevanter Marker zur Verlaufsbeurteilung der arteriellen Hypertonie herausgestellt (1, 2). Studien konnten zeigen, dass über einen längeren Zeitraum bestehende hohe Blutdruckwerte mit einer Beeinträchtigung der elastischen Dehnbarkeit der Aorta einhergehen (3, 4). Dabei ist eine verringerte elastische Dehnung großer Arterien mit einem erhöhten Risiko für kardiovaskuläre Ereignisse assoziiert (4). Jedoch ist nicht abschließend geklärt, ob eine eingeschränkte elastische Dehnbarkeit der arteriellen Gefäßwände eine arterielle Hypertonie begründet oder sich als deren Konsequenz entwickelt. Zu vermuten ist, dass beide Faktoren sich gegenseitig begünstigen (2).

Zur Quantifizierung der elastischen Dehnbarkeit der Gefäße kann die Distensibilität als Wert herangezogen werden, der die relative Änderung der Gefäßquerschnittsfläche für eine definierte Druckänderung bei bestimmter Gefäßlänge beschreibt. Die elastische Kapazität der aortalen Gefäßwand ermöglicht es, Anteile des linksventrikulären Schlagvolumens während der Systole zu speichern und die kontinuierliche Organperfusion während der Diastole aufrechtzuerhalten (5). Eine Einschränkung dieser Windkesselfunktion kann sich schwerwiegend auf das Herz-Kreislauf-System auswirken, wie durch einen Anstieg des systolischen Spitzendruckes, wodurch es zur Erhöhung der kardialen Nachlast kommt (6). Durch die zunehmende linksventrikuläre Belastung kann sich langfristig eine linksventrikuläre Myokardhypertrophie entwickeln (7).

Bereits bekannt ist, dass die Distensibilität des arteriellen Gefäßsystems mit zunehmendem Alter abnimmt (8). Auswertungen postmortal erhobener Daten zeigten jedoch, dass bereits im Kindes- und Jugendalter frühe arteriosklerotische Prozesse wie fibröse Plaques in der Aorta und den Koronararterien vorzufinden sind (9). Dabei korrelierte das Ausmaß der Läsionen stark mit dem Vorliegen einer arteriellen Hypertonie und Adipositas (10). Die weltweite Prävalenz der arteriellen

Hypertonie bei Kindern und Jugendlichen, welche als eine dauerhafte Erhöhung des systolischen und/oder diastolischen Blutdrucks über die alters-, größen- und geschlechterabhängigen Referenzwerte der 95. Perzentile definiert ist (11), hat in den vergangenen Jahren stetig zugenommen (12). Für die primäre Ätiologie der arteriellen Hypertonie stellt sich die Adipositas als wesentlicher Risikofaktor dar: Adipöse Kinder weisen ein etwa 3-mal höheres Risiko auf, an einem pathologisch hohen Bluthochdruck zu leiden als normalgewichtige Kinder (13). Eine sekundäre arterielle Hypertonie tritt als Folgeerkrankung anderer Grunderkrankungen auf, wobei bei Kindern die Aortenisthmusstenose (ISTA) die häufigste nicht-renale Ursache darstellt. Die ISTA, definiert als eine Lumeneinengung der Aorta im Bereich des Isthmus aortae, macht 5-10% aller angeborenen Herzerkrankungen aus (14). In bis zu 75% der Fälle ist eine ISTA zusätzlich erschwerend mit einer bikuspiden Aortenklappe vergesellschaftet (15). Trotz frühzeitiger Interventionsmöglichkeiten und etablierter Behandlungskonzepte sind Morbidität und Mortalität nach wie vor hoch (16), was nicht zuletzt auf eine persistierende arterielle Hypertonie zurückzuführen ist, die trotz erfolgreicher Reparatur bei mehr als 65% aller Betroffenen bestehen bleibt (14). Erhöhte Blutdruckwerte im Kindesalter stellen den stärksten Prädiktor für die Entwicklung einer arteriellen Hypertonie im Erwachsenenalter dar und erhöhen dadurch die langfristige kardiovaskuläre Morbidität und Mortalität (17).

Neuere Studien zeigen, dass eine hohe Natriumzufuhr blutdruckunabhängig mit einer Struktur- und Funktionsveränderung der großen elastischen Arterien einhergeht (18). Dabei werden Veränderungen im vaskulären Endothel und in der extrazellulären Matrix der arteriellen Gefäßwände als wichtigste Faktoren im Zusammenhang mit der verringerten Kapazität zur Dehnung der Arterien angesehen (18). Erwachsene Patient*innen, die eine natriumarme Diät einhielten, zeigten unabhängig ihrer Blutdruckwerte eine verbesserte Distensibilität der arteriellen Gefäßwände (19). Zusätzlich kardiovaskulär belastend steht ein erhöhter Natriumkonsum in Zusammenhang mit einer erhöhten Körperfettmasse bei Kindern wie auch bei Erwachsenen (20,

21). Eine hohe Natriumzufuhr kann demnach nicht nur über Erhöhung des Blutdrucks und der Körperfettmasse, sondern auch durch ihre direkte Einwirkung auf die Gefäßwände die kardiovaskuläre Morbidität und Mortalität beeinflussen.

1.2. Bildgebung von Gefäßwand- und Gewebeeigenschaften

Die kardiovaskuläre MRT (CMR) kann zur Untersuchung der Aorta genutzt werden und ermöglicht ohne den Einsatz ionisierender Strahlen eine dreidimensionale Darstellung des Gefäßes. Die Anatomie der Aorta sowie deren Beziehung zu benachbarten Strukturen können auf diese Weise zuverlässig dargestellt werden (22). Zur nicht-invasiven Beurteilung der Dehnbarkeit der Aorta wurden in den vergangenen Jahren unterschiedliche Techniken erprobt - darunter Methoden mittels intravaskulärer Sonographie, computertomografischer Angiographie, Echokardiographie, Oszillometrie (23, 24) und die Messung der peripheren Pulswellengeschwindigkeit (PWV). Während die Messung der peripheren PWV nicht-invasiv und einfach anzuwenden ist, ist sie bei Patient*innen mit ISTA ungeeignet, da die Lumenverengung abnormale Wellenreflexionen verursachen kann und somit eine relevante Fehlerquelle darstellt. Die CMR hingegen ermöglicht eine Quantifizierung der aortalen Distensibilität unabhängig vom Vorhandensein einer Stenose (25). Sie bietet sich daher als geeignetes Verfahren zur tiefergehenden Diagnostik von strukturellen und funktionellen Veränderungen der Aorta an.

Auch zur Untersuchung des im Gewebe gespeicherten Natriums ist die Untersuchung mittels MRT geeignet (26-28). Durch die ^{23}Na-MRT kann der Natriumkern, welcher nach dem ^{1}H-(Wasserstoff)-Kern das zweitstärkste Kernspinresonanzsignal aller in biologischen Geweben vorhandenen Kerne aufweist, detektiert werden (29). Bisher hat sich die ^{23}Na-MRT noch nicht in der klinischen Routine etabliert, konnte allerdings bereits an gesunden und hypertensiven Proband*innen erfolgreich zur Untersuchung der Natriumkonzentration der Haut und des Muskelgewebes angewandt werden (27).

2. Zielsetzung

Ziel der vorliegenden Dissertation war die Untersuchung der Distensibilität der Aorta beziehungsweise die Erhebung des Gewebenatriums in zwei kardiovaskulär gefährdeten Patient*innenpopulationen mit begleitender arterieller Hypertonie anhand nicht-invasiver MRT-Methoden, die in die klinische Routine integriert werden könnten. Die Ergebnisse könnten zur besseren Verlaufsbeurteilung der arteriellen Hypertonie und zur detaillierteren Evaluierung des individuellen kardiovaskulären Risikoprofils dienen.

Zunächst wurde in **Publikation 1** die Reproduzierbarkeit der Messmethodik zur Erhebung der aortalen Distensibilität mittels CMR analysiert. In **Publikation 2** wurde anhand der MRT-Methodik die kombinierte Auswirkung der arteriellen Hypertonie, der bikuspiden Aortenklappe und des Alters auf die Lokalisation und den Schweregrad einer Einschränkung der Distensibilität der Aorta ascendens (AoA) und Aorta descendens (AoD) in Patient*innen mit ISTA untersucht. Ziel der **Publikation 3** war es mittels eines MRT-basierten Ansatzes die Zusammenhänge zwischen Natriumspeicherung in Muskel und Haut, arterieller Hypertonie und Adipositas bei jugendlichen Patient*innen zu untersuchen.

3. Methodik

3.1. Studiendesign und Patient*innenkollektiv

In der Studie für **Publikation 1**, welche als retrospektive Analyse durchgeführt wurde, war das primäre Ziel die Untersuchung der Reproduzierbarkeit (inkl. Inter- und Intraobserver-Reliabilität) der Distensibilitätsmessungen mittels CMR. Nach den örtlichen Bestimmungen unterzeichneten alle Personen vor dem Eintritt in das klinisch-diagnostische MRT nach Aufklärung eine Einwilligung. Alle Studienteilnehmenden waren Patient*innen des Deutschen Herzzentrums Berlin (DHZB) und wurden nach klinischer Routine anhand eines standardisierten MRT-Protokolls

gescannt. Es wurden zunächst 33 Proband*innen mit variablen Indikationen zur MRT eingeschlossen, von denen zwei aufgrund geringer MRT-Bildqualität ausgeschlossen werden mussten (n=31). Der arterielle Blutdruck der oberen Extremitäten wurde zeitgleich zur MRT-Untersuchung erhoben. Auf Grundlage der in Publikation 1 untersuchten Messmethodik wurden die in Publikation 2 veröffentlichten Auswertungen durchgeführt.

Die der **Publikation 2** zugrundeliegende Studie wurde als bizentrische Querschnittsstudie, als Teil des EU-geförderten Cardioproof-Projekts (Proof of Concept of Model Based Cardiovascular Prediction, Clinical Trial Registernummer: NCT02591940, October 30, 2015) geplant und durchgeführt. Das primäre Ziel des Cardioproof-Projekts war die MRT-basierte prädiktive Modellierung der hämodynamischen Funktionen bei Patient*innen mit strukturellen Herzerkrankungen. Die bildbasierte Modellierung sollte Angaben über Flussmuster und Druckfelder in den betroffenen Gefäßabschnitten liefern und dadurch ein kardiovaskuläres Profiling ermöglichen. Als eine Komponente dieses Vorhabens wurde in der vorliegenden Studie die Untersuchung der Einschränkung der Distensibilität der AoA und AoD bei Patient*innen mit angeborener ISTA in Anbetracht einer bestehenden arteriellen Hypertonie (medikamentös behandelt/unbehandelt), einer biskupiden Aortenklappe und des Alters durchgeführt. Vor Beginn der Studie wurde ein positives Votum der Ethikkommission der medizinischen Fakultät der Charité - Universitätsmedizin Berlin (Nr. EA2/172/13) und durch die kooperierende Arbeitsgruppe ein positives Votum des National Research Ethics Service Committee des University College London (Nr. 15HC23) eingeholt. An zwei europäischen Universitätskliniken, am DHZB (n=84) und am University College London (n=37), wurden zwischen Januar 2014 und Dezember 2016 insgesamt 121 Patient*innen mit zuvor gestellter Diagnose einer ISTA eingeschlossen. Die Datenauswertung erfolgte aus einer gemeinsamen Studiendatenbank. Die Einschlusskriterien für die MRT-Studie waren eine bestätigte Diagnose einer ISTA mit Indikation zur diagnostischen Evaluierung nach Leitlinie der European Society of Cardiology (ESC) (22) und des American College of

Cardiology/American Heart Association (ACC/AHA) (30). Die Indikation wurde auf Grundlage von Echokardiographie-Befunden und Blutdruckmessungen gestellt, die auf einen Druckgradienten von mehr als 20 mmHg über der Stenose oder schwere Verengungen und/oder eine begleitende arterielle Hypertonie hinwiesen. Patient*innen mit Kontraindikationen zur MRT und/oder zusätzlichen komplexen angeborenen kardiovaskulären Fehlbildungen wurden ausgeschlossen. Alle Studienteilnehmenden erhielten eine transthorakale Echokardiographie zur Untersuchung des Druckgradienten über der ISTA und eine CMR im Rahmen der klinischen Routine. Gleichzeitig zur MRT erfolgte die Blutdruckmessungen an beiden oberen Extremitäten. In Kombination mit den erhobenen Blutdruckwerten konnte somit eine Berechnung der lokalisierten Distensibilität der AoA und AoD erfolgen. Als Referenzwerte dienten die von Voges et al. (2012) veröffentlichten Perzentilen (31).

Die Studie im Rahmen von **Publikation 3** wurde als Querschnittsstudie durchgeführt. Das primäre Ziel war die Analyse und Vorhersage kardiovaskulärer Risikofaktoren bei übergewichtigen Jugendlichen. In der vorliegenden Arbeit erfolgte die Untersuchung der Zusammenhänge zwischen Natriumspeicherung in Muskel und Haut, arterieller Hypertonie und Adipositas. Die Studie wurde durch die Ethikkommission der Charité - Universitätsmedizin Berlin (EA2/036/14) genehmigt. Es wurden aus dem DHZB und dem sozialpädiatrischen Zentrum der Charité - Universitätsmedizin Berlin zwischen 2014 und 2017 insgesamt 20 zuvor unbehandelte adipöse und 12 normalgewichtige Jugendliche rekrutiert und untersucht. Die Studienteilnehmenden wurden als adipös klassifiziert, wenn ihr Body-Mass-Index (BMI) die 97. Kromeyer-Hauschild-Perzentile überschritt (32). Bei den normalgewichtigen Kontrollen handelte es sich um Patient*innen, die aufgrund klinischer Indikationen einer routinemäßigen diagnostischen MRT-Untersuchung unterzogen wurden und diese freiwillig um das ^{23}Na-MRT-Protokoll ergänzen ließen. Patient*innen mit endokriner Adipositas (z.B. Glukokortikoid-induziert oder Prader-Willi-Syndrom), MRT-untauglichen

Implantaten oder medizinischen Geräten und/oder Klaustrophobie wurden ausgeschlossen. Der arterielle Blutdruck und die Herzfrequenz wurden zeitgleich zur MRT-Untersuchung erhoben.

Alle Studien, die in dieser Dissertation mit menschlichen Teilnehmenden durchgeführt wurden, entsprachen den ethischen Standards des institutionellen und nationalen Forschungsausschusses sowie den ethischen Richtlinien der Deklaration von Helsinki von 1964 und ihrer späteren Amendments. Alle Teilnehmenden gaben ihr schriftliches Einverständnis zur Studienteilnahme. Im Falle der Minderjährigkeit wurde das schriftliche Einverständnis der Sorgebevollmächtigten eingeholt.

3.2. MRT-Untersuchungsprotokolle

Alle Patient*innen in **Publikation 1 und 2** wurden nach klinischer Routine anhand standardisierter MRT-Protokolle gescannt. Die Untersuchungen wurden in Publikation 1 an einem 3,0-Tesla-MRT-Scanner (Ingenia, Philips Healthcare, Best, Niederlande) und in Publikation 2 an 1,5-Tesla-MRT-Scannern (Achieva, Philips Healthcare, Best, Niederlande und Avanto, Siemens, Erlangen, Deutschland) durchgeführt. Die MRT-Protokolle beinhalteten eine standardmäßige Cine-Steady-State-Free-Precession-(SSFP-)Sequenz. Zur Kopplung der Daten an die Eigenbewegung des Herzens wurde während der Messung ein EKG-Signal aufgezeichnet (EKG-Triggerung). Es erfolgte ein retrospektives EKG-Gating. Die Bildsequenzen umfassten 40 automatisch rekonstruierte Herzphasen. Typische Sequenzparameter am 1,5-Tesla-MRT-Scanner waren: Echozeit, echo time (TE) = 1,2 ms; Repetitionszeit, repetition time (TR) = 2,5 ms; Flipwinkel, flip angle (FA) = 60°; Voxelgröße, acquired voxel size (AVS): 1,80 x 1,70 x 6 mm^3. Die Gesamtdauer des Scans betrug 9 bis 14 Minuten. Weitere Details zu den MRT-Einstellungen sind den Publikationen 1 und 2 zu entnehmen (33, 34). In Publikation 1 wurden Cine-Aufnahmen im 4-Kammerblick mit Abbildung der AoD akquiriert. Zudem wurden transversale und orthogonale Querschnitte der AoD erhoben. In Publikation 2 wurden zur Aufnahme der AoA und AoD die

Schnittebenen senkrecht zum Gefäß und auf Höhe der Bifurkation der Arteria pulmonalis positioniert.

Im Rahmen der **Publikation 3** wurden alle Studienteilnehmenden anhand eines ^{23}Na-MRT-Protokolls gescannt. Die Bildgebung wurde in einem 3,0-Tesla-MRT-Scanner (Ingenia R 5.4, Philips Healthcare, Best, Niederlande) mithilfe einer ^{23}Na Sender/Empfänger-Kniespule (Rapid Biomedical, Rimpar, Deutschland) unter Anwendung einer 2D Spoiled Gradient-Echo-(GRE-)Sequenz durchgeführt. Sequenzparameter waren: Gesamtaufnahmezeit, time of acquisition (TA) = 20,5 min; TE = 2,138 ms; TR = 100 ms; FA = 90◦; Anzahl der Signalmittelung, number of signal average (NSA): 196; Auflösung: 3 × 3 × 30 mm^3. Alle Versuchspersonen ruhten mindestens 15 Minuten lang bevor ihre linke Wade am breitesten Umfang gescannt wurde. Vier Kalibrierphantome mit wässrigen Lösungen von 10, 20, 30 und 40 mmol/L NaCl wurden als Referenzstandards zusammen mit der Wade der Proband*innen gescannt. Gleichzeitig wurde der Gewebewassergehalt mittels ^{1}H-MRT unter Verwendung einer fettgesättigten, inversionspräparierten Spin-Echo-(SE-)Sequenz gemessen. Sequenzparameter waren: Inversionszeit, inversion time (TI) = 210 ms; TA = 6,27 min; TE = 12 ms; TR = 3000 ms; FA = 90◦; Auflösung: 1,5 × 1,5 × 5 mm^3.

3.3. Analyse und Auswertungen der MRT-Aufnahmen

In **Publikation 1 und 2** erfolgte die manuelle Auswertung der Gefäßdurchschnittsfläche in axialer Schnittführung während der endsystolischen und enddiastolischen Herzphase, entsprechend der maximalen und minimalen Gefäßerweiterung. In Publikation 1 erfolgte ausschließlich die Auswertung der AoD. Für Publikation 2 wurde der jeweilige Gefäßdurchmesser der AoA und AoD auf Höhe der Bifurkation der Arteria pulmonalis gemessen. Zur Erhebung der maximalen und minimalen Aortenquerschnittsfläche, die zur Berechnung der Distensibilität benötigt wird, wurde zunächst der längste und der kürzeste Durchmesser der aortalen Gefäßwand während des

gesamten Herzzyklus visuell nachvollzogen. Es wurde dementsprechend jeweils ein Schnittbild zum Zeitpunkt der maximalen bzw. minimalen Ausdehnung der Gefäßwand sowie unmittelbar davor und danach ausgewählt. Es folgte jeweils eine Bestimmung des Gefäßdurchmessers, welcher im späteren Verlauf zu einer Kreisfläche umgerechnet wurde. In Publikation 1 wurde zusätzlich zur durchmesserbasierten Messmethode die Gefäßquerschnittsfläche durch direkte Aortenwandkonturierung ausgemessen. Die Messungen wurden in jeder entsprechenden Schicht dreimal wiederholt, um jeweils einen Mittelwert pro Schicht zu berechnen. Zusätzlich wiederholte eine zweite Untersucherin alle Messungen, um die Interobserver-Reliabilität zu untersuchen. Beide Untersuchenden hatten mehr als zwei Jahre Erfahrung mit der Auswertung der Cine-Aufnahmen.

Um die lokale Distensibilität der Aorta zu berechnen, wurde folgende Formel verwendet:

$$\text{Distensibilität}_A\,[\frac{1}{\text{mmHg x } 10^3}] = \frac{(A_{max} - A_{min})}{A_{min}} \text{x } \frac{1}{PP}$$

Sie beschreibt die relative Änderung der Querschnittsfläche der Aorta im Verhältnis zur Pulsdruckänderung. A_{max} repräsentiert die systolische und A_{min} die diastolische Gefäßdurchschnittsfläche. Der Pulsdruck (PP) ist definiert als die Differenz zwischen systolischem und diastolischem Druck. Die Herleitung und weitere Details zur Berechnung sind den Publikationen 1 und 2 zu entnehmen (33, 34).

In **Publikation 3** wurden anhand des anatomischen Bildes (T1-gewichtete Spoiled-GRE-Sequenz) manuell Regions of Interest (ROI) auf Höhe des breitesten Querschnitts der linken Wade eingezeichnet. Entlang der Faszie wurden der Musculus triceps surae mit medialem und lateralem Musculus gastrocnemius und Musculus soleus, Haut, Tibia und subkutanem Fett ausgemessen. Die ROI des Muskelgewebes und des subkutanen Fetts wurden in der T1-gewichteten Sequenz eingezeichnet, während die ROI der Gesamtquerschnittsfläche der Wade, Haut und Phantomröhrchen anhand der ^{23}Na-MRT-Aufnahmen ausgemessen wurden. Die Signalintensität der vermessenen Bereiche wurde mittels linearer Trendanalyse in eine NaCl-Konzentration

umgerechnet, entsprechend des vordefinierten Gehaltes der Kalibrierungsphantome von 10, 20, 30 und 40 mmol/L. Da der Natriumgehalt im Fettgewebe durchschnittlich geringer ist als im Muskel, wurde zusätzlich untersucht, ob ein verminderter Natriumgehalt im Muskel auf eine vermehrte Anhäufung von Fett im Muskelgewebe zurückzuführen ist. Dabei wurden Voxel, die mehr als 30% über dem Intensitätsniveau des 10 mmol/L Phantomröhrchens lagen, (bei ^{1}H-T1-gewichteter Gewebesignalintensität) als Fettvoxel definiert. Der Fettgehalt des Muskelgewebes wurde anhand des Verhältnisses der Fettvoxel zur Gesamtzahl der Voxel innerhalb des Muskels beurteilt.

3.4. Statistische Analysen

In allen drei Studien wurden normalverteilte kontinuierliche Daten als Mittelwert mit Standardabweichung beschrieben. Bei nicht gegebener Normalverteilung wurden die Daten als Median mit Interquartilsabstand (Q3-Q1) ausgedrückt. Kategoriale Daten wurden als Häufigkeiten und Prozentsätze (%) dargestellt. Zur Analyse aller drei Studien wurden Tests auf Normalverteilung vor der darauffolgenden parametrischen und nicht-parametrischen statistischen Testung zum Gruppenvergleich durchgeführt. Unterschiede der Stichgruppen wurden bei Normalverteilung mit dem Student's t-Test verglichen, bzw. mit dem Wilcoxon-Test, wenn keine Normalverteilung vorlag. Der Chi-Quadrat-Test nach Pearson wurde in Kombination mit dem exakten Test nach Fisher zum Vergleich kategorialer Variablen verwendet. Univariate Korrelationen zwischen den Parametern wurden mit Hilfe der Pearson-Korrelationskoeffizienten errechnet. In Publikation 2 und 3 wurden Korrelationen mittels nicht-parametrischer Regressionsanalyse ausgewertet. Die Intra- und Interobserver-Reliabilität in Publikation 1 und 3 wurden mithilfe von Bland-Altman-Plots dargestellt. Der Intra-Klassen-Korrelationskoeffizient (ICC), als Indikator der Reliabilität, wurde bei Werten >0,7 als starke Korrelation bewertet. Die statistische Analyse der Publikation 1 erfolgte mit IBM SPSS Statistics für Windows (Version 24.0, SPSS Inc., Chicago, IL, USA). Für die statistische Auswertung der Publikation 2 und 3 wurde Stata

(Version 15.1, StataCorp, College Station, Texas, USA) verwendet. Alle Analysen wurden unter der Verwendung eines Signifikanzniveaus von $p<0,05$ durchgeführt.

4. Ergebnisse

Für die **Publikation 1** wurden zur Untersuchung der Reproduzierbarkeit der Distensibilitätsmessungen der Aorta insgesamt 31 Patient*innen in die Analyse einbezogen. Die Ergebnisse der durchmesser- bzw. flächenbasierten Messmethoden (Vermessung des Gefäßdurchmessers und anschließende Umrechnung in eine Kreisfläche bzw. direkte Messung der Gefäßquerschnittsfläche durch Aortenwandkonturierung) zur Erhebung der minimalen und maximalen Aortenquerschnittsfläche korrelierten linear (Pearson-Korrelationskoeffizient (CC) ≥0,971; jeweils $p<0,001$). Bei Auswertung per eingezeichneter Aortenwandkontur unterschied sich bei beiden Untersuchenden die Distensibilität der AoD aus den Aufnahmen im 4-Kammer-Blick von den streng orthogonalen Schnitten um etwa 25%. Dieser Unterschied war bei den entsprechenden Distensibilitätswerten der AoD auf Basis des Aortendurchmessers mit 12% geringer.

Die Untersuchung der Intraobserver-Reliabilität (n=10) zeigte für die flächenbasierte Messmethode die höchste Übereinstimmung unter Nutzung der Aufnahmen im 4-Kammer-Blick (ICC 0,97; 95% CI: 0,91-99), gefolgt von den orthogonalen und den transversalen Schnitten. Bei der durchmesserbasierten Messung der Distensibilität war die Übereinstimmung bei Messungen anhand der orthogonalen (ICC 0,97; 95% CI: 0,88-99) und der transversalen Schnitte (ICC 0,97; 95% CI: 0,89-99) etwas besser als anhand der Aufnahmen im 4-Kammer-Blick. In der Untersuchung der Interobserver-Reliabilität (n=31) zeigte sich unter Verwendung der flächenbasierten Messmethode die höchste Übereinstimmung bei Messungen anhand Aufnahmen in 4-Kammer-Ansicht (ICC 0,97; 95% CI: 0,93-99), gefolgt von den orthogonalen und den transversalen Schnitten. Bei der durchmesserbasierten Messmethode zur Erhebung der

Distensibilität war die Übereinstimmung ebenfalls bei Messungen anhand der 4-Kammer-Ansicht am höchsten (ICC 0,97; 95% CI: 0,94-99), gefolgt von den orthogonalen und den transversalen Aufnahmen.

Für die Fallzahlabschätzung der flächen- und durchmesserbasiert gemessenen Distensibilität der AoD zum Nachweis einer klinisch signifikanten Veränderung der aortalen Dehnbarkeit (90% Power; Signifikanzniveau=0,05) konnte folgendes festgestellt werden: Unter Verwendung der flächenbasierten Messmethode anhand von Aufnahmen im 4-Kammer-Blick genügen 24 Untersuchungen (n=19 + 25% Dropout) pro Gruppe, um eine klinisch relevante Differenz der Distensibilität von 0,8 $x10^{-3}mmHg^{-1}$ zu erkennen. In orthogonalen Aufnahmen benötigt man dafür eine Fallzahl von 28 Untersuchungen (n=22 + 25% Dropout). Bei der durchmesserbasierten Messmethode im 4-Kammer-Blick ist eine Anzahl von 23 Untersuchungen (n=18 + 25% Dropout) notwendig und im orthogonalen Schnitt eine Anzahl von 25 Untersuchungen (n=20 + 25% Dropout).

Für die als **Publikation 2** veröffentlichte zweizentrische Studie wurden 121 Studienteilnehmende in die Analyse einbezogen. Hypertensive ISTA-Patient*innen über 10 Jahre zeigten eine signifikant geringere Distensibilität der AoD im Vergleich zu normotensiven Patient*innen in ihrer Altersgruppe (-2,34 $x10^{-3}mmHg^{-1}$; p=0,020). In Hinblick auf die AoA konnte beobachtet werden, dass die Distensibilität bei Patient*innen mit koexistierender bikuspider Aortenklappe signifikant geringer war als bei Betroffenen mit trikuspider Aortenklappe (-2,59 $x10^{-3}mmHg^{-1}$; p=0,001). Insgesamt konnte eine Abnahme der Distensibilität der AoA und AoD mit zunehmendem Alter ab dem 10. Lebensjahr gezeigt werden.

Von der Gesamtkohorte (n=121) nahmen 37 Teilnehmende antihypertensive Medikamente ein. Von diesen erhielten 19 eine Monotherapie und 18 eine antihypertensive Doppel- oder Dreifachtherapie. Bei Patient*innen, welche unter Therapie normotensiv waren, war die

Distensibilität der AoD im Vergleich zu normotensiven Patient*innen ohne jegliche antihypertensive Therapie signifikant geringer (-1,32 $x10^{-3}mmHg^{-1}$; p=0,031). Hypertensive Patient*innen ohne antihypertensive Medikation zeigten eine weiter verringerte Distensibilität (-2,43 $x10^{-3}mmHg^{-1}$; p=0,020). Bei therapie-refraktären Patient*innen (d.h. unkontrollierte arterielle Hypertonie trotz medikamentöser Therapie) waren die geringsten Distensibilitätswerte der AoD zu beobachten (-3,40 $x10^{-3}mmHg^{-1}$; p=0,022).

Die Distensibilitätswerte wurden mit Referenzperzentilen gesunder Proband*innen (31) verglichen. Eine Einschränkung der Distensibilität der Aorta unterhalb der 5. Perzentile wurde in insgesamt 37,2% der Fälle für die AoA und in 43,0% für die AoD gefunden. Bei ISTA-Patient*innen älter als 10 Jahre korrelierte eine Einschränkung der Distensibilität (<5. Perzentile) der AoD vor allem mit dem Bestehen einer arteriellen Hypertonie (Odds Ratio (OR): 2,8; 95% Konfidenzintervall (CI): 1,08-7,2; p=0,033). Distensibiliätswerte der AoD unterhalb der 5. Perzentile wurde bei 49,3% aller hypertensiven Patient*innen >10 Jahre beobachtet, verglichen mit 26,7% bei normotensiven Teilnehmenden ihrer jeweiligen Altersgruppe. Eine vorliegende bikuspide Aortenklappe war in Betroffenen über 10 Jahre mit einer eingeschränkten Distensibilität (<5. Perzentile) der AoA assoziiert (OR: 3,1; 95% CI: 1,33-7,22; p=0,009). Bei ihnen wurde eine Beeinträchtigung der Distensibilität unter der 5. Perzentile der AoA bei 51,1% gesehen, verglichen mit nur 26,9% bei Patient*innen mit trikupider Aortenklappe. Bei Kombination aus arterieller Hypertonie und bikuspider Aortenklappe konnte in insgesamt 49,6% der Fälle eine Einschränkung (<5. Perzentile) der Distensibilität der AoA und in 51,4% der Fälle eine Einschränkung der Distensibilität der AoD gesehen werden. Im Vergleich dazu war bei normotensiven ISTA-Patient*innen mit physiologischer Trikuspidalklappe die Einschränkung der Distensibilität nur bei 21,1% in der AoA und bei 26,3% in der AoD vorhanden.

Im Rahmen der **Publikation 3** wurde der Natrium- und Wassergehalt des Gewebes bei insgesamt 32 Proband*innen analysiert, von denen 11 hypertensiv und adipös, 9 normotensiv und adipös und

12 normotensiv und normalgewichtig (Kontrollgruppe) waren. Der Natriumgehalt im Muskelgewebe in der Gruppe der hypertensiv-adipösen (11,95 mmol/L; Interquartilsabstand (IQR): 11,62–13,66) war signifikant niedriger als in der Gruppe der normotensiv-adipösen Patient*innen (13,63 mmol/L; IQR: 12,97–17,64; p=0,043) und der Kontrollgruppe (15,37 mmol/L; IQR: 14,12–16,08; p=0,012). Der Anteil des Fettgewebes innerhalb des Muskels unterschied sich dabei nicht zwischen den drei Gruppen. Es wurde auch keine Korrelation zwischen dem gemessenen Anteil des Fettgewebes und dem Natriumgehalt des Muskels gefunden (p=0,149). Der Natriumgehalt der Haut hingegen war in der Gruppe der normotensiv-adipösen (14,12 mmol/L; IQR: 13,15-15,83) signifikant höher als in der Kontrollgruppe (11,48 mmol/L; IQR: 10,48-12,80; p=0,004) und tendenziell höher als in der Gruppe der hypertensiv-adipösen Patient*innen (13,33 mmol/L; IQR: 11,53-14,22; p=0,144). Der Natriumgehalt im Gesamtquerschnitt aller Kompartimente betrug bei hypertensiv-adipösen 12,01 mmol/L (IQR: 11,41-12,89) und war damit signifikant niedriger als in der Gruppe der normotensiv-adipösen Patient*innen (p=0,045) und der Kontrollen (p=0,005). Es wurde eine negative Korrelation zwischen dem Natriumgehalt des Muskels und dem systolischen Blutdruck gefunden (p=0,0025, R^2=0,27). Diese Effekte standen in keinem Zusammenhang mit dem BMI. Zwischen Natriumgehalt der Haut und dem systolischen Blutdruck wurde ebenfalls keine signifikante Korrelation gefunden. Insgesamt konnte anhand von Bland-Altman-Plots eine geringe Interobserver-Variabilität bei der Messung des Natriumgehalts im Muskel nachgewiesen werden.

5. Diskussion

Im Rahmen der **Publikation 1** konnte eine ausgezeichnete Inter- und Intraobserver-Reliabilität zur Messung der Distensibilität der AoD beobachtet werden, unabhängig davon, ob die Messungen durchmesser- oder flächenbasiert durchgeführt wurden. In früheren Studien konnte bereits eine höhere Reproduzierbarkeit der aus CMR erhobenen Messergebnisse im Vergleich zur Echokardiographie gezeigt werden (35, 36). Dabei wurde eine hohe Korrelation zwischen in 4D-

Flussbildgebung gemessener PWV der Aorta und den entsprechenden Distensibilitätswerten festgestellt (37). Weiterhin konnte gezeigt werden, dass Distensibilitätswerte, die mittels der klinisch etablierten Aufnahme im 4-Kammer-Blick erhoben wurden, stark mit solchen aus streng orthogonalen Schnitten korrelieren. Die erhobenen Daten zeigen, dass die in standardmäßiger 4-Kammer-Ansicht gemessenen Distensibilitätswerte der Aorta gut mit denen aus streng orthogonalen Bildern übereinstimmen, jedoch dazu neigen, bei flächenbasierter Auswertung um etwa 25% und bei durchmesserbasierter Messung um etwa 12% überschätzt zu werden. Diese Abweichung ist eine Konsequenz des jeweiligen Anschnitts der Gefäßquerschnittsflächen aus unterschiedlichen Winkeln. Während orthogonal abgeleitete Bereiche nahezu kreisförmig sind, basieren die Bereiche im 4-Kammer-Blick auf einem Schrägschnitt des Gefäßes. Aus diesem Grund wurde bei Aufnahmen im 4-Kammer-Blick zur durchmesserbasierten Auswertung stets der kürzeste Durchmesser gewählt.

Anhand einer Fallzahlabschätzung konnte gezeigt werden, dass bereits durch eine kleine Anzahl von Untersuchungen eine klinisch signifikante Differenz der aortalen Distensibilität erkannt werden kann. Unter Verwendung der durchmesserbasierten Messmethode im 4-Kammer-Blick ist eine Anzahl von 23 Untersuchungen und in orthogonaler Aufnahme eine Anzahl von 25 Untersuchungen notwendig, um eine Differenz der Distensibilität von 0,8 $x10^{-3}mmHg^{-1}$ mit einer Power von 90% zu erkennen. Dies macht die in Publikation 1 verwendete Methode besonders geeignet für zukünftige Studien.

Zu den Limitationen dieser Studie gehört die geringe Anzahl der Studienteilnehmenden. Eine größere Kohorte könnte die Aussagekraft der Ergebnisse verbessern. Darüber hinaus wurde eine standardmäßige Cine-SSFP-Sequenz genutzt. Der Einfluss unterschiedlicher zeitlicher und räumlicher Auflösungen von Cine-SSFP-Sequenzen auf die Distensibilitätsmessung wurde nicht untersucht. Zum besseren Verständnis der Ergebnisse wäre weiterführend ein Vergleich mit anderen Markern für die arterielle Dehnbarkeit (z.B. PWV) hilfreich.

Auf Grundlage der untersuchten Messmethodik wurde die als **Publikation 2** veröffentlichte zweizentrische Studie durchgeführt. Es konnte gezeigt werden, dass ISTA-Patient*innen (>10 Jahre) mit bestehender arterieller Hypertonie signifikant niedrigere Distensibilitätswerte der AoD aufwiesen als normotensive Patient*innen ihrer jeweiligen Altersgruppe. Die Beeinträchtigung der Distensibilität der Aorta wurde in unserer Kohorte am deutlichsten bei Betroffenen über 10 Jahren beobachtet, mit zunehmender Abnahme der Distensibilität bei steigendem Alter. Entsprechend dieser Befunde fanden Juffermans et al. eine positive Korrelation zwischen verstärkter Versteifung der aortalen Gefäßwand von ISTA-Patient*innen und der Expositionsdauer gegenüber abnormaler Hämodynamik im Gefäß (38). Eine fehlende Normalisierung, z.B. durch eine unzureichende antihypertensive Behandlung, könnte somit zum Verlust der Dehnbarkeit der Aorta beitragen und damit das Risiko der Entwicklung kardiovaskulärer Komplikationen erhöhen. In Übereinstimmung mit diesen Konzepten zeigen unsere Daten die am stärksten beeinträchtigten Distensibilitätswerte bei therapierefraktärer arterieller Hypertonie, wohingegen gut eingestellte Blutdruckwerte zum Zeitpunkt der Studie mit einer verbesserten Distensibilität der AoD assoziiert waren.

Zur Berechnung der Distensibilität der Aorta konnte auf keine direkte Messung des zentralarteriellen Druckes zurückgegriffen werden, da eine solche aufgrund der Invasivität nicht in die Studie integriert wurde. Um eine nicht-invasive Beurteilung dennoch zu ermöglichen, verwendeten wir ein zuvor beschriebenes, auf der peripheren Blutdruckmessung basiertes Modell zur Abschätzung des zentralen Pulsdrucks, welches zuvor an ISTA-Patient*innen getestet wurde (25). Die Publikation 2 wurde als Querschnittsstudie geplant und durchgeführt, jedoch sind weiterführend Längsschnittstudien und größere Kohorten erforderlich, um die Kausalität der gefunden Zusammenhänge zu untersuchen.

Bei der Suche nach Mechanismen zur Erklärung des Zusammenhangs zwischen arterieller Hypertonie und der arteriellen Distensibilität wird der Natriumaufnahme und deren Auswirkung auf die Gefäße eine wichtige Rolle zugesprochen. Studien konnten bereits feststellen, dass eine

hohe Natriumzufuhr mit einer Struktur- und Funktionsveränderung der großen elastischen Arterien einhergeht (18). Die extrazelluläre Matrix der Arterienwand enthält mehrere Strukturproteine, darunter Kollagen und Elastin, welche durch Matrix-Metalloproteinasen (MMP) reguliert werden. MMPs werden durch eine natriumreiche Ernährung aktiviert, wodurch ein erhöhter Gehalt an transforming growth factor beta-1 (TGFß-1) verursacht wird (39). TFGß-1 wiederrum führt zur Fragmentierung der Elastinfasern, sowie zur Akkumulation von Kollagenfasern und somit zu einer Abnahme der elastischen Dehnbarkeit der arteriellen Gefäßwände (18, 40). Die nähere Betrachtung der Natriumspeicherung könnte daher zum besseren Verständnis der Pathophysiologie der arteriellen Hypertonie und deren kardiovaskulären Konsequenzen dienen.

Die Ergebnisse der **Publikation 3** zeigten, dass adipöse Jugendliche mit arterieller Hypertonie einen niedrigeren Natriumgehalt des Musculus triceps surae und einen niedrigeren Gesamtquerschnittsgehalt an Natrium aufwiesen als diejenigen ohne Hypertonie oder die normotensiven Kontrollen, unabhängig vom BMI. Entgegen der allgemeinen Annahme, dass der menschliche Körper im physiologischen Zustand unter erhöhter Salzbelastung durch eine gesteigerte renale Salzausscheidung den Anstieg des Blutdrucks regulieren kann, haben neuere Studie gezeigt, dass normotensive Proband*innen während einer akuten oder chronischen Salzbelastung weder schneller Natrium ausscheiden, noch eine stärkere Ausdehnung des Blutvolumens erfahren (41). Stattdessen wurde festgestellt, dass unter konstanter Salzaufnahme die tägliche Natriumausscheidung im Urin einen wöchentlichen Rhythmus zeigt, was zugleich für eine periodische Speicherung des Natriums spricht (42). In weiteren Studien konnte gezeigt werden, dass vor allem Muskelgewebe und Haut als Speicherort zur Pufferung von überschüssigem Natrium dienen (43, 44). Unsere Studie zeigt eine Beeinträchtigung dieser Puffermechanismen bei Jugendlichen: Während bei jungen adipösen Patient*innen ohne arterielle Hypertonie die Natriumspeicherung im Muskel nur geringfügig reduziert ist, beobachteten wir bei Patient*innen

mit arterieller Hypertonie eine Reduktion der Natriumspeicherung im Muskel. In anderen Kompartimenten wie der Haut, der Tibia und dem subkutanen Fettgewebe zeigte der Natriumgehalt bei hypertensiv-adipösen Patient*innen keinen signifikanten Unterschied, wobei eine potenzielle Verschiebung des Natriums in die benachbarten Kompartimente ausgeschlossen wurde. Dies könnte demnach bedeuten, dass Natrium in Adipösen mit arterieller Hypertonie nur vermindert im Gewebe gespeichert werden kann und es dadurch zu einer vermehrten intravaskulären Natriumaufnahme kommt. Auf diese Weise könnte ein Anstieg des Blutdrucks verursacht werden.

Im Rahmen der Studie 3 wurden keine Interventionen wie Salzbelastungstests oder eine Erhebung der Natriumausscheidung durchgeführt. Bei der Bewertung der Studienergebnisse sollte nicht nur an die Höhe der Natriumzufuhr, sondern auch an den individuellen Grad der Natriumsensitivität gedacht werden.

5.1. Klinische Bedeutung

Die frühzeitige Erkennung einer gestörten elastischen Dehnbarkeit der aortalen Gefäßwand ist von potenzieller prognostischer Bedeutung, da kardiovaskuläre Morbidität und Mortalität mit einer Abnahme der zentralarteriellen Dehnung verbunden sind. In Publikation 1 wurde die hohe Reproduzierbarkeit der Distensibilitätsmessungen anhand CMR nachgewiesen. Die Anwendbarkeit der Messmethodik konnte anschließend in Publikation 2 gezeigt werden. Messungen der Distensibilität der großen Arterien sind relativ einfach durchzuführen und spiegeln Veränderungen im zentralen Gefäßsystem wider. Die arterielle Distensibilität als neuartiger bildgebungsbasierter Marker für die Vorhersage des individuellen kardiovaskulären Risikos hat daher großes Potenzial, zur frühzeitigen Identifizierung von Risikopatient*innen beizutragen.

Anhand Publikation 2 konnte gezeigt werden, dass die Distensibilität der AoD bereits von der frühen Adoleszenz an bei ISTA-Patient*innen mit arterieller Hypertonie eingeschränkt ist.

Insbesondere Patient*innen mit hohen Blutdruckwerten trotz antihypertensiver Medikation waren betroffen. Es konnte ein deutlicher Zusammenhang zwischen adäquater Blutdruckkontrolle und verbesserter Distensibilität der aortalen Gefäßwand beobachtet werden. Dies verstärkt die Bedeutung einer frühzeitigen und vor allem geeigneten antihypertensiven Therapie. Die nicht-invasive Möglichkeit zur Erkennung von beginnenden Gefäßveränderungen könnte Ansätze zur Verbesserung angepasster Therapien liefern.

Weiterhin spielt die Früherkennung einer Dysregulation der Natriumspeicherung eine bedeutende Rolle in der Verlaufsbeurteilung der arteriellen Hypertonie. In Publikation 3 konnte durch nicht-invasive ^{23}Na-MRT-Technik das Speicherverhalten von Natrium im Gewebe untersucht werden. Die Ergebnisse deuten auf eine veränderte Regulierung der Natrium-Homöostase und -Speicherung bei Kindern und Jugendlichen mit arterieller Hypertonie hin, was der salzinduzierten arteriellen Hypertonie und deren Kompensationsmechanismen im Jugendalter eine neue Perspektive verleiht. Die Möglichkeit zur frühzeitigen Erkennung eines Missverhältnisses im Natriumhaushalt und dadurch bedingte Veränderungen im Speicherverhalten im Gewebe könnten helfen, frühzeitig Maßnahmen zu ergreifen, um kardiovaskuläre Langzeitfolgen zu verhindern.

5.2. Schlussfolgerung

Die zur Messung der Distensibilität der Aorta genutzte Methodik weist eine hohe Reproduzierbarkeit auf, kann mit wenig Aufwand in die klinische Routine integriert werden und zur frühen Detektion eines erhöhten kardiovaskulären Risikos beitragen. Die arterielle Hypertonie, die schon ab der frühen Adoleszenz ein großes kardiovaskuläres Risiko darstellt, geht mit einer Beeinträchtigung der aortalen Distensibilität und einer veränderten Natriumspeicherung einher. Die Verfahren zur Erhebung der Distensibilität großer arterieller Gefäße und des Gewebenatriums mittels MRT können zur Verlaufsbeurteilung einer arteriellen Hypertonie genutzt werden. Die Möglichkeit zur nicht-invasiven Evaluation des zentralen Gefäßsystems und der Natrium-

Homöostase des Gewebes können zur Verbesserung von Behandlungsstrategien beitragen und dabei helfen, Risikopatient*innen frühzeitig zu identifizieren.

Literaturverzeichnis

1. Maldonado J, Pereira T, Polonia J, Silva JA, Morais J, Marques M, participants in the EP. Arterial stiffness predicts cardiovascular outcome in a low-to-moderate cardiovascular risk population: the EDIVA (Estudo de DIstensibilidade VAscular) project. Journal of hypertension. 2011;29(4):669-75.

2. Mitchell GF. Arterial stiffness and hypertension: chicken or egg? Hypertension. 2014;64(2):210-4.

3. Safar ME, Levy BI, Struijker-Boudier H. Current perspectives on arterial stiffness and pulse pressure in hypertension and cardiovascular diseases. Circulation. 2003;107(22):2864-9.

4. Glasser SP, Arnett DK, McVeigh GE, Finkelstein SM, Bank AJ, Morgan DJ, Cohn JN. Vascular compliance and cardiovascular disease: a risk factor or a marker? Am J Hypertens. 1997;10(10 Pt 1):1175-89.

5. Belz GG. Elastic properties and Windkessel function of the human aorta. Cardiovascular drugs and therapy. 1995;9(1):73-83.

6. Leung MC, Meredith IT, Cameron JD. Aortic stiffness affects the coronary blood flow response to percutaneous coronary intervention. Am J Physiol Heart Circ Physiol. 2006;290(2):H624-30.

7. Eren M, Gorgulu S, Uslu N, Celik S, Dagdeviren B, Tezel T. Relation between aortic stiffness and left ventricular diastolic function in patients with hypertension, diabetes, or both. Heart. 2004;90(1):37-43.

8. Ganten M, Krautter U, Hosch W, Hansmann J, von Tengg-Kobligk H, Delorme S, Kauczor HU, Kauffmann GW, Bock M. Age related changes of human aortic distensibility: evaluation with ECG-gated CT. Eur Radiol. 2007;17(3):701-8.

9. Berenson GS, Srinivasan SR, Bao W, Newman WP, 3rd, Tracy RE, Wattigney WA. Association between multiple cardiovascular risk factors and atherosclerosis in children and young adults. The Bogalusa Heart Study. N Engl J Med. 1998;338(23):1650-6.

10. Strong JP, Malcom GT, McMahan CA, Tracy RE, Newman WP, 3rd, Herderick EE, Cornhill JF. Prevalence and extent of atherosclerosis in adolescents and young adults: implications for prevention from the Pathobiological Determinants of Atherosclerosis in Youth Study. JAMA. 1999;281(8):727-35.

11. Flynn JT, Kaelber DC, Baker-Smith CM, Blowey D, Carroll AE, Daniels SR, de Ferranti SD, Dionne JM, Falkner B, Flinn SK, Gidding SS, Goodwin C, Leu MG, Powers ME, Rea C, Samuels J, Simasek M, Thaker VV, Urbina EM, Subcommittee On S, Management Of High Blood Pressure In C. Clinical Practice Guideline for Screening and Management of High Blood Pressure in Children and Adolescents. Pediatrics. 2017;140(3).

12. Song P, Zhang Y, Yu J, Zha M, Zhu Y, Rahimi K, Rudan I. Global Prevalence of Hypertension in Children: A Systematic Review and Meta-analysis. JAMA Pediatr. 2019:1-10.

13. Sorof J, Daniels S. Obesity hypertension in children: a problem of epidemic proportions. Hypertension. 2002;40(4):441-7.

14. Canniffe C, Ou P, Walsh K, Bonnet D, Celermajer D. Hypertension after repair of aortic coarctation--a systematic review. Int J Cardiol. 2013;167(6):2456-61.

15. Tanous D, Benson LN, Horlick EM. Coarctation of the aorta: evaluation and management. Curr Opin Cardiol. 2009;24(6):509-15.

16. Toro-Salazar OH, Steinberger J, Thomas W, Rocchini AP, Carpenter B, Moller JH. Long-term follow-up of patients after coarctation of the aorta repair. Am J Cardiol. 2002;89(5):541-7.

17. Chen X, Wang Y. Tracking of blood pressure from childhood to adulthood: a systematic review and meta-regression analysis. Circulation. 2008;117(25):3171-80.

18. Safar ME, Thuilliez C, Richard V, Benetos A. Pressure-independent contribution of sodium to large artery structure and function in hypertension. Cardiovasc Res. 2000;46(2):269-76.

19. Avolio AP, Clyde KM, Beard TC, Cooke HM, Ho KK, O'Rourke MF. Improved arterial distensibility in normotensive subjects on a low salt diet. Arteriosclerosis. 1986;6(2):166-9.

20. Ma Y, He FJ, MacGregor GA. High salt intake: independent risk factor for obesity? Hypertension. 2015;66(4):843-9.

21. Zhu H, Pollock NK, Kotak I, Gutin B, Wang X, Bhagatwala J, Parikh S, Harshfield GA, Dong Y. Dietary sodium, adiposity, and inflammation in healthy adolescents. Pediatrics. 2014;133(3):e635-42.

22. Erbel R, Aboyans V, Boileau C, Bossone E, Bartolomeo RD, Eggebrecht H, Evangelista A, Falk V, Frank H, Gaemperli O, Grabenwoger M, Haverich A, Iung B, Manolis AJ, Meijboom F, Nienaber CA, Roffi M, Rousseau H, Sechtem U, Sirnes PA, Allmen RS, Vrints CJ, Guidelines ESCCfP. 2014 ESC Guidelines on the diagnosis and treatment of aortic diseases: Document covering acute and chronic aortic diseases of the thoracic and abdominal aorta of the adult. The

Task Force for the Diagnosis and Treatment of Aortic Diseases of the European Society of Cardiology (ESC). Eur Heart J. 2014;35(41):2873-926.

23. Urbina EM, Williams RV, Alpert BS, Collins RT, Daniels SR, Hayman L, Jacobson M, Mahoney L, Mietus-Snyder M, Rocchini A, Steinberger J, McCrindle B, American Heart Association Atherosclerosis H, Obesity in Youth Committee of the Council on Cardiovascular Disease in the Y. Noninvasive assessment of subclinical atherosclerosis in children and adolescents: recommendations for standard assessment for clinical research: a scientific statement from the American Heart Association. Hypertension. 2009;54(5):919-50.

24. Cavalcante JL, Lima JA, Redheuil A, Al-Mallah MH. Aortic stiffness: current understanding and future directions. J Am Coll Cardiol. 2011;57(14):1511-22.

25. Kelm M, Goubergrits L, Fernandes JF, Biocca L, Pongiglione G, Muthurangu V, Khushnood A, Secinaro A, Chinali M, Schubert S, Berger F, Kuehne T, group C. MRI as a tool for non-invasive vascular profiling: a pilot study in patients with aortic coarctation. Expert Rev Med Devices. 2016;13(1):103-12.

26. Kopp C, Linz P, Wachsmuth L, Dahlmann A, Horbach T, Schofl C, Renz W, Santoro D, Niendorf T, Muller DN, Neininger M, Cavallaro A, Eckardt KU, Schmieder RE, Luft FC, Uder M, Titze J. (23)Na magnetic resonance imaging of tissue sodium. Hypertension. 2012;59(1):167-72.

27. Kopp C, Linz P, Dahlmann A, Hammon M, Jantsch J, Muller DN, Schmieder RE, Cavallaro A, Eckardt KU, Uder M, Luft FC, Titze J. 23Na magnetic resonance imaging-determined tissue sodium in healthy subjects and hypertensive patients. Hypertension. 2013;61(3):635-40.

28. Dahlmann A, Dorfelt K, Eicher F, Linz P, Kopp C, Mossinger I, Horn S, Buschges-Seraphin B, Wabel P, Hammon M, Cavallaro A, Eckardt KU, Kotanko P, Levin NW, Johannes B, Uder M, Luft FC, Muller DN, Titze JM. Magnetic resonance-determined sodium removal from tissue stores in hemodialysis patients. Kidney Int. 2015;87(2):434-41.

29. Madelin G, Lee JS, Regatte RR, Jerschow A. Sodium MRI: methods and applications. Prog Nucl Magn Reson Spectrosc. 2014;79:14-47.

30. Stout KK, Daniels CJ, Aboulhosn JA, Bozkurt B, Broberg CS, Colman JM, Crumb SR, Dearani JA, Fuller S, Gurvitz M, Khairy P, Landzberg MJ, Saidi A, Valente AM, Van Hare GF. 2018 AHA/ACC Guideline for the Management of Adults With Congenital Heart Disease: Executive Summary: A Report of the American College of Cardiology/American Heart Association Task Force on Clinical Practice Guidelines. J Am Coll Cardiol. 2019;73(12):1494-563.

31. Voges I, Jerosch-Herold M, Hedderich J, Pardun E, Hart C, Gabbert DD, Hansen JH, Petko C, Kramer HH, Rickers C. Normal values of aortic dimensions, distensibility, and pulse wave velocity in children and young adults: a cross-sectional study. Journal of cardiovascular magnetic resonance : official journal of the Society for Cardiovascular Magnetic Resonance. 2012;14:77.

32. Kromeyer-Hauschild K, Wabitsch, M., Kunze, D., Geller F., Geiß H.C., Hesse V., von Hippel A., Jaeger U., Johnsen D., Korte W., Menner K., Müller G., Müller J.M., Niemann-Pilatus A., Remer T., Schaefer F., Wittchen H.-U., Zabransky S., Zellner K., Ziegler A., Hebebrand J. Perzentile für den Body-mass-Index für das Kindes- und Jugendalter unter Heranziehung verschiedener deutscher Stichproben. Monatsschr Kinderheilkd. 2001;149(149):807–18.

33. Ghorbani N, Muthurangu V, Khushnood A, Goubergrits L, Nordmeyer S, Fernandes JF, Lee CB, Runte K, Roth S, Schubert S, Kelle S, Berger F, Kuehne T, Kelm M. Impact of valve morphology, hypertension and age on aortic wall properties in patients with coarctation: a two-centre cross-sectional study. BMJ Open. 2020;10(3):e034853.

34. Stoiber L, Ghorbani N, Kelm M, Kuehne T, Rank N, Lapinskas T, Stehning C, Pieske B, Falk V, Gebker R, Kelle S. Validation of simple measures of aortic distensibility based on standard 4-chamber cine CMR: a new approach for clinical studies. Clin Res Cardiol. 2019.

35. Grothues F, Smith GC, Moon JC, Bellenger NG, Collins P, Klein HU, Pennell DJ. Comparison of interstudy reproducibility of cardiovascular magnetic resonance with two-dimensional echocardiography in normal subjects and in patients with heart failure or left ventricular hypertrophy. Am J Cardiol. 2002;90(1):29-34.

36. Morton G, Schuster A, Jogiya R, Kutty S, Beerbaum P, Nagel E. Inter-study reproducibility of cardiovascular magnetic resonance myocardial feature tracking. Journal of cardiovascular magnetic resonance : official journal of the Society for Cardiovascular Magnetic Resonance. 2012;14:43.

37. Harloff A, Mirzaee H, Lodemann T, Hagenlocher P, Wehrum T, Stuplich J, Hennemuth A, Hennig J, Grundmann S, Vach W. Determination of aortic stiffness using 4D flow cardiovascular magnetic resonance - a population-based study. Journal of cardiovascular magnetic resonance : official journal of the Society for Cardiovascular Magnetic Resonance. 2018;20(1):43.

38. Juffermans JF, Nederend I, van den Boogaard PJ, Ten Harkel ADJ, Hazekamp MG, Lamb HJ, Roest AAW, Westenberg JJM. The effects of age at correction of aortic coarctation and recurrent obstruction on adolescent patients: MRI evaluation of wall shear stress and pulse wave velocity. Eur Radiol Exp. 2019;3(1):24.

39. Salvi P, Giannattasio C, Parati G. High sodium intake and arterial stiffness. Journal of hypertension. 2018;36(4):754-8.

40. Safar ME, Temmar M, Kakou A, Lacolley P, Thornton SN. Sodium intake and vascular stiffness in hypertension. Hypertension. 2009;54(2):203-9.

41. Kurtz TW, DiCarlo SE, Pravenec M, Schmidlin O, Tanaka M, Morris RC, Jr. An alternative hypothesis to the widely held view that renal excretion of sodium accounts for resistance to salt-induced hypertension. Kidney Int. 2016;90(5):965-73.

42. Rakova N, Juttner K, Dahlmann A, Schroder A, Linz P, Kopp C, Rauh M, Goller U, Beck L, Agureev A, Vassilieva G, Lenkova L, Johannes B, Wabel P, Moissl U, Vienken J, Gerzer R, Eckardt KU, Muller DN, Kirsch K, Morukov B, Luft FC, Titze J. Long-term space flight simulation reveals infradian rhythmicity in human Na(+) balance. Cell Metab. 2013;17(1):125-31.

43. Selvarajah V, Connolly K, McEniery C, Wilkinson I. Skin Sodium and Hypertension: a Paradigm Shift? Curr Hypertens Rep. 2018;20(11):94.

44. Olde Engberink RHG, Selvarajah V, Vogt L. Clinical impact of tissue sodium storage. Pediatr Nephrol. 2019.

Eiddesstattliche Versicherung

„Ich, **Niky Ghorbani**, versichere an Eides statt durch meine eigenhändige Unterschrift, dass ich die vorgelegte Dissertation mit dem Thema: **„Nicht-invasive MRT-Diagnostik von Gefäßwand- und Gewebeeigenschaften in zwei Risikopopulationen mit arterieller Hypertonie“** selbstständig und ohne nicht offengelegte Hilfe Dritter verfasst und keine anderen als die angegebenen Quellen und Hilfsmittel genutzt habe.

Alle Stellen, die wörtlich oder dem Sinne nach auf Publikationen oder Vorträgen anderer Autoren/innen beruhen, sind als solche in korrekter Zitierung kenntlich gemacht. Die Abschnitte zu Methodik (insbesondere praktische Arbeiten, Laborbestimmungen, statistische Aufarbeitung) und Resultaten (insbesondere Abbildungen, Graphiken und Tabellen) werden von mir verantwortet.

Meine Anteile an etwaigen Publikationen zu dieser Dissertation entsprechen denen, die in der untenstehenden gemeinsamen Erklärung mit dem/der Erstbetreuer/in, angegeben sind. Für sämtliche im Rahmen der Dissertation entstandenen Publikationen wurden die Richtlinien des ICMJE (International Committee of Medical Journal Editors; www.icmje.og) zur Autorenschaft eingehalten. Ich erkläre ferner, dass ich mich zur Einhaltung der Satzung der Charité - Universitätsmedizin Berlin zur Sicherung Guter Wissenschaftlicher Praxis verpflichte.

Weiterhin versichere ich, dass ich diese Dissertation weder in gleicher noch in ähnlicher Form bereits an einer anderen Fakultät eingereicht habe.

Die Bedeutung dieser eidesstattlichen Versicherung und die strafrechtlichen Folgen einer unwahren eidesstattlichen Versicherung (§§156, 161 des Strafgesetzbuches) sind mir bekannt und bewusst.“

Datum Unterschrift

Anteilserklärung an den erfolgten Publikationen

Die Promovendin **Niky Ghorbani** hatte folgenden Anteil an den folgenden Publikationen:

Publikation 1:

Stoiber, L., **Ghorbani, N**., Kelm, M., Kuehne, T., Rank, N., Lapinskas, T., Stehning, C., Pieske, B., Falk, V., Gebker, R., Kelle, S. "Validation of simple measures of aortic distensibility based on standard 4-chamber cine CMR: a new approach for clinical studies." *Clin Res Cardiol. (2019)*

Beitrag im Einzelnen:

- Umfassende Einarbeitung in den Stand der Literatur hinsichtlich nicht-invasiver Methoden zur Messung der elastischen Dehnbarkeit von Gefäßen mit Schwerpunkt CMR
- Einarbeitung in die Software zur Auswertung und Post-Prozessierung der CMR-Bilddaten
- Etablierung der Messmethode (in Kooperation mit Dr. med. univ. L. Stoiber)
- Eigenständige Durchführung aller radiologischen Messungen der CMR-Bilddaten als zweite Untersucherin
- Mithilfe zur Dokumentation und Aufarbeitung aller erhobenen Daten in der Studiendatenbank
- Mithilfe bei der Interpretation der Ergebnisse und deren klinischer Bedeutung (in enger Zusammenarbeit mit Dr. med. univ. L. Stoiber)
- Kritische Revision des finalen Manuskripts

Publikation 2:

Ghorbani, N., Muthurangu V., Khushnood A., Goubergrits L,, Nordmeyer S., Fernandes J.F., Lee C.B., Runte K., Roth S., Schubert S., Kelle S., Berger F., Kuehne T., Kelm M., "Impact of Valve Morphology, Hypertension and Age on Aortic Wall Properties in Patients with Coarctation: a two-centre cross-sectional study" *BMJ Open (2020)*

Beitrag im Einzelnen:

- Umfassende Einarbeitung in den Stand der Literatur hinsichtlich CMR-Bildgebung, Aortenisthmusstenose, Distensibilität (physikalische Hintergründe und Berechnung), arterielle Hypertonie und deren Zusammenhänge
- Einarbeitung in die Software zur Auswertung und Post-Prozessierung der CMR-Bilddaten
- Weiterentwicklung der Messmethode zur Verbesserung der Präzision in interdisziplinärer Absprache mit Prof. Dr.-Ing. L. Goubergrits und M.Sc. J.F. Fernandes

- Eigenständige Datenerfassung der Studienpopulation (klinische Parameter)
- Eigenständige Durchführung aller radiologischen Messungen der CMR-Bilddaten und deren Erfassung in der Studiendatenbank
- Eigenständige Erweiterung der Studiendatenbank zur Ermöglichung einer detaillierteren Gruppeneinteilung
- Koordination und Kommunikation zwischen DHZB und der Partnergruppe am University College London
- Wesentlicher Anteil an der Datenauswertung und statistischen Analyse (in enger Zusammenarbeit mit Dr. M. Kelm)
- Eigenständige Interpretation der Daten und Einordnung in den wissenschaftlichen Kontext
- Eigenständige Konzeption und Erstellung von Tabellen und Grafiken (Tabelle 1, Figure 1, Figure 2)
- Eigenständige Konzeption, Verfassung und Einreichung des Manuskripts (inhaltliche Kommentare und Korrekturlesungen von Prof. Dr. T. Kühne und Dr. M. Kelm)
- Revision des Manuskripts und Umsetzung der Reviewer-Kommentare

Publikation 3:

Roth, S., Marko, L., Birukov, A., Hennemuth, A., Kuhnen, P., Jones, A., **Ghorbani, N**., Linz, P., Muller, D. N., Wiegand, S., Berger, F., Kuehne, T., Kelm, M. "Tissue Sodium Content and Arterial Hypertension in Obese Adolescents." *J Clin Med (2019)*

Beitrag im Einzelnen:

- Einarbeitung in den Stand der Literatur hinsichtlich ^{23}Na-MRT (technische Hintergründe und Anwendungsfelder), Adipositas und arterieller Hypertonie und deren Zusammenhänge
- Beteiligung an der Aufarbeitung der Studiendatenbank (klinische Parameter)
- Beteiligung an der Diskussion und Interpretation der Ergebnisse
- Kritische Revision des finalen Manuskripts

_____

Unterschrift, Datum und Stempel des/der erstbetreuenden Hochschullehrers/in

_____

Unterschrift des Doktoranden/der Doktorandin

Publikation 1

Stoiber L, **Ghorbani N**, Kelm M, Kuehne T, Rank N, Lapinskas T, Stehning C, Pieske B, Falk V, Gebker R, Kelle S. Validation of simple measures of aortic distensibility based on standard 4-chamber cine CMR: a new approach for clinical studies. Clin Res Cardiol. 2019.

DOI: 10.1007/s00392-019-01525-8

Clinical Research in Cardiology
https://doi.org/10.1007/s00392-019-01525-8

ORIGINAL PAPER

Validation of simple measures of aortic distensibility based on standard 4-chamber cine CMR: a new approach for clinical studies

Lukas Stoiber[1,2] · Niky Ghorbani[3] · Marcus Kelm[3,6] · Titus Kuehne[3,6] · Nina Rank[1,2] · Tomas Lapinskas[1,4,6] · Christian Stehning[7] · Burkert Pieske[1,5,6] · Volkmar Falk[2,6] · Rolf Gebker[1] · Sebastian Kelle[1,5,6]

Received: 10 April 2019 / Accepted: 2 July 2019

Abstract

Objective Aortic distensibility (AD) represents a well-established parameter of aortic stiffness. It remains unclear, however, whether AD can be obtained with high reproducibility in standard 4-chamber cine CMR images of the descending aorta. This study investigated the intra- and inter-observer agreement of AD based on different angles of the aorta and provided a sample size calculation of AD for future trials.

Methods Thirty-one patients underwent CMR. Angulation of the descending aorta was performed to obtain strictly transversal and orthogonal cross-sectional aortic areas. AD was obtained both area and diameter based.

Results For area-based values, inter-observer agreement was highest for 4-chamber AD (ICC 0.97; 95% CI 0.93–99), followed by orthogonal AD (ICC 0.96; 95% CI 0.91–98) and transversal AD (ICC 0.93; 95% CI 0.80–97). For diameter-based values, agreement was also highest for 4-chamber AD (ICC 0.97; 95% CI 0.94–99), followed by orthogonal AD (ICC 0.96; 95% CI 0.92–98) and transversal AD (ICC 0.91; 95% CI 0.77–96). Bland–Altman plots confirmed a small variation among observers. Sample size calculation showed a sample size of 12 patients to detect a change in 4-chamber AD of 1×10^{-3} $mmHg^{-1}$ with either the area or diameter approach.

Conclusion AD measurements are highly reproducible and allow an accurate and rapid assessment of arterial compliance from standard 4-chamber cine CMR.

Electronic supplementary material The online version of this article (https://doi.org/10.1007/s00392-019-01525-8) contains supplementary material, which is available to authorized users.

Extended author information available on the last page of the article

Published online: 13 July 2019

Graphic abstract

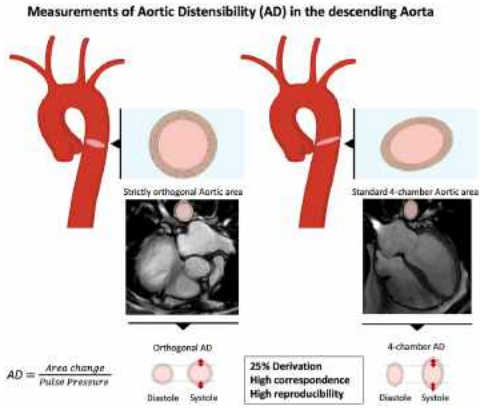

Keywords Aortic distensibility · Compliance · Cardiac magnetic resonance imaging · Cine MRI · Reproducibility

List of abbreviations

AA	Aortic areas
AC	Aortic compliance
AD	Aortic distensibility
BP	Blood pressure
CMR	Cardiac magnetic resonance tomography
ICC	Intra-class coefficient
MRI	Magnetic resonance imaging
PP	Pulse pressure
PWV	Pulse wave velocity
SD	Standard deviation
SSFP	Steady-state free precession sequence

Introduction

Arterial compliance, the tendency of blood vessels to stretch in response to the pulsatile blood flow, has significant physiological effects on blood pressure (BP) [1–3]. The cushioning function of the aorta may be impaired due to structural degeneration of the aortic wall, increasing stiffness and thus the afterload for the left ventricle [3].

Aortic distensibility (AD) provides an estimation of these elastic properties and normalizes arterial compliance with the size of the vessel, allowing for a better comparison between individuals [4].

Previously, several authors have made significant contributions to assess aortic compliance with various imaging methods [5–8]. Measurements of AD can give information even on subclinical vascular changes and are being investigated as predictors of cardiovascular morbidity [4, 9–11]. Newer preclinical and clinical studies are focusing on mechanisms of influencing AD. Moreover, we recently showed AD to be a potential biomarker to act as a non-invasive control in interventional hypertension trials [4].

Currently, cardiac magnetic resonance tomography (CMR) is regarded as a gold standard to assess areas of different parts of the aorta to calculate AD. However, some aspects regarding the meaningfulness and interpretability of AD in the descending aorta remain unresolved. Even though the descending aorta is incidentally imaged in every standard 4-chamber view cine steady-state free precession sequence (SSFP) of the heart, it remains uncertain whether these images can be used to calculate AD in daily clinical practice adequately. The current study aimed to systematically analyze reproducibility (with intra- and inter-observer agreement) of cine imaging in the evaluation of AD. Our measurements were acquired using various types of angulation of the descending aorta in CMR.

Methods

We performed CMR in 31 subjects (mean age 57 years) with variable indications. The study complies with the Declaration of Helsinki. Institutional Review Board approval was not necessary due to a retrospective analysis of clinical data. According to local law, all individuals signed informed consent before entering the clinical MRI. The data were anonymized and none of the observers had the possibility

of identifying patient information when analyzing the data. All images were acquired using a Philips Ingenia 3.0 Tesla Scanner (Philips Healthcare, Best, the Netherlands). Cine images were acquired during breath holds of 10–15 s using vector electrocardiogram gating and steady-state free precession sequence [4]. All study participants were scanned using the same imaging protocol, which consisted of angulation of the descending aorta to obtain strictly transversally and orthogonally cut cross-sectional areas of the aorta [16]. Fifty images per cardiac cycle were obtained. AD was determined as the change in the cross-sectional aortic area per unit change in BP, as previously reported [4, 10, 16, 17]. Office BP was obtained during the MRI with an automatic brachial oscillometric monitor after at least 5 min of rest [4]. Two experienced observers then performed post-processing of the CMR dataset with the Medis Suite Version 2.1. (Medis, Leiden, The Netherlands). Both observers had more than 2 years of experience with general CMR imaging. Qmass software was used to contour the inner diameter of the aortic wall. Maximum and minimum aortic areas were calculated by (i) tracing the largest and smallest extension of the aortic wall contour throughout the cardiac cycle and (ii) tracing aortic diameters to calculate a hypothetic circle aiming to obtain a strictly circular aortic area. We first assessed cross-sectional areas of the descending aorta obtained in standard 4-chamber cine images. In a second step, we performed the same measurements in images based on strictly transversal or orthogonal cuts. Figure 1 illustrates the three different angles used at the time of image acquisition. All measurements were repeated three times and then averaged. To calculate AD, we first determined aortic strain, defined as the relative change in area, and then normalized this value with the peripheral pulse pressure (PP) obtained at the time point of the CMR (average of three PP values). The formula used for the AD calculation has been published previously [4, 10, 16, 17].

Sample size calculation

To detect a clinically significant change of 0.5, 0.8 and 1×10^{-3} $mmHg^{-1}$ in aortic distensibility with the power of 90% and a significance level (α) of 5%, the sample size calculations were performed using the following formula:

$$n = f(\alpha, P) \cdot \sigma^2 \cdot 2/\delta^2$$

where α is the significance level, P the required power, n the sample size and f the value of the factor for different values of α and P ($f = 10.5$ for $\alpha = 0.05$ and $P = 0.090$), with σ the

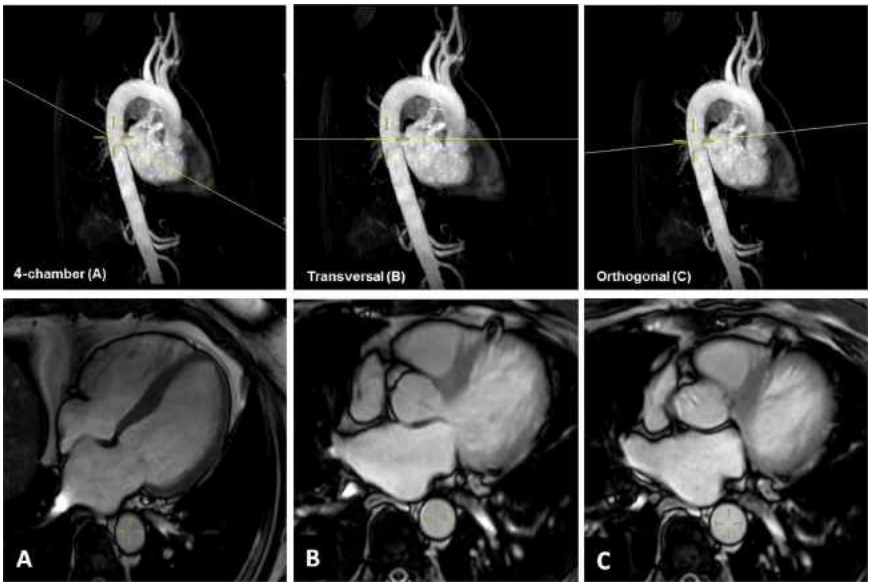

Fig. 1 Illustration of CMR angulation of the descending aorta at the time of image acquisition and corresponding 4-chamber (**a**), transversal (**b**) and orthogonal (**c**) aortic areas. Image **a** shows a standard 4-chamber SSFP image where the slightly oval areas of the descending aorta can easily be tracked without further technical planning. Images **b** and **c** demand proper planning and are not performed in daily practice clinical imaging of the heart

standard deviation of differences between two measurements and δ the target difference to be detected [18, 19].

Statistical analysis

All data are presented as mean ± standard deviation. Differences in mean values were compared using Student's *T* test if data were normally distributed or the Wilcoxon test if normality could not be assumed. Kolmogorov–Smirnov test was used to assess distribution. Univariate correlations between parameters were obtained using Pearson's correlation coefficients. Intra- and inter-observer variability is displayed in Bland–Altman plots. The intra-class correlation coefficient (ICC) was considered excellent with a value of > 0.7 [20]. A *P* value < 0.05 was considered statistically significant. Statistical analysis was performed using IBM SPSS Statistics for Windows (Version 24.0, SPSS Inc., Chicago, IL, USA).

Results

Study population

Thirty-three patients were included in this analysis. Two patients had to be excluded due to low image quality. The mean age was 57 years, 13/33 (39%) were female and mean BP was 122/68 mmHg.

Values of aortic areas, aortic strain, and aortic distensibility

Table 1 provides an overview of the minimal and maximal aortic areas, aortic distensibility and strain derived from either aortic area or aortic diameter. The values displayed are those obtained from observer 1. Pearson correlation coefficients are represented.

Values of aortic distensibility among two observers

Figure 1S illustrates the distribution of AD values obtained by two observers depending on the angulation used at the time of image acquisition. Table 2 outlines the differences in absolute values of AD between two observers. In both observers, the classic 4-chamber AD differed from the strictly orthogonal cuts by about 25% when using traced aortic contours for AD calculation (3.26 ± 2.28 vs. 2.49 ± 1.96 10^{-3} $mmHg^{-1}$ for observer 1 and 2.93 ± 2.37 vs. 2.35 ± 2.06 10^{-3} $mmHg^{-1}$ for observer 2). As expected, this difference was smaller in the corresponding values for AD based on aortic diameter (about 12%). Pearson's values for correlation between orthogonal AD and 4-chamber AD as well as for transversal AD and 4-chamber are listed in Table 3.

Interestingly, the highest values for correlation and reproducibility were found for 4-chamber AD measures both in area- and in diameter-based measurements. Figure 2 provides the correlation between orthogonal AD and the classic 4-chamber AD for both observers. For observer 1, the

Table 1 Overview of minimal and maximal aortic areas and aortic distensibility and strain derived from either aortic area or aortic diameter. Pearson correlation coefficients are represented. Values represent measurements of observer 1

Parameter ($n = 31$)	Area	Diameter	Pearson CC	*P* value CC*
Minimal areas of descending aorta (mm^2)				
Transversal angulation	445.09 ± 178.65	419.11 ± 156.24	0.993	< 0.001
Orthogonal angulation	442.35 ± 159.38	420.86 ± 146.24	0.994	< 0.001
Classic 4-chamber angulation	482.82 ± 167.14	432.24 ± 153.93	0.986	< 0.001
Maximal areas of descending aorta (mm^2)				
Transversal angulation	497.67 ± 184.50	476.04 ± 161.41	0.989	< 0.001
Orthogonal angulation	487.51 ± 159.62	470.08 ± 149.95	0.992	< 0.001
Classic 4-chamber angulation	549.18 ± 171.16	487.60 ± 156.93	0.971	< 0.001
Aortic strain (mm^2)				
Transversal angulation	13.08 ± 6.44	14.76 ± 6.35	0.819	< 0.001
Orthogonal angulation	11.67 ± 6.77	13.00 ± 6.97	0.785	< 0.001
Classic 4-chamber angulation	15.27 ± 7.38	14.42 ± 7.71	0.798	< 0.001
Aortic distensibility (10^{-3} $mmHg^{-1}$)				
Transversal angulation	2.80 ± 1.99	3.11 ± 1.83	0.882	< 0.001
Orthogonal angulation	2.49 ± 1.96	2.74 ± 1.98	0.911	< 0.001
Classic 4-chamber angulation	3.26 ± 2.28	3.08 ± 2.36	0.910	< 0.001

Data are expressed as mean and standard deviation

CC correlation coefficient

**P* values indicating the level of correlation

Table 2 Aortic area- and aortic diameter-derived measurements of aortic distensibility (AD) in two observers

Parameter ($n=31$)	Observer 1	Observer 2	Pearson CC	P value CC*
AD (10^{-3} mmHg^{-1}) based on aortic area				
Transversal angulation	2.80 ± 1.99	2.26 ± 2.06	0.895	< 0.001
Orthogonal angulation	2.49 ± 1.96	2.35 ± 2.06	0.921	< 0.001
Classic 4-chamber angulation	3.26 ± 2.28	2.93 ± 2.37	0.948	< 0.001
AD (10^{-3} mmHg^{-1}) based on aortic diameter				
Transversal angulation	3.11 ± 1.84	2.61 ± 1.78	0.854	< 0.001
Orthogonal angulation	2.74 ± 1.99	2.62 ± 2.10	0.928	< 0.001
Classic 4-chamber angulation	3.08 ± 2.36	2.85 ± 2.29	0.949	< 0.001

Data are expressed as mean and standard deviation

CC correlation coefficient

**P* values indicating the level of correlation

Table 3 Pearson's values for correlation between orthogonal AD and classic 4-chamber AD as well as for transversal AD and classic 4-chamber AD

	Observer 1 4-chamber angulation	Observer 2 4-chamber angulation
Area-based AD (10^{-3} mmHg^{-1})		
Orthogonal angulation	Pear = 0.92 (R^2 = 0.8451)	Pear = 0.92 (R^2 = 0.8451)
Transversal angulation	Pear = 0.90 (R^2 = 0.8067)	Pear = 0.90 (R^2 = 0.805)
Diameter-based AD (10^{-3} mmHg^{-1})		
Orthogonal angulation	Pear = 0.87 (R^2 = 0.7558)	Pear = 0.90 (R^2 = 0.8175)
Transversal angulation	Pear = 0.80 (R^2 = 0.6412)	Pear = 0.85 (R^2 = 0.7187)

Pear Pearson's correlation coefficient

corresponding R^2 values were 0.8451 for area-based AD and 0.7558 for diameter-based AD. For observer 2, the respective R^2 values were 0.8451 and 0.8175.

Intra- and inter-observer agreement

Figure 3 shows the Bland–Altman plots demonstrating intra- and inter-observer variability for AD values obtained from contoured (A) or diameter-based (B) aortic areas, depending on the angulation of the aorta at the time of image acquisition. Table 4 outlines the reproducibility giving the mean difference between two measurements and the corresponding intra-class correlation coefficient (ICC). Inter-observer agreement was excellent in both approaches used: for area-based AD, agreement was highest for 4-chamber AD (ICC 0.97; 95% CI 0.93–99), followed by orthogonal AD (ICC 0.96; 95% CI 0.91–98) and transversal AD (ICC 0.93; 95% CI 0.80–97). For diameter-based AD, agreement was also highest for 4-chamber AD (ICC 0.97; 95% CI 0.94–99), followed by orthogonal AD (ICC 0.96; 95% CI 0.92–98) and transversal AD (ICC 0.91; 95% CI 0.77–96).

Sample size calculation

Changes in reproducibility influence the sample size required to detect significant differences in AD. The sample sizes required for each AD value are given in Table 5.

Discussion

The present work was designed to investigate the reproducibility of AD calculation in standard 4-chamber cine CMR imaging. Our data demonstrate the following:

1. Assessment of AD through conventional 4-chamber cine images is easy and correlates highly with AD derived from a strictly orthogonal angulation of the aorta.
2. Excellent inter-observer and intra-observer reproducibility were observed for AD, irrespective of whether measurements were based on aortic diameter or manually traced aortic area.

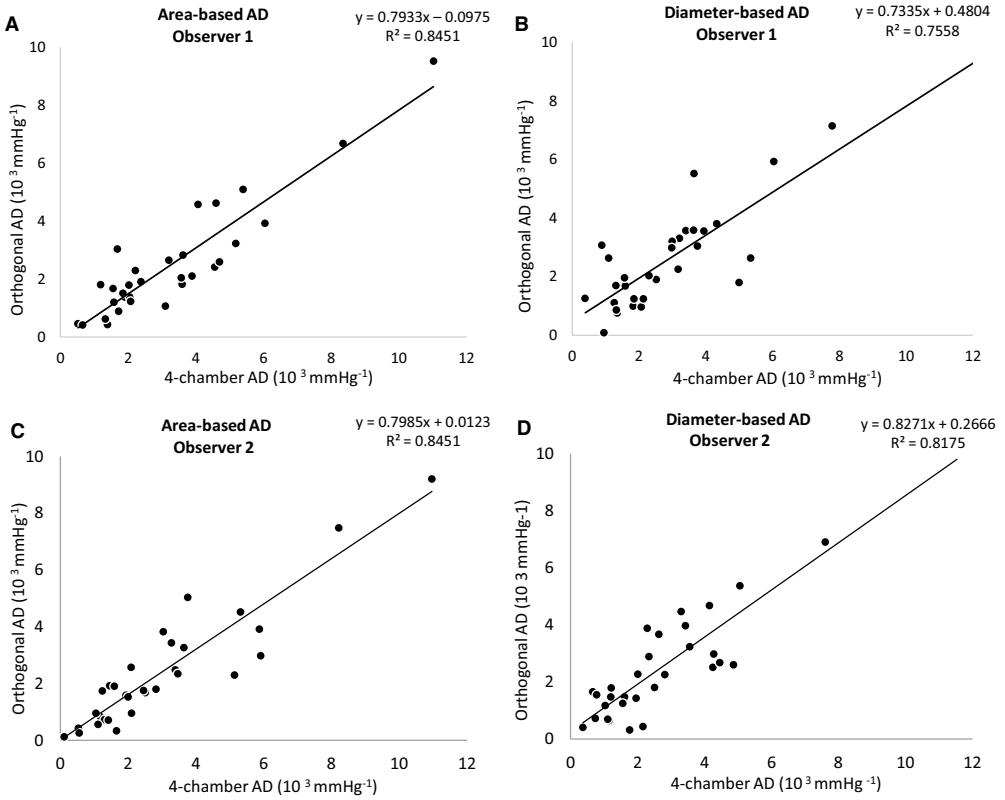

Fig. 2 Correlation between orthogonal AD and the classic 4-chamber AD with the corresponding R^2 values. Results are provided for Observer 1 (A + B) and Observer 2 (C + D) for both area-based AD and diameter-based AD

3. The sample size calculation demonstrated a minimal number of $n = 12$ subjects to detect even small changes in AD.

Relationships of pulse pressure (PP) and flow are illustrated by impedance curves, which show higher frequencies when the aortic arch becomes stiffer and then reflects pulse waves earlier [21]. While determinants of peripheral resistance are simple to acquire, parameters of aortic stiffness require consideration of the distending PP, vascular tone and site of measurement [3]. As a gold standard for arterial stiffness, PWV requires certain geometric assumptions and extended planning and remains time consuming. Recently, 4D flow CMR has been shown to directly assess PWV in reduced time and to have a high correlation with AD values [22]. Measures of AD are relatively simple to obtain and reflect alterations in the central vasculature even in the absence of overt cardiovascular disease. No additional scans are needed to calculate AD. Thus, focusing on AD as a novel imaging biomarker for the prediction of cardiovascular risk has significant potential to improve individually adapted therapies [23].

While previous research aimed to assess AD in vivo, newer studies focus on therapeutic concepts to reduce arterial stiffness [11–14]. Both medical control of heart rate and modulation of the sympathetic nervous system by renal denervation have shown promising results to improve AD. [12–15] In preclinical studies, heart rate reduction with ivabradine has shown to improve arterial stiffness and diastolic function [14, 15]. Targeting AD might thus play an essential role in the management of heart failure with preserved ejection fraction (HFPEF).

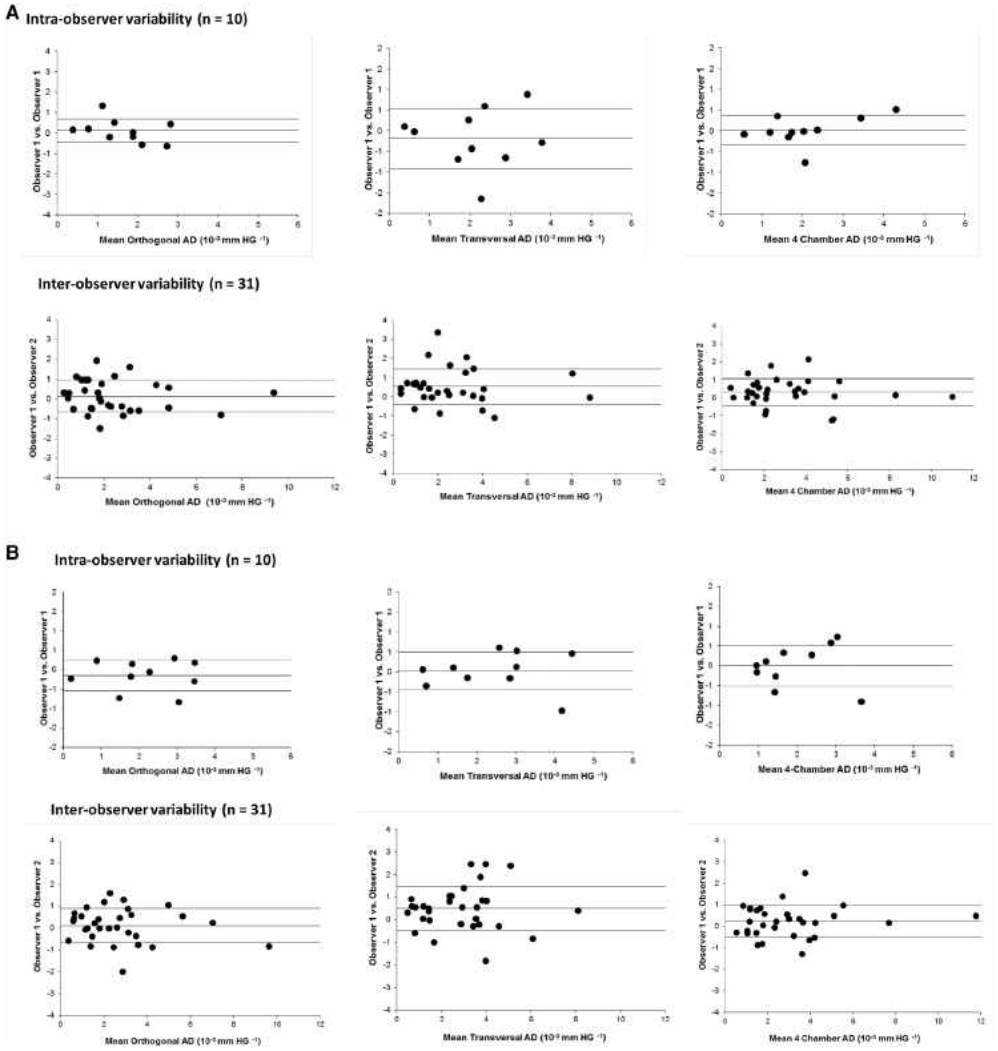

Fig. 3 Bland–Altman plots demonstrating intra- and inter-observer variability for AD values obtained from contoured aortic areas (**a**) or diameter-based values (**b**) depending on the angulation of the aorta at the time of image acquisition

Reproducibility and accuracy of CMR were previously shown to be high, especially compared to those of echocardiography [24, 25]. We assumed that AD estimation would be feasible when focusing on images of the descending aorta that are available in every standard 4-chamber cine sequence of the heart (Fig. 1) [19]. For this purpose, we retrospectively analyzed already existing CMR data. Images were taken in diameter and area. Resulting values differed by about 15% (Fig. 4).

Based on the outlined data, we can assume that AD taken in standard 4-chamber cine images corresponds well with strictly orthogonal images but tends to overestimate values by about 25% (Table 3, Fig. 4). This deviation is a consequence of the geometry of cross-sectional vessel areas

Table 4 Intra-observer and inter-observer reproducibility for aortic distensibility based on aortic areas or diameters

Parameter	Mean difference ± SD	ICC (95% CI)
AD (10^{-3} mmHg^{-1}) based on aortic area		
Intra-observer ($n = 10$)		
AD transversal angulation	−0.19 ± 0.73	0.81 (0.41–0.95)
AD orthogonal angulation	0.11 ± 0.58	0.87 (0.50–0.97)
AD classic 4-chamber angulation	0.13 ± 0.35	0.97 (0.91–0.99)
Inter-observer ($n = 31$)		
AD transversal angulation	−0.54 ± 0.94	0.93 (0.80–0.97)
AD orthogonal angulation	−0.13 ± 0.81	0.96 (0.91–0.98)
AD classic 4-chamber angulation	−0.32 ± 0.76	0.97 (0.93–0.99)
AD (10^{-3} mmHg^{-1}) based on aortic diameter		
Intra-observer ($n = 10$)		
AD transversal angulation	0.02 ± 0.47	0.97 (0.89–0.99)
AD orthogonal angulation	−0.14 ± 0.40	0.97 (0.88–0.99)
AD classic 4-chamber angulation	0.01 ± 0.52	0.93 (0.73–0.98)
Inter-observer ($n = 31$)		
AD transversal angulation	−0.50 ± 0.98	0.91 (0.77–0.96)
AD orthogonal angulation	−0.12 ± 0.78	0.96 (0.92–0.98)
AD classic 4-chamber angulation	−0.23 ± 0.75	0.97 (0.94–0.99)

Data are expressed as mean and standard deviation. Mean difference = mean difference between the two measurements; coefficient of variability = SD of the mean difference between two measurements divided by the mean value of the parameter (Grothues et al. [19])

ICC intra-class correlation coefficient, CI = confidence interval

Table 5 Sample size calculations for area-based AD and diameter-based AD to detect a clinically significant change of 0.5, 0.8 and one 10^{-3} mmHg^{-1} in aortic distensibility (with 90% power and an α error of 0.05)

Parameter	Mean difference ± SD	Sample size (n)		
		0.5	0.8	1
AD (10^{-3} mmHg^{-1}) based on aortic area				
AD transversal angulation	−0.54 ± 0.94	74	29	19
AD orthogonal angulation	−0.13 ± 0.81	55	22	14
AD classic 4-chamber angulation	−0.32 ± 0.76	48	19	12
AD (10^{-3} mmHg^{-1}) based on the aortic diameter				
AD transversal angulation	−0.50 ± 0.98	81	32	20
AD orthogonal angulation	−0.12 ± 0.78	51	20	13
AD classic 4-chamber angulation	−0.23 ± 0.75	47	18	12

Data are expressed as mean and standard deviation

ICC intra-class correlation coefficient, *CI* confidence interval, *SD* standard deviation

displayed with different angulations. While orthogonally derived areas are nearly circular, the areas in the 4-chamber view are based on an oblique section of the vessel in this projection. Values of inter- and intra-observer agreement were excellent in our data, underlining the high potential for retrospective analyses (Fig. 3). To give an impression of how this measurement technique will perform in daily practice, the correlation curves of two different observers are shown in Fig. 2.

CMR was shown to provide highly accurate and reproducible measures, especially when values are derived three times [18, 19, 26]. We used this strategy and averaged three measurements to improve reproducibility. Given the above evidence, AD obtained by tracing of the aortic wall is justified to be used in daily clinical practice for risk prediction.

Recently, two studies investigated AD measurement as a non-invasive tool to control the effect of renal denervation [4, 11]. These studies included 58 and 28 patients, respectively. Based on the present work, it seems that even fewer patients are necessary to detect small changes in AD when using conventional 4-chamber cine CMR images. The sample size calculation given in Table 5 shows that, e.g., 25 exams ($n = 19$ plus 25% dropout) per arm are necessary to detect a difference of 0.8 10^{-3} mmHg^{-1} in AD with a power of 90%. This makes our technique especially suitable for retrospective analyses of CMR datasets.

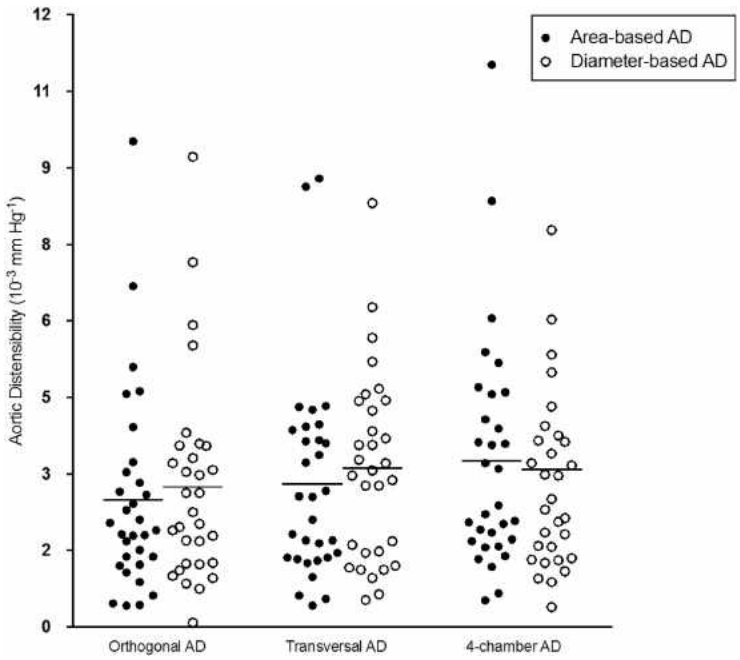

Fig. 4 Distribution of AD values depending on the angulation used at the time of image acquisition. Aortic areas were acquired either by directly contoured aortic areas (black spots) or based on diameter measurements (white spots)

Conclusions

AD measurements using conventional 4-chamber cine imaging are feasible and highly reproducible and reflect the elastic properties of the descending aorta accordingly. This allows an accurate and rapid assessment of arterial compliance and may help to predict changes in the central vasculature at an early stage, eventually preventing evolution toward left ventricular remodeling and dysfunction. Using automated contouring and 3D acquisition of the aorta, future trials could assess AD among different segments to increase accuracy and diagnostic value. In addition, our approach might be even used in a retrospective analysis of studies on already existing CMR data.

Limitations

Among the major limits of our study is the relatively small number of patients included. A larger cohort could enhance the power of our results and outline more subtle differences among different angulations. We used a standard CMR cine sequence; the effect of different temporal and spatial resolutions of SSFP cine sequences on AD measurements has not been evaluated. There is a lack of comparison of our results with other markers of arterial compliance (e.g., PWV) and the absence of centrally measured BP. The invasiveness would, however, have limited the conduct of this study. Another limitation is the use of peripheral PP in our investigation. Central aortic PP would provide a more accurate absolute measure of AD.

Acknowledgements We want to thank our MR technicians for helping with the high-quality CMR examinations. We also thank Anne Wölffel-Gale for editorial assistance.

Author contributions LS and SK wrote the main manuscript text. All authors reviewed the manuscript.

Data availability statement The datasets generated during and analyzed during the current study are available from the corresponding author on reasonable request.

Compliance with ethical standards

Conflict of interest TL received support from the Hospital of Lithuanian University of Health Sciences. TL, SK, VF, and BP received support from the DZHK (German Center for Cardiovascular Research), Partner Site Berlin. SK was supported by Philips Healthcare. CS is an employee of Philips Healthcare. VF reports grants and other support from Abbott, Medtronic, Boston Scientific, and Edwards Lifesciences and other support from Biotronik, Berlin Heart, and Novartis Pharma,

outside of the submitted work. VF is also on the advisory board for Medtronic, Berlin Heart, Novartis Pharma, and Boston Scientific.

References

1. Mitchell GF, Lacourcière Y, Ouellet JP et al (2003) Determinants of elevated pulse pressure in middle-aged and older subjects with uncomplicated systolic hypertension: the role of proximal aortic diameter and the aortic, pressure-flow relationship. Circulation 108:1592–1598. https://doi.org/10.1161/01.CIR.0000093435.04334.1F
2. DiBona GF (2005) Physiology in perspective: the wisdom of the body. Neural control of the kidney. Am J Physiol Regul Integr Comp Physiol 289:R633–R641. https://doi.org/10.1152/ajpregu.00258.2005
3. O'Rourke M (1995) Mechanical principles in arterial disease. Hypertension 26:2–9. https://doi.org/10.1161/01.HYP.26.1.2
4. Stoiber L, Mahfoud F, Zamani SM et al (2018) Renal sympathetic denervation restores aortic distensibility in patients with resistant hypertension: data from a multi-center trial. Clin Res Cardiol 107:642–652. https://doi.org/10.1007/s00392-018-1229-z
5. Forbat SM, Mohiaddin RH, Yang GZ et al (1995) Measurement of regional aortic compliance by MR imaging: a study of reproducibility. J Magn Reson Imaging 5:635–639. https://doi.org/10.1002/jmri.1880050604
6. Shan Y, Lin J, Xu P et al (2012) Comprehensive assessment of aortic compliance and brachial endothelial function using 3.0-T high-resolution MRI: a feasibility study. J Comput Assist Tomogr 36:437–442. https://doi.org/10.1097/RCT.0b013e31825b823e
7. Nelson AJ, Worthley SG, Cameron JD et al (2009) Cardiovascular magnetic resonance-derived aortic distensibility: validation and observed regional differences in the elderly. J Hypertens 27:535–542. https://doi.org/10.1097/HJH.0b013e32831e4599
8. Massmann A, Stemler J, Fries P et al (2017) Automated oscillometric blood pressure and pulse-wave acquisition for evaluation of vascular stiffness in atherosclerosis. Clin Res Cardiol 106:514–524. https://doi.org/10.1007/s00392-017-1080-7
9. Rose JL, Lalande A, Bouchot O et al (2010) Influence of age and sex on aortic distensibility assessed by MRI in healthy subjects. Magn Reson Imaging 28:255–263. https://doi.org/10.1016/j.mri.2009.07.001
10. Redheuil A, Yu WC, Wu CO et al (2010) Reduced ascending aortic strain and distensibility: earliest manifestations of vascular aging in humans. Hypertension 55:319–326. https://doi.org/10.1161/HYPERTENSIONAHA.109.141275
11. Fengler K, Rommel K-P, Blazek S et al (2018) Cardiac magnetic resonance assessment of central and peripheral vascular function in patients undergoing renal sympathetic denervation as predictor for blood pressure response. Clin Res Cardiol. https://doi.org/10.1007/s00392-018-1267-6
12. Hohneck AL, Fries P, Ströder J et al (2019) Effects of heart rate reduction with ivabradine on vascular stiffness and endothelial function in chronic stable coronary artery disease. J Hypertens. https://doi.org/10.1097/hjh.0000000000001984
13. Hohl M, Linz D, Fries P et al (2016) Modulation of the sympathetic nervous system by renal denervation prevents reduction of aortic distensibility in atherosclerosis prone ApoE-deficient rats. J Transl Med. https://doi.org/10.1186/s12967-016-0914-9
14. Reil JC, Hohl M, Reil GH et al (2013) Heart rate reduction by If-inhibition improves vascular stiffness and left ventricular systolic and diastolic function in a mouse model of heart failure with preserved ejection fraction. Eur Heart J 34:2839–2849. https://doi.org/10.1093/eurheartj/ehs218
15. Custodis F, Fries P, Mller A et al (2012) Heart rate reduction by ivabradine improves aortic compliance in apolipoprotein E-deficient mice. J Vasc Res 49:432–440. https://doi.org/10.1159/000339547
16. Resnick LM, Militianu D, Cunnings AJ et al (1997) Direct magnetic resonance determination of aortic distensibility in essential hypertension: relation to age, abdominal visceral fat, and in situ intracellular free magnesium. Hypertension 30:654–659. https://doi.org/10.1161/01.HYP.30.3.654
17. Doltra A, Hartmann A, Stawowy P et al (2016) Effects of renal denervation on renal artery function in humans: preliminary study. PLoS ONE. https://doi.org/10.1371/journal.pone.0150662
18. Lapinskas T, Grune J, Zamani SM et al (2017) Cardiovascular magnetic resonance feature tracking in small animals—a preliminary study on reproducibility and sample size calculation. BMC Med Imaging 17:1. https://doi.org/10.1186/s12880-017-0223-7
19. Grothues F, Smith GC, Moon JCC et al (2002) Comparison of interstudy reproducibility of cardiovascular magnetic resonance with two-dimensional echocardiography in normal subjects and in patients with heart failure or left ventricular hypertrophy. Am J Cardiol 90:29–34
20. Oppo K, Leen E, Angerson WJ et al (1998) Doppler perfusion index: an interobserver and intraobserver reproducibility study. Radiology 208:453–457. https://doi.org/10.1148/radiology.208.2.9680575
21. O'Rourke MF, Nichols WW (2005) Aortic diameter, aortic stiffness, and wave reflection increase with age and isolated systolic hypertension. Hypertension 45:652–658
22. Harloff A, Mirzaee H, Lodemann T et al (2018) Determination of aortic stiffness using 4D flow cardiovascular magnetic resonance—a population-based study. J Cardiovasc Magn Reson. https://doi.org/10.1186/s12968-018-0461-z
23. Ge Y, Wang TJ (2012) Identifying novel biomarkers for cardiovascular disease risk prediction. J Intern Med 272:430–439
24. Hendel RC, Kramer CM, Patel MR et al (2006) ACCF/ACR/SCCT/SCMR/ASNC/NASCI/SCAI/SIR 2006 appropriateness criteria for cardiac computed tomography and cardiac magnetic resonance imaging. J Am Coll Cardiol 48:1475–1497. https://doi.org/10.1016/j.echo.2007.06.011
25. Morton G, Schuster A, Jogiya R et al (2012) Inter-study reproducibility of cardiovascular magnetic resonance myocardial feature tracking. J Cardiovasc Magn Reson. https://doi.org/10.1186/1532-429X-14-43
26. MacEira AM, Mohiaddin RH (2012) Cardiovascular magnetic resonance in systemic hypertension. J. Cardiovasc. Magn, Reson, p 14

Affiliations

Lukas Stoiber[1,2] · Niky Ghorbani[3] · Marcus Kelm[3,6] · Titus Kuehne[3,6] · Nina Rank[1,2] · Tomas Lapinskas[1,4,6] · Christian Stehning[7] · Burkert Pieske[1,5,6] · Volkmar Falk[2,6] · Rolf Gebker[1] · Sebastian Kelle[1,5,6]

✉ Lukas Stoiber
stoiber@dhzb.de

[1] Department of Internal Medicine/Cardiology, German Heart Center Berlin, Berlin, Germany

[2] Department of Cardiothoracic and Vascular Surgery, German Heart Center Berlin, Berlin, Germany

[3] Department of Congenital Heart Disease/Pediatric Cardiology, German Heart Center Berlin, Berlin, Germany

[4] Department of Cardiology, Medical Academy, Lithuanian University of Health Sciences, Kaunas, Lithuania

[5] Department of Internal Medicine and Cardiology, Charité-Universitätsmedizin Berlin, Berlin, Germany

[6] DZHK (German Centre for Cardiovascular Research), Partner Site, Berlin, Germany

[7] Philips Health Care, Hamburg, Germany

Publikation 2

Ghorbani N, Muthurangu V, Khushnood A, Goubergrits L, Nordmeyer S, Fernandes JF, Lee CB, Runte K, Roth S, Schubert S, Kelle S, Berger F, Kuehne T, Kelm M. Impact of valve morphology, hypertension and age on aortic wall properties in patients with coarctation: a two-centre cross-sectional study. BMJ Open. 2020;10(3):e034853.

DOI: 10.1136/bmjopen-2019-034853

BMJ Open

Impact of valve morphology, hypertension and age on aortic wall properties in patients with coarctation: a two-centre cross-sectional study

Niky Ghorbani,[1,2] Vivek Muthurangu,[3] Abbas Khushnood,[3] Leonid Goubergrits,[1,2] Sarah Nordmeyer,[1,2] Joao Filipe Fernandes,[1] Chong-Bin Lee,[1,4] Kilian Runte,[1] Sophie Roth,[1] Stephan Schubert,[2,5] Sebastian Kelle,[4,5] Felix Berger,[2,5] Titus Kuehne,[1,2,5] Marcus Kelm [1,2,6]

To cite: Ghorbani N, Muthurangu V, Khushnood A, *et al*. Impact of valve morphology, hypertension and age on aortic wall properties in patients with coarctation: a two-centre cross-sectional study. *BMJ Open* 2020;**10**:e034853. doi:10.1136/bmjopen-2019-034853

► Prepublication history for this paper is available online. To view these files, please visit the journal online (http://dx.doi.org/10.1136/bmjopen-2019-034853).

Received 18 November 2019
Revised 13 February 2020
Accepted 04 March 2020

For numbered affiliations see end of article.

Correspondence to
Dr Marcus Kelm;
mkelm@dhzb.de

ABSTRACT

Objective We aimed to investigate the combined effects of arterial hypertension, bicuspid aortic valve disease (BAVD) and age on the distensibility of the ascending and descending aortas in patients with aortic coarctation.

Design Cross-sectional study.

Setting The study was conducted at two university medical centres, located in Berlin and London.

Participants A total of 121 patients with aortic coarctation (ages 1–71 years) underwent cardiac MRI, echocardiography and blood pressure measurements.

Outcome measures Cross-sectional diameters of the ascending and descending aortas were assessed to compute aortic area distensibility. Findings were compared with age-specific reference values. The study complied with the Strengthening the Reporting of Observational Studies in Epidemiology statement and reporting guidelines.

Results Impaired distensibility (below fifth percentile) was seen in 37% of all patients with coarctation in the ascending aorta and in 43% in the descending aorta. BAVD (43%) and arterial hypertension (72%) were present across all ages. In patients >10 years distensibility impairment of the ascending aorta was predominantly associated with BAVD (OR 3.1, 95% CI 1.33 to 7.22, p=0.009). Distensibility impairment of the descending aorta was predominantly associated with arterial hypertension (OR 2.8, 95% CI 1.08 to 7.2, p=0.033) and was most pronounced in patients with uncontrolled hypertension despite antihypertensive treatment.

Conclusion From early adolescence on, both arterial hypertension and BAVD have a major impact on aortic distensibility. Their specific effects differ in strength and localisation (descending vs ascending aorta). Moreover, adequate blood pressure control is associated with improved distensibility. These findings could contribute to the understanding of cardiovascular complications and the management of patients with aortic coarctation.

Strengths and limitations of this study

- The two-centre study investigates the combined impact of arterial hypertension, bicuspid aortic valve disease and age on the presence, location and severity of aortic distensibility impairment in patients with aortic coarctation.
- The study further characterises the effects of antihypertensive treatment and adequate blood pressure control on aortic distensibility.
- Using observational cross-sectional data precludes the authors from directly inferring causal relationships and individual longitudinal courses of distensibility alterations.

INTRODUCTION

Aortic coarctation (CoA) accounts for 5%–10% of all congenital heart defects.[1] Despite progress made in early treatment concepts, morbidity and mortality remain high.[2] Arterial hypertension (HTN) persists in more than 65% of all patients despite successful repair,[1 3] commonly leading to cardiovascular and cerebrovascular complications and subsequently impaired long-term outcome.[2 3] In up to 75% of cases[4] CoA occurs in combination with bicuspid aortic valve disease (BAVD), which is also associated with vascular complications such as dilation of the aorta.

HTN, BAVD and age are each known to affect the distensibility of the aorta and thus on its Windkessel function that usually enables partial storage of left ventricular stroke volume during systole and the maintenance of continuous organ perfusion during diastole. Persisting HTN has been demonstrated to be associated with impaired elastic capacity of the aorta[5] and thus an increased afterload that can contribute to relevant cardiovascular remodelling processes. In addition to HTN, the elasticity of the ascending aorta is frequently impaired in BAVD, as wall stresses[6] are typically elevated and elastic fibre content

of the medial layer decreases[7] in the presence of permanent non-laminar flow profiles. Furthermore, ageing has been shown to contribute to a loss of vascular elasticity throughout life.[8]

Although HTN, BAVD and age have each been associated with impaired elasticity, little is known about their combined impact. The specific impact of each risk factor on the impairment of vascular properties and the effects of antihypertensive treatment can be of clinical relevance. We therefore aimed to investigate the combined effects of HTN (with and without antihypertensive treatment), BAVD and age on the presence, location and severity of aortic distensibility impairment in patients with CoA using a non-invasive MRI-based approach.

METHODS

Study design, population and patient involvement

This observational study was carried out at two centres, located in Berlin, German Heart Centre Berlin (n=84) and London, University College London (n=37). The study population consisted of 121 consecutive outpatients with known CoA between January 2014 and December 2016. Key inclusion criteria for the MRI study were (1) a confirmed diagnosis of CoA with (2) an indication for diagnostic evaluation according to European Society of Cardiology (ESC)[9] and American College of Cardiology/American Heart Association (ACC/AHA) guidelines[10] due to (2A) echocardiography or blood pressure measurements indicating pressure gradients across the stenosis exceeding 20 mm Hg or (2B) severe narrowing and/or (2C) HTN that were (3) without relevant contraindications for MRI and were (4) without any additional complex congenital cardiovascular malformations. As this was a non-invasive study, MRI was also performed in patients with unclear treatment indications, where ESC and/or ACC/AHA guideline indications where suspected. The study complied with the Strengthening the Reporting of Observational Studies in Epidemiology statement.

In this study, all patients underwent echocardiography and cardiac MRI in conjunction with blood pressure measurements of the upper extremities. MRI-based approaches have recently been demonstrated to be feasible and reliable measures for non-invasive assessment of aortic compliance and the resulting distensibility in patients with CoA.[11 12] Patients were considered hypertensive (HTN group) where the diagnosis of HTN was made according to clinical guidelines[13 14] and with consideration of paediatric percentiles where appropriate.[14] For all computations, blood pressures at the time of MRI examination in comfortably placed patients with back support for at least 5 min were used. Baseline characteristics are shown in table 1.

The diagnosis of BAVD was made based on cine MRI data, acquired orthogonally to the native valve plane. Calculated aortic area distensibility was compared with percentiles of healthy individuals published by Voges *et al*.[15] Distensibility impairment was defined as patients with measurements below the fifth percentile.

Patient and public involvement

We did not directly include patient and public involvement in this study, but the research design has been motivated by direct interactions and regular discussions with our patients. We are also sharing study results with participants and provide a plain-language summary for patients and patient and public involvement representatives on request.

Image acquisition

Data were acquired on 1.5 T clinical MR systems (including Achieva; Philips Healthcare, Best, The Netherlands; and Avanto, Siemens, Erlangen, Germany). The cardiac MRI protocol included standard balanced fast field echo cine imaging with at least two slices covering the ascending and descending aortas to assess diameter changes for each vessel. The imaging planes were positioned perpendicular to the vessel at the level of the pulmonary artery bifurcation. In case of imaging artefacts due to previous stenting, the plane covering the descending aorta was placed more distally, yet remained above the level of the diaphragm. Typical imaging parameters were: voxel size 1.80×1.70×6 mm, reconstructed voxel size 1×1×6 mm, echo time=1.2 ms, repetition time=2.5 ms, flip angle 60°, retrospective cardiac gating, 40 automatically reconstructed cardiac phases. Scan duration in total was 9–14 min.

Image postprocessing and analysis

MRI cine images were analysed manually using View Forum (Philips Medical Systems Nederland; View Forum R6.3V1L7 SP1). Analysis was carried on-site for the respective patient group. The slices to be examined were manually selected at the level of pulmonary artery bifurcation (figure 1). Cross-sectional diameters of the ascending and descending aortas were measured during the end-systolic and end-diastolic heart phase, during the maximal and minimal expansion of the vessel. For each localisation, three slices nearby the point of maximal/minimal visual vessel extension were selected. For each measurement, three diameters were measured and the average was calculated. Diameters were chosen at the shortest distance and were subsequently converted to cross-sectional areas in order to minimise minor angulation errors. The arterial compliance is defined as the change in arterial blood volume (ΔV) relative to a given change in the arterial blood pressure (ΔP): C=ΔV/ΔP. Clinically, an alternative version of arterial compliance is used in which the cross-sectional area (A) of the aorta replaces the vessel volume. Aortic area compliance in this paper is defined as the change in the cross-sectional area of the aorta per unit of change in pulse pressure (PP):

$$C_{area} = \frac{A_{max} - A_{min}}{PP_{aorta}}$$

To achieve comparability within the study population, cross-sectional aortic area compliance was converted to

Table 1 Patient characteristics; median and lower and upper quantiles (Q1;Q3) and n (%)

	Total study group (n=121)	Non-HTN group (n=34)	HTN group (n=87)	P value
Characteristics				
Age (years)	22 (15;31)	22 (16;30)	23 (15;31)	0.760
Male (n, %)	80 (66)	22 (65)	58 (67)	0.838
Weight (kg)	66.2 (51;78)	59.25 (50.2;74)	68 (51;80)	0.183
Height (cm)	169 (153;177.5)	167 (152.6;178)	170 (153;177.5)	0.674
BMI (kg/m²)	22.3 (19.36;25.16)	21.24 (19.36;23.72)	22.64 (19.1;25.3)	0.324
BSA (m²)	1.74 (1.5;1.95)	1.66 (1.47;1.93)	1.8 (1.47;1.97)	0.190
Bicuspid aortic valve (n, %)	52/121 (43)	15/34 (44)	37/87 (43)	0.874
Previous episodes of HTN and/or exercise HTN (n, %)	98/121 (81)	11/34 (32)	87/87 (100)	0.002
Systolic BP (mm Hg)	136 (122;148)	116 (110;122)	142 (134;152)	<0.001
Diastolic BP (mm Hg)	69 (62;77)	66.5 (58;75)	72 (63;80)	0.006
Echocardiographic pressure drop across stenosis (mm Hg)	25 (13;41)	25 (13;35)	25 (14;45)	0.289
Patients with echocardiographic pressure drop above 20 mm Hg (n, %)	81 (67)	23 (68)	58 (67)	0.918
Previous treatment				
Balloon angioplasty (n, %)	45/121 (37)	9/34 (26)	36/87 (41)	0.129
Stenting (n, %)	23/121 (19)	4/34 (12)	19/87 (22)	0.206
Surgical reconstruction (n, %)	73/121 (60)	23/34 (68)	50/87 (57)	0.306
Antihypertensive medication (n, %)	37/121 (31)	11/34 (32)	26/87 (30)	0.791
Type of medication				
Beta blockers (n, %)	23/121 (19)	7/34 (21)	16/87 (18)	0.783
ACE inhibitors (n, %)	22/121 (18)	7/34 (21)	15/87 (17)	0.669
Calcium channel blockers (n, %)	11/121 (9)	1/34 (3)	10/87 (11)	0.143
Angiotensin receptor blockers (n, %)	4/121 (3)	1/34 (3)	3/87 (3)	0.889
Diuretics (n, %)	7/121 (6)	3/34 (9)	4/87 (5)	0.373
Diameter of the aorta				
Ascending aorta, minimum (mm)	25 (19.9;30)	26.05 (19.2;30)	24.2 (20;30.3)	0.802
Ascending aorta, maximum (mm)	29.09 (24;33.1)	29.45 (24;32.7)	28.4 (23.8;33.8)	0.762
Descending aorta, minimum (mm)	17.9 (14.7;20.9)	16.84 (13.8;20.3)	17.9 (15;21)	0.378
Descending aorta, maximum (mm)	20 (16.2;23.3)	19.25 (15.8;23)	20.1 (16.2;23.4)	0.500

Pressure drop across the stenosis: maximal pressure in mm Hg across the coarctated segment measured by echocardiography; ascending and descending aortas (minimum) describing end-diastolic cross-sectional diameter; ascending and descending aortas (maximum) describing end-systolic cross-sectional diameter.
Continuous data are expressed as median and IQR (Q1;Q3), p values are from Wilcoxon-Mann-Whitney test. Categorical data are presented as frequencies and percentage (%), p values are from Pearson's χ^2 test.
BMI, body mass index; BP, blood pressure; BSA, body surface area; HTN, hypertension.

area distensibility (D_{area}), defined as the relative change in the cross-sectional area of the aorta.

$$D_{area}\left(\frac{1}{mmHg\times 10^3}\right) = \frac{A_{max}-A_{min}}{A_{min}} \times \frac{1}{PP}$$

A_{max} represents the systolic cross-sectional area and A_{min} the diastolic area. PP is defined as the difference between systolic and diastolic pressure ($P_{systolic}$–$P_{diastolic}$). Previous studies have demonstrated[12] that a non-invasive sphygmomanometer-based blood pressure measurement on the left arm can be expected to be higher than aortic PP. Hence, we used a linear model for generating the aortic PP with given values such as mean arterial pressure (MAP) $\left(MAP = \frac{2}{3}xP_{diastolic} + \frac{1}{3}xP_{systolic}\right)$ and PP measured by cuff on the left arm (PP_{LA}), as described in Kelm *et al*[12]:

$$PP_{aorta} = PP_{LA}x\left(0.3133xMAP_{LA} + 28.366\right) / \left(MAP_{LA} - 22\right)$$

The linear model is only valid on the condition that the aortic PP is less than or equal to peripheral PP.

Statistical analysis

Continuous data are expressed as median and IQR (Q1;Q3) unless stated otherwise. Categorical data are

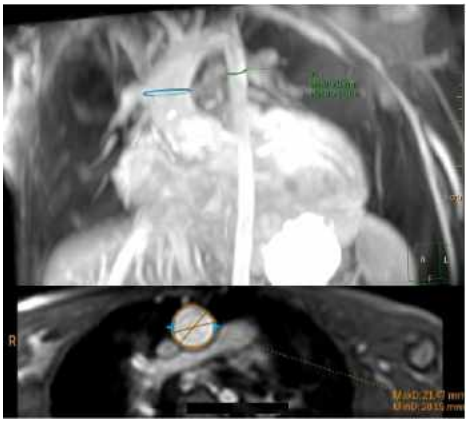

Figure 1 Locations of cross-sectional diameter measurements of the ascending and descending aortas, measured during the end-systolic and end-diastolic heart phase

presented as frequencies and percentages (%). Data distribution was tested using Shapiro-Wilk and Shapiro-Francia tests. Wilcoxon-Mann-Whitney test was used to assess continuous data for differences between groups (HTN vs non-HTN). Pearson's χ^2 test was used in conjunction with Fisher's exact test to compare categorical variables between groups. Non-parametric regression was performed to assess multifactorial effects on the distensibility of the aorta. Multifactorial influences leading to distensibility impairment were assessed using logistic regression. Predictive margins were calculated and plotted to visualise the combined effects of BAVD, HTN, medication and age. Stata V.15.1 was used for statistical analysis. P values <0.05 were considered statistically significant.

RESULTS

A two-centre cohort of patients with CoA was included in the analysis, in which the patient populations did not significantly differ between the participating centres. Seventy-two per cent (87/121) of patients were hypertensive at the time of examination. BAVD was found in 43% (52/121) of subjects. Patient characteristics of the study population divided into the two groups (HTN group and non-HTN group) are shown in table 1. There were no significant differences between the two groups regarding patients' characteristics or previous treatment. Median echocardiographic pressure gradients and the number of patients with a pressure drop above 20 mm Hg did not differ between groups.

In patients above the age of 10 years, aortic distensibility of the ascending and descending aortas decreased with age (figure 2). While no significant differences in distensibility of the ascending aorta were found between normotensive patients and patients with HTN (figure 2A), a multifactorial model revealed that patients with HTN and CoA above the age of 10 years showed significantly lower distensibility of the descending aorta compared with normotensive subjects in their age groups (figure 2B). In patients with CoA and coexisting BAVD older than 10 years of age, distensibility of the ascending aorta was significantly lower than patients with tricuspid aortic valve (figure 2C), while BAVD showed no impact on the distensibility of the descending aorta (figure 2D). These effects were not found in patients below the age of 10 years.

Of the total cohort, 37 patients were under antihypertensive medication. From these patients, 19 were on monotherapy and 18 were on dual or triple therapy. Compared with normotensive patients without antihypertensive medication, the estimated distensibility of the descending aorta was (1) significantly lower in normotensive patients, who were under antihypertensive treatment at the time of examination (estimated effect: -1.32×10^{-3} mm Hg^{-1}, p=0.031). Furthermore (2), in patients with HTN without antihypertensive medication even further reduced distensibility of the descending aorta (estimated effect: -2.43×10^{-3} mm Hg^{-1}, p=0.020) was found, and (3) was lowest in patients with HTN and CoA under antihypertensive medication, that is, patients with uncontrolled HTN despite therapy (estimated effect: -3.40×10^{-3} mm Hg^{-1}, p=0.022). There were no drug-specific effects on distensibility of the ascending or descending aorta. The effects are illustrated in figure 3. No significant differences were found between previous surgical or interventional treatment.

In comparison to reference data from healthy individuals,[15] distensibility impairment below the fifth percentile was found in the ascending aorta in 37.2% and in the descending aorta in 43.0% of all patients with CoA. Patients with CoA with a combination of BAVD and HTN had impaired distensibility of the ascending aorta in 49.6% and distensibility impairment of the descending aorta in 51.4%. In normotensive patients with CoA and physiological tricuspid valve, impaired distensibility was present in just 21.1% in the ascending aorta and 26.3% in the descending aorta.

In patients below 10 years of age, no associations were found between BAVD and impaired distensibility in the ascending (p=0.519) or the descending (p=0.889) aorta. Also, HTN and impaired distensibility showed no significant correlation, either in the ascending (p=0.635) or in the descending (p=0.207) aorta. In patients above the age of 10 years, distensibility impairment of the ascending aorta was more common in BAVD (OR 3.1, 95% CI 1.33 to 7.22, p=0.009). In these patients with BAVD, impaired distensibility of the ascending aorta was seen in 51.1%, compared with 26.9% in patients with a tricuspid valve. Associations between BAVD and impaired distensibility of the ascending aorta further increased with age, whereas no such associations were found in the descending aorta. Patients with HTN above the age of 10 years showed no association with distensibility impairment in the ascending

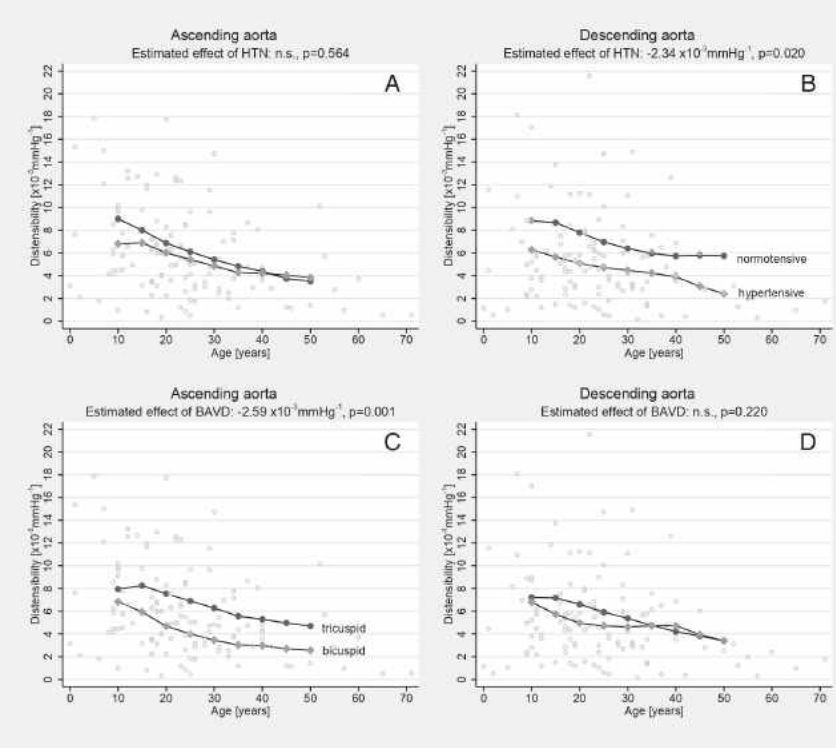

Figure 2 Aortic distensibility of the ascending aorta (left) and descending aorta (right) in patients with or without accompanying HTN or BAVD, plotted against age. It includes the effects of (A) HTN on the ascending aorta, (B) HTN on the descending aorta, (C) BAVD on the ascending aorta and (D) BAVD on the descending aorta; BAVD, bicuspid aortic valve disease; HTN, hypertension.

aorta (p=0.239), whereas distensibility impairment of the descending aorta was correlated with HTN (OR 2.8, 95% CI 1.08 to 7.2, p=0.033). Distensibility impairment of the descending aorta below the fifth percentile was seen in 49.3% of all patients with HTN >10 years, compared with 26.7% in normotensive patients.

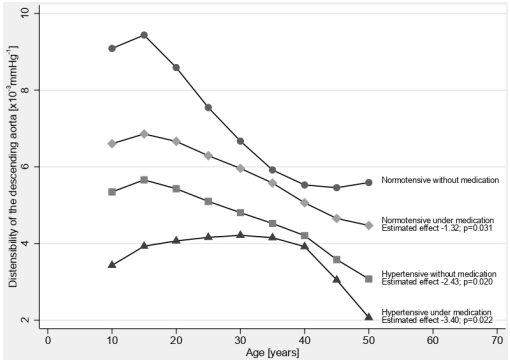

Figure 3 Estimated effects of antihypertensive medication on the distensibility of the descending aorta, compared with normotensive patients without medication (reference).

The combined impact of BAVD and HTN on distensibility impairment below the fifth percentile in patients with CoA aged 10–50 years is shown in figure 4. In patients with HTN, 95% CIs of the estimated risk for distensibility impairment of the descending aorta did not overlap from the age of 30 years onwards. In patients with BAVD, the same effects were observed for the ascending aorta in patients above 30 years.

Significant differences in cross-sectional diameters of the ascending aorta between patients with BAVD and patients with tricuspid valve and CoA were observed. Compared with patients with tricuspid aortic valve, those with BAVD had significantly larger end-diastolic and end-systolic diameters of the ascending aorta: minimum 22.6 (18.9;28.5) mm in tricuspid valve morphology vs 28 (22.3;36.1) mm in BAVD, p<0.001; maximum 27 (21.9;31) mm vs 30.7 (24.9;38.7) mm in BAVD, p=0.002.

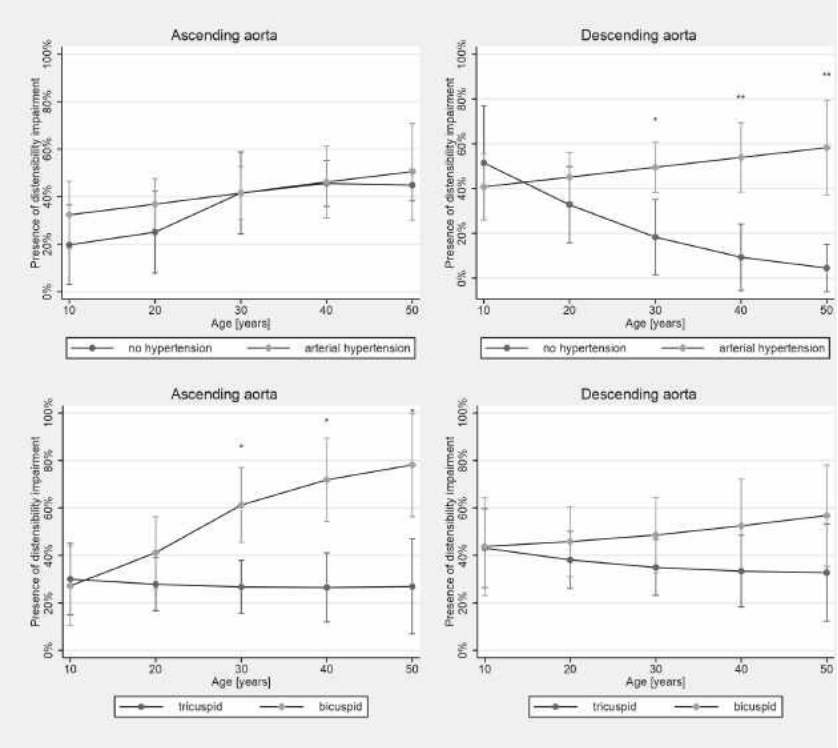

Figure 4 Marginal effects and 95% CIs for impaired aortic distensibility (below the fifth percentile) of the ascending and descending aortas, in patients with or without hypertension (HTN) or bicuspid aortic valve disease (BAVD), plotted against age (*p<0.05; **p<0.01).

DISCUSSION

In our cohort, aortic distensibility was impaired in almost half of all patients with CoA. In those above the age of 10 years, BAVD had a significant effect on distensibility impairment of the ascending aorta, whereas HTN predominantly affected the descending aorta. Additionally, antihypertensive treatment was associated with improved distensibility. However, when compared with normotensive patients without medical treatment, normotensive patients under antihypertensive medication had significantly lower distensibility across all ages. Distensibility was even lower in untreated patients with HTN, and lowest in those with uncontrolled HTN despite antihypertensive therapy.

Increased aortic stiffness (impairment of the Windkessel capacity) is considered as a marker for vascular disease and cardiovascular outcome.[16] An example can demonstrate the immediate impact of reduced distensibility on Windkessel capacity: in a 30-year-old male patient with physiological (50th percentile) distensibility of the ascending (7.5×10^{-3} mm Hg^{-1}) and descending (5.5×10^{-3} mm Hg^{-1}) aortas, the expected overall Windkessel volume of the thoracic aorta is 33.2 mL. With impaired distensibility (below the fifth percentile), the Windkessel volume of the thoracic aorta would decrease by approximately one-third to 22.2 mL (−33.13%). This can induce various severe consequences for blood circulation in the cardiovascular system, such as increases in systolic blood pressure and cardiac afterload, diminished diastolic function[17] and coronary blood flow,[18] and left ventricular hypertrophy.[17] High systolic pressure was found to directly result in fractures of the elastic laminae and an increase in collagen fibres, further accelerating the loss of arterial elasticity, ultimately leading to vascular dysfunction, heart failure and cardiovascular events.[19]

Distensibility impairment in our cohort was most clearly observed in patients above the age of 10 years. This supports a concept of aortic distensibility in which the duration a patient is exposed to risk factors can be crucial for the development of distensibility impairment and thus for the likelihood of subsequent cardiovascular events. In line with these findings, increased wall stiffening in patients with CoA and prolonged exposure to abnormal haemodynamics was recently suggested.[20] However, despite early surgical repair, the distensibility

of the aorta can remain impaired in CoA, as has been observed in patients with tetralogy of Fallot.[21 22]

A previous study showed that the development of postoperative systemic HTN depends on the duration of preoperative HTN in CoA[23] and suggested that the extent of decrease in aortic distensibility is related to the patients' age at surgery.[24] Possible concepts of the underlying pathophysiology include an ongoing remodelling process of the pressure-sensitive baroreceptors located in the aortic arch, which adapt to the limited contractility of the vessel wall and higher pressure states over time.[25] Preoperative HTN and a lack of normalisation due to, for example, inadequate antihypertensive treatment after surgical repair may be important causes of subsequent loss of aortic elasticity and thus cardiovascular complications in patients with CoA. In accordance with these concepts, our data show the most impaired distensibility values among patients with uncontrolled HTN despite antihypertensive therapy, whereas well-adjusted blood pressures at the time of the study were associated with improved aortic distensibility of the descending aorta. There is a lack of longitudinal studies regarding the reversibility of distensibility impairment under antihypertensive medication in patients with CoA. However, it has been shown that adequate HTN control may also prevent HTN-related complications,[13] such as coronary artery disease, sudden cardiac death, heart failure and cerebrovascular accidents.[3]

Patients with BAVD are known to be affected by severe alterations in flow profiles[26] and degenerative changes in the tunica media of the ascending aorta, which also influence the elasticity of the aorta.[7 27] Previous studies have shown increased regional wall shear stress in the ascending aorta of patients with BAVD to correspond with extracellular matrix dysregulation and elastic fibre degeneration.[6] The bicuspid valve may further contribute by speeding up the progression of aortic wall complications such as aortic dilatation,[27] aneurysm, rupture and dissection.[28] Dilated and aneurysmatic areas in BAVD were previously reported to show reduced aortic elasticity.[29]

Our results confirm significantly impaired distensibility of the ascending aorta in patients with CoA and BAVD where aortic dilation was present, starting in childhood. The high prevalence of BAVD and its association with dilatation may superimpose the effects of HTN on the distensibility impairment of the ascending aorta. However, in patients with tricuspid valves, effects of HTN were equally limited to the descending aorta. The high risk for distensibility impairment of the ascending aorta suggests that the presence and severity of BAVD and associated turbulent flow may be important contributors to vascular pathology.

Several techniques have been introduced to assess vascular properties, including invasive intravascular ultrasound,[30] CT angiography,[31] echocardiography, pulse wave velocity (PWV) and MRI.[32] While peripheral PWV measures can be non-invasive and easily applied, they are unsuitable in patients with vascular stenosis, as the narrowing can be a relevant source of error due to abnormal wave reflections.[12] In contrast to PWV as a current reference standard for assessing arterial stiffness,[32] the area distensibility used in this study allows localised quantification of elastic capacity,[33] regardless of the presence of a stenosis. Although the calculation of the area compliance is a relatively new method, its reliability has been previously demonstrated in CoA.[12]

Limitations

The calculation of area distensibility depends on manual postprocessing of cardiac imaging data, and therefore individual experience as well as training can be essential for precise measurements. To ensure comparability and consistency of aortic compliance and distensibility measurements, the interobserver variability has been assessed.[34] To reduce the risk of overestimating vessel diameters, angulation errors were reduced using minimal cross-sectional diameters of the vessel. Furthermore, central blood pressure estimations are required for distensibility calculation and were not directly assessed by invasive heart catheterisation. To allow a non-invasive assessment, we used a previously described cuff pressure-based model for central PP estimation[33] that has been tested in patients with CoA.[12] All blood pressure measurements were simultaneously obtained to MRI measurements.

The cross-sectional study was not designed to identify a specific age cut-off. The age of 10 years (from which significant associations were found within our model) is only descriptive for our study cohort. Longitudinal studies and larger cohorts are required to assess to which extent these mechanisms apply in principle and why they are more pronounced in adolescents and adults. Moreover, the study was not intended to assess subgroups of heterogeneous previous interventional or surgical techniques.

The comparison of aortic distensibility in CoA with healthy individuals was based on published percentiles by Voges *et al*. The comparability was ensured by considering the used methods, including sequence parameters as well as data analysis workflow. Published percentiles covered age ranges from 2 to 30 years. As our cohort included older patients, percentile graphs were extrapolated for older patients.

CONCLUSION

From early adolescence on, BAVD and HTN were both associated with an impairment of aortic distensibility in patients with CoA. Their specific effects differ in strength and localisation: BAVD had its main effect on the distensibility of the ascending aorta, whereas HTN affected the distensibility of the descending aorta. Whether antihypertensive medication is capable of preventing the onset or reversing existing distensibility impairment remains unclear. However, adequate blood pressure control was associated with improved distensibility. Therefore, antihypertensive treatment and the early non-invasive detection of alterations may be pertinent strategies for the

prevention and reduction of distensibility impairment of the aorta.

Author affiliations
[1]Charité–Universitätsmedizin, Institute for Computational and Imaging Science in Cardiovascular Medicine, Berlin, Germany
[2]Department of Congenital Heart Disease, Deutsches Herzzentrum Berlin, Berlin, Germany
[3]Centre for Cardiovascular Imaging, UCL Institute of Cardiovascular Science, London, UK
[4]Department of Internal Medicine/Cardiology, Deutsches Herzzentrum, Berlin, Germany
[5]DZHK (German Centre for Cardiovascular Research), Partner Site Berlin, Germany
[6]BIH (Berlin Institute of Health), Berlin, Germany

Acknowledgements We thank Anne Gale for editorial assistance and Alireza Khasheei for his technical support. MK is a participant in the Charité Digital Clinician Scientist Program funded by DFG.

Contributors TK, VM and MK were responsible for conception and design of the study. MK and AK contributed to subject recruitment. MK and NG acquired imaging data. NG and LG established the measurement method. NG contributed to data acquisition and analysed and interpreted the data. MK and NG conducted the statistical analysis. NG drafted the manuscript. MK and TK critically revised and reviewed the manuscript. SN, JFF, CBL, KR, SR, SS, SK and FB provided feedback on drafts, read and approved the final manuscript. NG wrote the final draft. All authors approved the final manuscript and agree to be accountable for all aspects of the work.

Funding This study was funded by the European Commission under the ICT Program (grant agreement: 611232). LG and MK have received funding in a project supported by the German Research Foundation (DFG, grant 223533535, Berlin, Germany). MK is a participant in the Charité Digital Clinician Scientist Program funded by DFG.

Competing interests None declared.

Patient and public involvement Patients and/or the public were not involved in the design, or conduct, or reporting, or dissemination plans of this research.

Patient consent for publication Not required.

Ethics approval All procedures performed in this study involving human participants were in accordance with the ethical standards of the institutional and national research committee and with the 1964 Helsinki declaration and its later amendments. This study was approved by the local ethics committees (Ethikkommission–Charité–Universitätsmedizin Berlin: EA2/172/13 and National Research Ethics Service Committee London: 15HC23). Written informed consent was obtained from all individual participants and/or their guardians included in the study.

Provenance and peer review Not commissioned; externally peer reviewed.

Data availability statement Data are available upon reasonable request. Please contact the corresponding author to discuss requests for availability of deidentified participant data.

ORCID iD
Marcus Kelm http://orcid.org/0000-0003-4971-0452

REFERENCES

1 Canniffe C, Ou P, Walsh K, *et al*. Hypertension after repair of aortic coarctation--a systematic review. *Int J Cardiol* 2013;167:2456–61.
2 Toro-Salazar OH, Steinberger J, Thomas W, *et al*. Long-Term follow-up of patients after coarctation of the aorta repair. *Am J Cardiol* 2002;89:541–7.
3 Lee MGY, Allen SL, Kawasaki R, *et al*. High prevalence of hypertension and end-organ damage late after coarctation repair in normal Arches. *Ann Thorac Surg* 2015;100:647–53.
4 Tanous D, Benson LN, Horlick EM. Coarctation of the aorta: evaluation and management. *Curr Opin Cardiol* 2009;24:509–15.
5 Safar ME, Levy BI, Struijker-Boudier H. Current perspectives on arterial stiffness and pulse pressure in hypertension and cardiovascular diseases. *Circulation* 2003;107:2864–9.
6 Guzzardi DG, Barker AJ, van Ooij P, *et al*. Valve-Related hemodynamics mediate human bicuspid Aortopathy: insights from wall shear stress mapping. *J Am Coll Cardiol* 2015;66:892–900.
7 Fedak PWM, Verma S, David TE, *et al*. Clinical and pathophysiological implications of a bicuspid aortic valve. *Circulation* 2002;106:900–4.
8 Rose J-L, Lalande A, Bouchot O, *et al*. Influence of age and sex on aortic distensibility assessed by MRI in healthy subjects. *Magn Reson Imaging* 2010;28:255–63.
9 Baumgartner H, Bonhoeffer P, De Groot NMS, *et al*. Esc guidelines for the management of grown-up congenital heart disease (new version 2010). *Eur Heart J* 2010;31:2915–57.
10 Warnes CA, Williams RG, Bashore TM, *et al*. ACC/AHA 2008 guidelines for the management of adults with congenital heart disease: a report of the American College of Cardiology/American heart association Task force on practice guidelines (writing Committee to develop guidelines on the management of adults with congenital heart disease). *Circulation* 2008;118:e714–833.
11 Schäfer M, Morgan GJ, Mitchell MB, *et al*. Impact of different coarctation therapies on aortic stiffness: phase-contrast MRI study. *Int J Cardiovasc Imaging* 2018;34:1459–69.
12 Kelm M, Goubergrits L, Fernandes JF, *et al*. Mri as a tool for non-invasive vascular profiling: a pilot study in patients with aortic coarctation. *Expert Rev Med Devices* 2016;13:103–12.
13 Mancia G, Fagard R, Narkiewicz K, *et al*. ESH/ESC guidelines for the management of arterial hypertension: the task force for the management of arterial hypertension of the European Society of hypertension (ESH) and of the European Society of cardiology (ESC). *J Hypertens* 2013;2013:1281–357.
14 Flynn JT, Kaelber DC, Baker-Smith CM, *et al*. Clinical practice guideline for screening and management of high blood pressure in children and adolescents. *Pediatrics* 2017;140:e20171904.
15 Voges I, Jerosch-Herold M, Hedderich J, *et al*. Normal values of aortic dimensions, distensibility, and pulse wave velocity in children and young adults: a cross-sectional study. *J Cardiovasc Magn Reson* 2012;14:77.
16 Maldonado J, Pereira T, Polónia J, *et al*. Arterial stiffness predicts cardiovascular outcome in a low-to-moderate cardiovascular risk population: the EDIVA (Estudo de DIstensibilidade vascular) project. *J Hypertens* 2011;29:669–75.
17 Eren M, Gorgulu S, Uslu N, *et al*. Relation between aortic stiffness and left ventricular diastolic function in patients with hypertension, diabetes, or both. *Heart* 2004;90:37–43.
18 Leung MCH, Meredith IT, Cameron JD. Aortic stiffness affects the coronary blood flow response to percutaneous coronary intervention. *Am J Physiol Heart Circ Physiol* 2006;290:H624–30.
19 Sun Z, Aging SZ. Aging, arterial stiffness, and hypertension. *Hypertension* 2015;65:252–6.
20 Juffermans JF, Nederend I, van den Boogaard PJ, *et al*. The effects of age at correction of aortic coarctation and recurrent obstruction on adolescent patients: MRI evaluation of wall shear stress and pulse wave velocity. *Eur Radiol Exp* 2019;3:24.
21 Schäfer M, Browne LP, Morgan GJ, *et al*. Reduced proximal aortic compliance and elevated wall shear stress after early repair of tetralogy of Fallot. *J Thorac Cardiovasc Surg* 2018;156:2239–49.
22 Voges I, Kees J, Jerosch-Herold M, *et al*. Aortic stiffening and its impact on left atrial volumes and function in patients after successful coarctation repair: a multiparametric cardiovascular magnetic resonance study. *J Cardiovasc Magn Reson* 2016;18:56.
23 de Divitiis M, Pilla C, Kattenhorn M, *et al*. Vascular dysfunction after repair of coarctation of the aorta: impact of early surgery. *Circulation* 2001;104:I165–70.
24 Brili S, Dernellis J, Aggeli C, *et al*. Aortic elastic properties in patients with repaired coarctation of aorta. *Am J Cardiol* 1998;82:1140–3.
25 Kenny D, Polson JW, Martin RP, *et al*. Relationship of aortic pulse wave velocity and baroreceptor reflex sensitivity to blood pressure control in patients with repaired coarctation of the aorta. *Am Heart J* 2011;162:398–404.
26 Mahadevia R, Barker AJ, Schnell S, *et al*. Bicuspid aortic cusp fusion morphology alters aortic three-dimensional outflow patterns, wall shear stress, and expression of aortopathy. *Circulation* 2014;129:673–82.
27 Nistri S, Grande-Allen J, Noale M, *et al*. Aortic elasticity and size in bicuspid aortic valve syndrome. *Eur Heart J* 2008;29:472–9.

28 Keshavarz-Motamed Z, Garcia J, Kadem L. Fluid dynamics of coarctation of the aorta and effect of bicuspid aortic valve. *PLoS One* 2013;8:e72394.
29 Grotenhuis HB, Ottenkamp J, Westenberg JJM, *et al*. Reduced aortic elasticity and dilatation are associated with aortic regurgitation and left ventricular hypertrophy in nonstenotic bicuspid aortic valve patients. *J Am Coll Cardiol* 2007;49:1660–5.
30 Stefanadis C, Stratos C, Vlachopoulos C, *et al*. Pressure-diameter relation of the human aorta. A new method of determination by the application of a special ultrasonic dimension catheter. *Circulation* 1995;92:2210–9.
31 Ahmadi N, Nabavi V, Hajsadeghi F, *et al*. Impaired aortic distensibility measured by computed tomography is associated with the severity of coronary artery disease. *Int J Cardiovasc Imaging* 2011;27:459–69.
32 Cavalcante JL, Lima JAC, Redheuil A, *et al*. Aortic stiffness: current understanding and future directions. *J Am Coll Cardiol* 2011;57:1511–22.
33 Saouti N, Marcus JT, Vonk Noordegraaf A, *et al*. Aortic function quantified: the heart's essential cushion. *J Appl Physiol* 2012;113:1285–91. (1985).
34 Stoiber L, Ghorbani N, Kelm M, *et al*. Validation of simple measures of aortic distensibility based on standard 4-chamber cine CMR: a new approach for clinical studies. *Clin Res Cardiol* 2019. doi:10.1007/s00392-019-01525-8. [Epub ahead of print: 13 Jul 2019].

Publikation 3

Roth S, Marko L, Birukov A, Hennemuth A, Kuhnen P, Jones A, **Ghorbani N**, Linz P, Muller DN, Wiegand S, Berger F, Kuehne T, Kelm M. Tissue Sodium Content and Arterial Hypertension in Obese Adolescents. J Clin Med. 2019;8(12).

DOI: 10.3390/jcm8122036

Journal of
Clinical Medicine

MDPI

Article

Tissue Sodium Content and Arterial Hypertension in Obese Adolescents

Sophie Roth [1,2], Lajos Markó [3,4,5,6], Anna Birukov [3,4,5,6], Anja Hennemuth [1], Peter Kühnen [7], Alexander Jones [8], Niky Ghorbani [1], Peter Linz [9], Dominik N Müller [3,4,5,6], Susanna Wiegand [7], Felix Berger [2,3], Titus Kuehne [1,2,3] and Marcus Kelm [1,2,*]

1 Institute for Computational and Imaging Science in Cardiovascular Medicine, Charité–Universitätsmedizin 13353 Berlin, Germany; sophie.roth@charite.de (S.R.); anja.hennemuth@charite.de (A.H.); niky.ghorbani@charite.de (N.G.); titus.kuehne@dhzb.de (T.K.)
2 Deutsches Herzzentrum Berlin, Department of Congenital Heart Disease, 13353 Berlin, Germany; berger@dhzb.de
3 DZHK (German Centre for Cardiovascular Research), partner site Berlin, 10785 Berlin, Germany; lajosmarko@yahoo.com (L.M.); anna.birukov@charite.de (A.B.); dominik.mueller@mdc-berlin.de (D.N.M.)
4 Max Delbruck Center for Molecular Medicine, 13092 Berlin, Germany
5 Berlin Institute of Health (BIH), 10178 Berlin, Germany
6 Experimental and Clinical Research Center, a joint cooperation between the Charité Medical Faculty and the Max Delbruck Center for Molecular Medicine, 13125 Berlin, Germany
7 Department of Paediatrics, Charité–Universitätsmedizin Berlin, 13353 Berlin, Germany; peter.kuehnen@charite.de (P.K.); susanna.wiegand@charite.de (S.W.)
8 Department of Paediatrics, University of Oxford, Oxford OX3 9DU, UK; alexander.jones@paediatrics.ox.ac.uk
9 Institute of Radiology, Friedrich-Alexander-University Erlangen-Nürnberg, 91054 Erlangen, Germany; Peter.Linz@uk-erlangen.de
* Correspondence: mkelm@dhzb.de; Tel.: +49-(0)30-4593-2864; Fax: +49-(0)30-4505-76983

Received: 25 September 2019; Accepted: 15 November 2019; Published: 21 November 2019

Abstract: Early-onset obesity is known to culminate in type 2 diabetes, arterial hypertension and subsequent cardiovascular disease. The role of sodium (Na^+) homeostasis in this process is incompletely understood, yet correlations between Na^+ accumulation and hypertension have been observed in adults. We aimed to investigate these associations in adolescents. A cohort of 32 adolescents (13–17 years), comprising 20 obese patients, of whom 11 were hypertensive, as well as 12 age-matched controls, underwent ^{23}Na-MRI of the left lower leg with a standard clinical 3T scanner. Median triceps surae muscle Na^+ content in hypertensive obese (11.95 mmol/L [interquartile range 11.62–13.66]) was significantly lower than in normotensive obese (13.63 mmol/L [12.97–17.64]; $p = 0.043$) or controls (15.37 mmol/L [14.12–16.08]; $p = 0.012$). No significant differences were found between normotensive obese and controls. Skin Na^+ content in hypertensive obese (13.33 mmol/L [11.53–14.22] did not differ to normotensive obese (14.12 mmol/L [13.15–15.83]) or controls (11.48 mmol/L [10.48–12.80]), whereas normotensive obese had higher values compared to controls ($p = 0.004$). Arterial hypertension in obese adolescents is associated with low muscle Na^+ content. These findings suggest an early dysregulation of Na^+ homeostasis in cardiometabolic disease. Further research is needed to determine whether this association is causal and how it evolves in the transition to adulthood.

Keywords: obesity; sodium; hypertension; adolescents; MRI; MR-spectroscopy

1. Introduction

Since the 1980s, the prevalence of obesity in many countries has doubled, affecting an estimated 603.7 million adults and 107.7 million children [1]. Globally, four million deaths per year have been attributed to increased body mass index (BMI), often due to associated cardiovascular disease (CVD) [1]. It is assumed that the course for the development of CVD is already set in childhood, but the exact mechanisms have remained unknown [1]. Amongst others, there are indications for chronic over-activity of the sympathetic nervous system and the renin–angiotensin–aldosterone system (RAAS) [2], as well as obesity-driven low-grade systemic inflammation-promoting type 2 diabetes [3].

Nutrition is known to play an important role in the pathogenesis of obesity, and mineral sodium (Na^+) has been discussed as an essential risk factor for CVD. Many factors may mediate the ability of high salt intake to increase blood pressure, however, their relative contributions to the pathogenesis of salt-induced hypertension are controversial [4,5]. Although several studies report deleterious effects, including a rise in blood pressure and the emergence of chronic kidney disease, some other studies have found more neutral effects [4]. Nevertheless, the rate of deaths from cardiovascular causes has been attributed to sodium consumption, and was found to be lower in regions and cultures with reduced salt intake [5]. In overweight adults, sodium-induced increases in circulating volume and hypertension have been described, which can elevate mortality by promoting left ventricular hypertrophy, altering vascular resistance and ultimately leading to heart failure [6].

Intake and accrual of Na^+ over the life course may, therefore, be an important determinant of CVD risk. Measurement of Na^+ status is routinely done by analysis of spot or 24 h urines. However, doubts have been raised about the suitability of 24 h urinary Na^+ excretion for estimating exact salt intake [7]. Whether urinary Na^+ excretion is at all reflecting tissue Na^+ content is currently unknown.

In recent studies, ^{23}Na-magnetic resonance imaging (MRI) has been introduced as a reliable, non-invasive method to quantify Na^+ tissue content [8–13] that overcomes this limitation. It has been suggested that tissue Na^+ accumulation with ageing could be implicated in the pathogenesis of refractory hypertension in adults [9]. However, these studies were of adult patients with advanced disease, where the independent effects of ageing, as well as hypertension and diet-related obesity, were difficult to separate. Only little is known about Na^+ storage in children and adolescents. However, studies in younger populations would have the advantage of excluding the effects of advanced ageing or long-established disease. To overcome this knowledge gap, the study investigates the associations between Na^+ storage, hypertension and obesity in adolescent patients.

2. Materials and Methods

In this cross-sectional study twenty, previously untreated obese (aged 13–17 [median 14] years) and twelve normal-weight "control" (aged 13–16 [median 15] years) adolescents were studied. Obese and control subjects were matched for sex and age. Obese patients were recruited prospectively from the social–paediatric centre (Charité–Universitätsmedizin Berlin) between 2014 and 2017, and they were further divided into two sub-groups, according to their blood pressure status. They were defined as obese if their body mass index (BMI) exceeded the 97th Kromeyer–Hauschild percentile according to sex and age [14]. Controls were patients undergoing routine clinical diagnostic MRI for non-cardiac and non-endocrinologic reasons that volunteered to have our ^{23}Na-MRI protocol added. The primary outcome was the absolute muscle sodium content; the secondary outcome was skin sodium content. Subjects with implanted devices not compatible with MRI and those with claustrophobia were excluded. Written informed consent from participants or their legal guardians was obtained before enrolment. The study was approved by the institutional ethics review board of the Charité–Universitaetsmedizin Berlin (approval reference number EA2/036/14) and conducted according to the principles of the Declaration of Helsinki.

Additionally to known blood pressure status, at the time of MRI, the subjects were comfortably seated with back support for at least five minutes while arterial blood pressure was measured on the right upper arm using an oscillometric Dinamap pro-100 device (Critikon, Milwaukee, WI, USA).

Cuff size was chosen appropriately to arm circumference. As there is still no single value threshold available in obese and overweight children (BMI >85th percentile) and even adult guideline values vary between ACC and ESC guidelines [14–16], in this study, hypertension was defined if systolic and/or diastolic values exceeded age-, gender- and height-specific (95th) [16] reference percentiles.

Anthropometric data were acquired using standardised clinical protocols and participants completed a questionnaire about salt intake, answering on a scale of 1–10 according to their agreement with the question asked. An oral glucose-tolerance test (OGTT) was performed and HbA1c, fasten insulin and glucose were measured. Homeostatic model assessment (HOMA) indices above 2.0 were considered hyperinsulinism.

All subjects rested for at least 15 min before their left calf was scanned at its widest circumference. Imaging was performed on a Philips Ingenia 3.0 Tesla MR scanner (Ingenia R 5.4, Philips Healthcare, Best, The Netherlands) with a ^{23}Na send/receive knee-coil (Rapid Biomedical, Rimpar, Germany), following previously validated methods, using a 2D-spoiled gradient echo sequence (total acquisition time, TA = 20.5 min; echo time, TE = 2.138 ms; repetition time, TR = 100 ms; flip angle, FA = 90°; 196 averages, resolution: $3 \times 3 \times 30$ mm^3) [9,10]. Four calibration phantoms containing aqueous solutions of 10, 20, 30, and 40 mmol/L NaCl were scanned as reference standards, together with the subject's calf. Simultaneously, tissue water content was measured by ^{1}H-MRI, using a fat-saturated inversion-prepared SE sequence (inversion time, TI = 210 ms; TA = 6.27 min; TE = 12 ms; TR = 3000 ms; FA = 90°; 1 average, resolution: $1.5 \times 1.5 \times 5$ mm^3), as implemented by other investigators [11].

Using ImageJ (NIH, version 1.50i) and the anatomical image (T1-weighted spoiled gradient echo sequence) as guidance, regions of interest (ROI) were drawn as centrally as possible whilst excluding prominent vascular structures, which are rich in Na^+. Relevant ROIs included the total leg, triceps surae muscle, as the largest muscle of the calf (with medial and lateral gastrocnemius and soleus; referred in the text as "muscle"), skin, tibial bone and subcutaneous fat. Muscle ROIs and subcutaneous ROIs were marked on the T1-weighted sequence, while skin ROI, total leg ROI and phantom ROIs were drawn on the Na^+ image, as already described by other authors [11]. ROI areas were assessed through each ROI's voxel count and measured in arbitrary units (AU).

The signal intensity of each ROI was measured and linear trend analysis was used to translate this intensity to a NaCl concentration, according to the calibration phantoms' predefined contents of 10, 20, 30, and 40 mmol/L [17]. A calibration standard for tissue water was based on the water content of the 10 mmol/L NaCl tube. Previous studies have suggested ^{1}H-MRI as a means to non-invasively assess tissue water content changes, based on a linear relationship between ^{1}H-MRI measurements and actual water content [9]. Thus, the combination of water and Na^+ measurements allows the differentiation of a water-dependent Na^+ storage (e.g., oedema) from water-independent Na^+ storage (e.g., bound to glycosaminoglycans) [18].

Since fat tissue is rather low in Na^+ content, we assessed whether decreased Na^+ content in muscle might be due to increased muscle fat accumulation. Muscle fat content was assessed by the ratio of fat-voxels and the total number of voxels within the muscle. As described by Kopp et al., ^{1}H-T1-weighted tissue signal intensities greater than 30% above the intensity level of the phantom tubes were defined "fat-voxels" [19]. The ratio of fat-voxels and the total number of voxels within the muscle was used to assess fatty muscle degeneration.

Data are expressed as median and interquartile range (Q1–Q3) unless otherwise stated. Data were tested for normality using the Shapiro–Wilk and Shapiro–Francia tests. Data were analysed for stochastic dominance among the three groups by applying a non-parametric Kruskal–Wallis test, followed by a Bonferroni-corrected Dunn's test as a nonparametric, pairwise, multiple comparison procedure. Pearson's chi-square test was used with Fisher's exact test for comparison of categorical variables. To plot the combined effects of BMI and hypertension on Na^+ content in muscle, predictive margins were calculated and plotted. Correlations were assessed by non-parametric multivariate regression analysis. Multifactorial effects (and their 95% confidence interval, CI) were assessed using robust regression. Significance level was set at $p = 0.05$ and 95% confidence intervals were

calculated. Inter-observer variability was evaluated for Na^+ measurements of 25 different subjects using a Bland–Altman plot. Stata (Version 15.1, StataCorp, College Station, Texas, USA) was used for statistical analysis.

3. Results

Na^+ content and tissue water content was analysed in a total of 32 subjects, of which 11 were hypertensive obese patients, nine normotensive obese patients and 12 normal-weight controls. The characteristics of these three groups are shown in Table 1. Age and sex did not significantly differ between groups, and BMI did not differ between both obesity groups (Figure 1a). Heart rate, systolic and diastolic blood pressure did not differ between normotensive obese and controls, but did between those two groups and hypertensive obese (Figure 1b–d, respectively). Only one patient had isolated diastolic blood pressure values exceeding the 95th percentile. All remaining hypertensive patients had systolic hypertension.

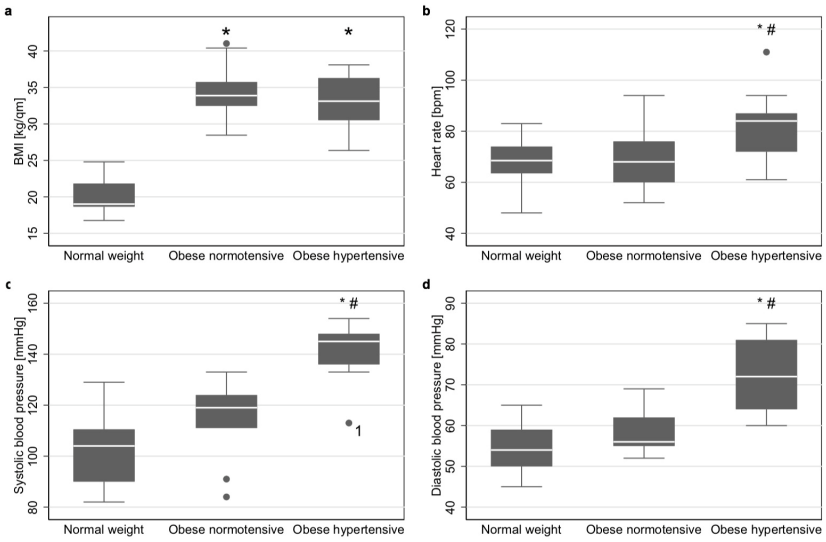

Figure 1. Group characteristics. (**a**) Boxplots of body-mass index (BMI) of controls, normotensive obese and hypertensive obese. (**b**) Boxplots of heart rate of controls, normotensive obese and hypertensive obese. (**c**) Boxplots of systolic blood pressure of controls, normotensive obese and hypertensive obese. (**d**) Boxplots of diastolic blood pressure of controls, normotensive obese and hypertensive obese. Tests were performed using a Kruskal–Wallis Test (N = 32) with inter-group p-values according to Bonferroni corrected Dunn's test. * p-value < 0.05 compared to controls # p-value < 0.05 compared to normotensive obese. [1]diastolic hypertension (above the 95th percentile).

Table 1. Baseline characteristics. Median (interquartile range), unless stated otherwise.

Subjects	Controls (n = 12)	Normoten–Sive Obese (n = 9)	Hyperten–Sive Obese (n = 11)	*p* Value Normotensive Obese vs. Controls	*p* Value Hypertensive Obese vs. Controls	*p* Value Hypertensive Obese vs. Normotensive Obese	*p* Value Overall
Age [years]	15 (14–16)	15 (14–16)	14 (13–14)	1.000	0.088	0.060	0.072
Male Gender (n)	4 (33%)	4 (44%)	5 (45%)				0.808
Cross-Sectional Total Leg Area (mm^2)	3830 (3536–4387)	6862 (5917–7244)	5912 (5217–6369)	<0.001	0.0007	0.533	<0.001
Tibial Bone Area (mm^2)	229 (208–244)	311 (245–322)	284 (225–317)	0.011	0.117	0.478	0.022
Total muscle area (mm^2)	2265 (1989–2482)	3196 (2780–3565)	2960 (2750–3377)	0.002	0.003	1.000	0.001
Subcutaneous Fat Area (mm^2)	1084 (950–1363)	2526 (2078–3787)	2128 (1824–2939)	<0.001	0.001	0.758	<0.001
Questionnaire							
"How much do you like salty food?"	7 (5.5–7.5)	6 (5–8)	5 (3–8)	1.000	0.400	0.352	0.419
"How often do you add more salt to your food"	3.5 (2–6.5)	3(1–5)	2 (1–3)	0.497	0.059	0.504	0.129
"How much do you like salty snacks such as crisps?"	8 (5.5–8)	5 (4–7)	7 (4–9)	0.242	0.916	0.552	0.379
"How often do you eat in fast food restaurants?"	4 (2.5–4.5)	4 (3–5)	3 (2–4)	1.000	0.088	0.126	0.124
"How much money do you usually spend there?" (€)	5 (2.8–8)	9 (5–10)	5 (4–9.5)	0.197	1.000	0.161	0.218
"How often do you drink beverages without additional flavour?"	7 (5–9.5)	10 (9–10)	10 (8–10)	0.166	0.058	1.000	0.122
"How much do you drink daily?" (L)	1.5 (1.1–2)	1.5 (1–2.5)	2 (1–2.3)	0.601	0.524	1.000	0.587

Questionnaire on a scale from 1–10 (1 = I strongly agree; 10 = I strongly disagree) unless stated otherwise.

3.1. Tissue Na^+, Water and Fat Content

We found significant differences in tibial bone Na^+ content, subcutaneous fat Na^+ content and water content of muscle, skin, tibial bone and subcutaneous fat in none of the groups (Supplementary Figure S1).

Muscle Na^+ content did not differ ($p = 1.00$) between controls (15.37 mmol/L [interquartile range 14.12–16.08]) and normotensive obese (13.63 mmol/L [12.97–17.64]), but was significantly lower than both of these groups ($p = 0.012$ and $p = 0.043$, respectively) in hypertensive obese (11.95 mmol/L [11.62–13.66]) (Figure 2a). The Bland–Altman plot showed only low inter-observer variability in muscle Na^+ content, due to variations in data processing (Supplementary Figure S2).

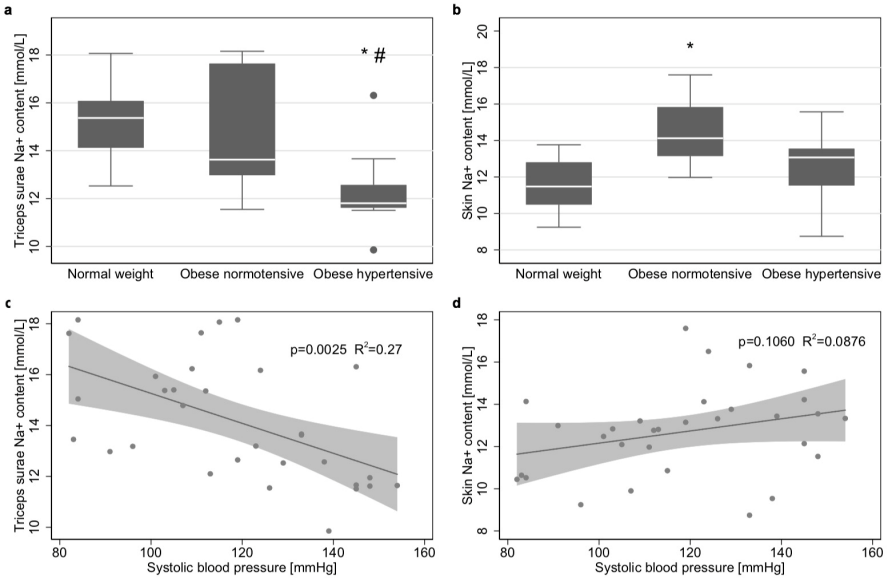

Figure 2. Na^+ content in different tissues. (**a**) Boxplots of triceps surae muscle Na^+ of controls, normotensive obese and hypertensive obese. (**b**) Boxplots of skin Na^+ content of controls, normotensive obese and hypertensive obese. Tests were performed using a Kruskal–Wallis Test (N = 32) with inter-group p-values according to Bonferroni corrected Dunn's test. * p-value <0.05 compared to controls # p-value <0.05 compared to normotensive obese. [1]diastolic hypertension (above the 95th percentile). (**c**) The scatter plot and the linear regression model show an inverse correlation between triceps surae Na^+ content and systolic blood pressure ($p = 0.0025$, $R^2 = 0.27$, N = 32). (**d**) Scatter plot and the linear regression model, showing no significant correlation between skin Na^+ content and systolic blood pressure (p = 0.1060 $R^2 = 0.09$).

In contrast, skin Na^+ content in normotensive obese (14.12 mmol/L [13.15–15.83]) was significantly higher ($p = 0.004$) than in controls (11.48 mmol/L [10.48–12.80]), while it tended to be higher in hypertensive obese (13.33 mmol/L [11.53–14.22]; $p = 0.144$). There was no difference between obese adolescents with or without hypertension ($p = 0.237$) (Figure 2b).

Cross-sectional total Na^+ content of all compartments in hypertensive obese was 12.01 mmol/L [11.41–12.89] and was significantly lower than in normotensive obese (p = 0.045) and controls ($p = 0.005$). Total Na^+ content did not significantly differ between controls (15.15 mmol/L [12.70–15.69]) and normotensive obese (13.02 mmol/L [12.39–14.98]; $p = 0.866$).

The proportion of fat tissue within the muscle did not vary between all three groups. No significant correlation was found ($p = 0.149$, $R^2 = 0.037$) between the amount (area) of fat tissue and muscle sodium content (Table 1).

3.2. Na^+ Content and Arterial Hypertension

As recent studies have reported correlations between Na^+ accumulation and hypertension in adults [9], we further investigated these aspects in an adolescent cohort: an inverse correlation was found between muscle Na^+ content and systolic blood pressure ($p = 0.0025$; $R^2 = 0.27$; Figure 2c) and cross-sectional total sodium content (p=0.0173, R^2=0.12). These effects were not attributed to BMI. In obese patients, no significant correlations were found between BMI and muscle Na^+ content and total cross-sectional Na^+ content. No significant correlation was found between skin Na^+ content and systolic blood pressure (Figure 2d).

Since a relationship between arterial hypertension and heart rate increase was described in the literature for obesity, heart rates were also compared between groups2. The heart rate in hypertensive obese (84 [72–87]) was significantly higher (p = 0.008 and p = 0.025, respectively) than in controls (69 [64–74]) and normotensive obese (68 [60–76]). Between controls and normotensive obese, heart rate did not differ ($p = 0.386$, Figure 1b).

A logistic regression model (Figure 3) in obese showed that the probability of hypertension was significantly associated with lower muscle Na^+ content ($p = 0.038$). The risk for hypertension and its uncertainty is also shown in the figure, and was increased to >80% in patients with triceps surae muscle Na^+ content below 12 mmol/L.

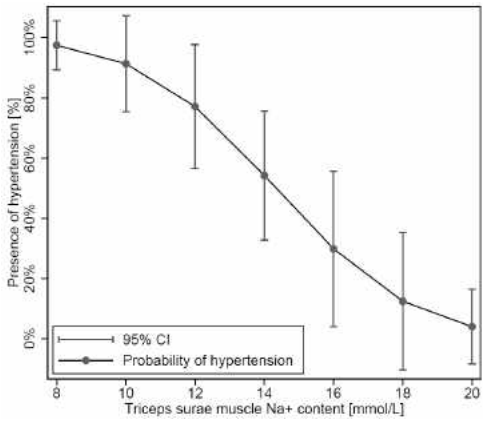

Figure 3. Logistic model showing the probability of hypertension according to muscle Na^+ content with 95% confidence intervals (CI). ($p = 0.038$; N = 32).

3.3. Sex Differences in Na^+ Content and Arterial Hypertension

Sex differences were assessed for all storage compartments. No significant sex-specific differences were found for muscle Na^+ content. Additionally, the associations between arterial hypertension and muscle sodium content, as well as total sodium content, were independent of the patient's sex. Robust linear regression demonstrated associations ($p < 0.001$; $R^2 = 0.40$) between skin Na^+ content and independent variables of (1) female sex (Coef. −1.31 95% CI −2.52 to −0.10, $p = 0.034$) and (2) being normotensive obese (Coef. 2.69 95% CI 1.20 to 4.19, $p = 0.001$) but not (3) being hypertensive obese ($p = 0.201$). Tibial bone Na^+ content was significantly lower in obese females (4.71 mmol/L [1.38–6.63]) than in obese males (7.45 mmol/L [6.10–9.14]; $p = 0.025$). Robust linear regression showed an association ($p = 0.023$; $R^2 = 0.25$) between tibial bone Na^+ content and independent variables of (1) female sex

(Coef. −3.20, 95% CI −5.85 to −0.55, $p = 0.020$), but not (2) being hypertensive obese ($p = 0.624$) or (3) normotensive obese ($p = 0.389$). In other compartments, we did not find sex-specific differences in Na^+ content.

3.4. Salt Intake, Tissue Na^+ and Glucose Metabolism

The responses to the questionnaire items in all groups are shown in Table 1. In all items, no differences were found between groups regarding salt appetite or salty fast food craving.

Hyperinsulinism, reflected by a HOMA index of 2.0 or higher, was found in 87% of all obese patients. We found a weak correlation between HbA1c and systolic blood pressure ($p = 0.088$; $R^2 = 0.18$ n = 19; Figure 4a), but a stronger one between Na^+ content of the whole leg and blood glucose levels after 1 h ($p = 0.034$; $R^2 = 0.63$; n = 11; Figure 4b) and 2 h of OGTT (p = 0.084; $R^2 = 0.56$; n = 11; Figure 4c). These effects were not found in other tissue compartments.

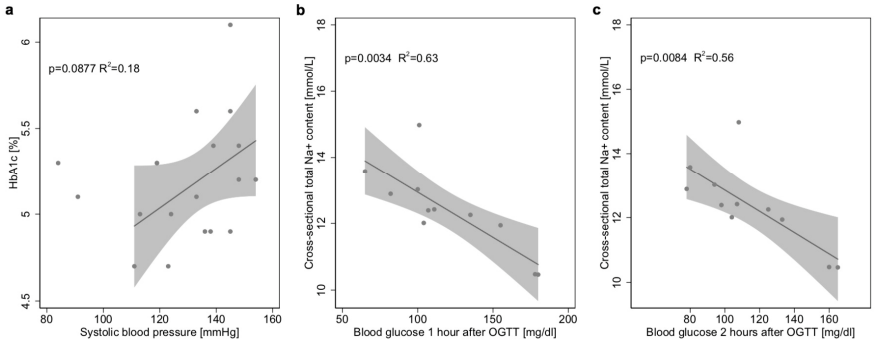

Figure 4. Tissue Na^+ and glucose metabolism. (**a**) Linear regression model with 95% CI combined with scatter plot, showing no significant correlation between HbA1c and systolic blood pressure (n = 19). (**b**) Linear regression model with 95% CI, combined with scatter plot showing a significant correlation between Na^+ of the whole leg and blood glucose 1 h after an oral glucose tolerance test (OGTT, $p = 0.0034$ $R^2 = 0.63$, n = 11). (**c**) The linear regression model with 95% CI, combined with scatter plot showing a significant correlation between Na^+ of the whole leg and blood glucose 2 h after an OGTT ($p = 0.0084$ $R^2 = 0.56$, n = 11).

3.5. Power Calculation

A power calculation using a Satterthwaite's t-test for unequal variances, based on relevant differences in muscle sodium content, and a group A (hypertensive obese) mean of 12.8 ± 1.877 and a group B (control) mean of 15.248 ± 1.657 mmol/L, a total sample size of N = 23 for both groups and a level of significance of 5% (two-sided), resulted in an estimated power of 92%. To estimate statistical power of differences between normotensive and hypertensive obese, a Group A (normotensive obese) mean of 14.9 ± 2.6190 and a Group B (control) mean of 15.248 ± 1.657 mmol/L, a total sample size of N = 20 for both groups and a level of significance of 5% (two-sided) resulted in an estimated power of 57%.

4. Discussion

Little progress has been made in preventing the emergence of cardiovascular risk factors, such as obesity and hypertension in their early stages [1,20]. The pathophysiological link between these conditions and the role of mineral Na^+ intake remains incompletely understood, hampering the development of targeted prevention measures. In previous studies, tissue Na^+ accumulation has been proposed as a factor in the pathogenesis of hypertension, based on findings of raised tissue Na^+ in hypertensive adults [9], but its association with blood pressure status in childhood has not been

studied before. We found that obese adolescents with hypertension had lower triceps surae muscle Na^+ and lower total cross-sectional Na^+ content than those without hypertension or normotensive controls. These effects were independent of the patients' BMI. When comparing our results with those of hypertensive adults, one must be aware that these studies, to our knowledge, do not consistently provide information on patients' weight [9]. Future studies should, therefore, further investigate to what extent tissue sodium storage in hypertensive and normotensive adults is linked to mechanisms of ageing and obesity.

4.1. Tissue Na^+ Contents in Adults

^{23}Na-MRI has been established as a non-invasive method for the quantification of Na^+ content in different tissues [9–13,21]. Although our picture of Na^+ homeostasis and tissue storage is still fragmented, this novel approach has made it possible to gain a considerable amount of knowledge in recent years. Tissue Na^+ content was previously found to be elevated, among others, in patients with lipoedema [22], acute heart failure [11] or acute kidney disease [12] and chronic kidney disease [13]. In patients with refractory hypertension, women showed increased skin Na^+ content compared to controls, whereas men showed higher muscle Na^+ content compared to controls [9]. Increasing age further intensifies these differences in compartment distribution [17]. Additionally, sex differences have been described in a recent study [17]. In our study, we found higher skin and tibial bone Na^+ content in males. Although these findings are in line with previous studies for the skin, the tibial bone has not yet been described as a compartment for sodium storage/depletion in patients with normal renal function, as its overall sodium content is typically much lower than that in the muscle/skin.

4.2. Na^+ and Blood Pressure

The World Health Organization (WHO) recommends less than 2 g/day Na^+ in adults, and even lower doses in children [23]. As the actual mean daily intake of Na^+ is as high as 3.6 g/day in the US, UK, and Germany, we presume high salt intake also plays an important role in our study cohort [5]. Using questionnaires to semi-quantify the "salt appetite" of our participants, we did not observe any differences between the groups. However, to record the actual salt intake, complex measurements of nutritional composition would be required.

Salt-loading studies with salt-resistant subjects have shown that, during acute or chronic salt-loading, normotensive salt-resistant subjects do not excrete Na^+ faster, nor do they experience more blood volume expansion. Instead, they substantially retain Na^+ in a rhythmical manner, which is in line with our concept of relevant tissue Na^+ buffers [24,25]. Impairment of these buffer mechanisms in our "early disease stage" study could be an important contributor to the onset of arterial hypertension: while, in obese young patients without hypertension, Na^+ storage in the muscle (the largest previously described buffer compartment) is only slightly reduced, in those with hypertension we observed an accentuated reduction of Na^+ storage in muscle. In other compartments, such as the skin, tibial bone and subcutaneous fat, Na^+ did not show significant differences in hypertensive obese, excluding a potential Na^+ shift to those compartments nearby.

Previous studies observed salt-sensitivity in some individuals, which describes an increase in blood pressure as a response to increases in dietary Na^+ intake and vice versa [20,25,26]. In this context, the RAAS seems to be an important factor: it controls the vascular tone and—through Na^+ reabsorption—the intravascular volume homeostasis, as well as the heart rate, through Angiotensin II activation [2,27]. Presuming similar Na^+ intake in all groups, without a significant shift to other compartments, impaired muscle Na^+ storage in hypertensive obese can result in elevated Na^+ excretion through two major mechanisms: 1) altered RAAS suppression [28] and 2) pressure natriuresis as a regulatory response mechanism in salt-sensitive hypertensive subjects [29] through hypertension itself. Elevated heart rates in our cohort of hypertensive obese are in line with an overactivation of the sympathetic nervous system that has been described as an essential factor in the pathogenesis of obesity-induced hypertension in rabbits, dogs and humans [2].

In adults with long-term hypertension, recent reports suggest osmotically inactive Na^+ storage in the skin via negatively charged glycosaminoglycans as binding partners [18]. We found elevated skin Na^+ content in normotensive obese compared to normal-weight controls. However, these effects were not found in hypertensive obese. Therefore, no such conclusions can be made for skin Na^+ content in adolescents.

Before Na^+ transfers from the vascular system to tissue, there are two barriers to overcome: the negatively charged endothelial glycocalyx layer and the endothelial Na^+ channel ENaC [30]. Therefore, Na^+ homeostasis and salt sensitivity in arterial hypertension might be associated not only with a subnormal ability to excrete sodium load, but also with vascular endothelial dysfunction [24,27]. Whereas in patients with different stages of chronic kidney disease, salt restriction can reduce blood pressure [31], no controlled studies have been performed to demonstrate that hypertensive subjects excrete sodium more slowly and retain more of it than normotensive subjects.

One could, therefore, speculate whether regulatory mechanisms in adolescents are different from those observed in older patients. If the muscle, as a main Na^+ storage compartment, stores less, maintenance of blood sodium homeostasis will depend more on excretion and other storage compartments. This may reflect a compensatory mechanism at an early stage of the disease-preventing tissue Na^+ overload, and further research will be needed to investigate the hormonal cascades involved, as well as absolute Na^+ excretion, as plasma Na^+ needs to maintain stable.

4.3. Na^+ Homeostasis and Hyperinsulinism

Insulin alone has long been thought to cause Na^+ retention, with enough effects to contribute to arterial hypertension [32,33]. A study by Brands and colleagues showed that such Na^+-retaining effects may be limited to uncontrolled Type II diabetes [32]. In 11 maintenance haemodialysis patients, higher muscle sodium content was, in a similar way, associated with insulin resistance [34]. Furthermore, in the soleus muscle of salt-sensitive hypertensive Dahl rats, the RAAS was shown to activate the NF-κB pro-inflammatory pathway, inducing moderate hyperinsulinemia and insulin resistance [33]. A recent study also demonstrated a positive statistical correlation between Na^+ intake and insulin resistance in obese children and adolescents [35]. A majority (87.5%) of our disease cohort not only had hyperinsulinism, but were also showing a trend between HbA1c and blood pressure, even at this early stage of the disease.

Although the relation between obesity and hyper-caloric diets is known, the association between obesity and Na^+ still remains unclear, as the quantification of salt intake is measured highly subjectively, through questionnaires or food records, unless investigators have the unusual opportunity of controlling their subjects' nutrition completely, as done by Titze et al. in their space flight simulations [25]. In our study, we used salt questionnaires to assess the habits of salt intake and did not note any elevation of salt consumption or salty fast food craving in hypertensive or normotensive obese compared to our controls.

4.4. ^{23}Na-MRI

Due to its non-invasive nature, ^{23}Na-MRI is increasingly used in clinical research projects, even though it requires the use of specific non-proton coils and yields a certain complexity in image acquisition and post-processing [8–13,21].

Our study was performed at a 3 Tesla clinical scanner with a previously described measurement set-up [9,10]. A calibration curve using aqueous reference saline solutions was generated alongside to all scans, and 196 signal averages were applied to improve image homogeneity. We also determined intra- and inter-observer variability that did not show any significant differences between measurements. Compartments were assessed separately, as the total-cross-sectional Na^+ content (shown for completeness) can be prone to averaging artefacts when different tissue types are combined, and the effects of the largest storage compartments (the muscle) may dominate.

4.5. Limitations

Within this study, we did not perform interventions such as salt loading tests, and, furthermore, assessments of the RAAS and Na^+ excretion were not part of the study protocol. As indicated by our findings, future prospective and longitudinal studies should further evaluate the impact of such interventions and assess the complex interplay of hormonal axes (including the RAAS), as well as their linkage to the inflammation and glucose/insulin metabolism, as this may be of high relevance in future treatment-planning strategies. Furthermore, and as already stated above, salt intake was not measured quantitatively.

Statistical power to assess differences in muscle sodium content between controls and hypertensive obese was 92%, however, it was 57% for differences between controls and normotensive obese, due to sample size and the large heterogeneity within normotensive obese. These findings may be of use for future study planning.

5. Clinical Outlook and Conclusions

In obese adolescents with hyperinsulinism, arterial hypertension occurs in the presence of low muscle tissue Na^+ content, independent of the patient's BMI. These findings suggest a different regulation of muscle Na^+ homeostasis and storage in early-onset obesity for hypertension compared to normotensive patients, adding a new perspective to salt-induced hypertension and salt sensitivity, if main storage compartments store less. The role of Na^+ storage, salt sensitivity and insulin resistance in the initial stages of arterial hypertension, and the extent of the compensatory mechanisms that can become maladaptive at a later stage of the disease, as well as differences to isolated arterial hypertension in adults, remain to be further investigated in future clinical research.

Supplementary Materials: The following are available online at http://www.mdpi.com/2077-0383/8/12/2036/s1, Figure S1: Na^+ and water content in different tissues, Figure S2: Bland-Altman Plot illustrating the inter-observer variability in the post-processing of the ^{23}Na MRI data, Figure S3: Sex-specific tibial bone Na^+.

Author Contributions: Conceptualization, T.K., D.N.M. and M.K.; Methodology, P.L., D.N.M., L.M.; Software, A.H.; Formal Analysis S.R., A.H., A.B., N.G., P.K., M.K.; Investigation, M.K., S.R.; Resources, T.K., F.B., S.W., S.K.; Data Curation, S.R.; Writing—Original Draft Preparation, S.R., M.K.; Writing—Review and Editing, T.K., A.J., S.W., S.K., F.B.; Visualization, M.K.; Supervision, T.K., F.B., S.W.; Project Administration, T.K., M.K.; Funding Acquisition, T.K., A.J., M.K. All authors read and approved the final manuscript and agree to be accountable for all aspects of the work.

Funding: This study was partially funded by the European Commission under the FP7-ICT Program (Grant No: 600932, Brussels, Belgium). M.K. receives funding from the Berlin Institute of Health (BIH, Berlin, Germany) within the Digital Clinician Scientist Program (07/2019-07/2022).

Acknowledgments: We thank Alireza Khasheei for technical support and Anne Wölffel-Gale for editorial assistance.

Conflicts of Interest: The authors declare no conflict of interest.

References

1. Afshin, A.; Afshin, A.; Forouzanfar, M.H.; Reitsma, M.B.; Sur, P.; Estep, K.; Lee, A.; Marczak, L.; Mokdad, A.H.; Moradi-Lakeh, M.; et al. Health effects of overweight and obesity in 195 countries over 25 years. *N. Engl. J. Med.* **2017**, *377*, 13–27.
2. Hall, J.E.; da Silva, A.A.; do Carmo, J.M.; Dubinion, J.; Hamza, S.; Munusamy, S.; Smith, G.; Stec, D.E. Obesity-induced hypertension: Role of sympathetic nervous system, leptin, and melanocortins. *J. Biol. Chem.* **2010**, *285*, 17271–17276. [CrossRef] [PubMed]
3. Tchkonia, T.; Thomou, T.; Zhu, Y.; Karagiannides, I.; Pothoulakis, C.; Jensen, M.D.; Kirkland, J.L. Mechanisms and metabolic implications of regional differences among fat depots. *Cell Metab.* **2013**, *17*, 644–656. [CrossRef] [PubMed]

4. Malta, D.; Petersen, K.S.; Johnson, C.; Trieu, K.; Rae, S.; Jefferson, K.; Santos, J.A.; Wong, M.M.Y.; Raj, T.S.; Webster, J.; et al. High sodium intake increases blood pressure and risk of kidney disease. From the Science of Salt: A regularly updated systematic review of salt and health outcomes (August 2016 to March 2017). *J. Clin. Hypertens.* **2018**, *20*, 1654–1665. [CrossRef] [PubMed]
5. Mozaffarian, D.; Fahimi, S.; Singh, G.M.; Micha, R.; Khatibzadeh, S.; Engell, R.E.; Lim, S.; Danaei, G.; Ezzati, M.; Powles, J. Global sodium consumption and death from cardiovascular causes. *N. Engl. J. Med.* **2014**, *371*, 624–634. [CrossRef] [PubMed]
6. He, J.; Ogden, L.G.; Vupputuri, S.; Bazzano, L.A.; Loria, C.; Whelton, P.K. Dietary sodium intake and subsequent risk of cardiovascular disease in overweight adults. *Jama* **1999**, *282*, 2027–2034. [CrossRef]
7. Lerchl, K.; Lerchl, K.; Rakova, N.; Dahlmann, A.; Rauh, M.; Goller, U.; Basner, M.; Dinges, D.F.; Beck, L.; Agureev, A.; et al. Agreement between 24-hour salt ingestion and sodium excretion in a controlled environment. *Hypertension* **2015**, *66*, 850–857. [CrossRef]
8. Kopp, C.; Linz, P.; Wachsmuth, L.; Dahlmann, A.; Horbach, T.; Schofl, C.; Renz, W.; Santoro, D.; Niendorf, T.; Muller, D.N.; et al. ^{23}Na magnetic resonance imaging of tissue sodium. *Hypertension* **2012**, *59*, 167–172. [CrossRef]
9. Kopp, C.; Linz, P.; Dahlmann, A.; Hammon, M.; Jantsch, J.; Muller, D.N.; Schmieder, R.E.; Cavallaro, A.; Eckardt, K.U.; Uder, M.; et al. ^{23}Na magnetic resonance imaging-determined tissue sodium in healthy subjects and hypertensive patients. *Hypertension* **2013**, *61*, 635–640. [CrossRef]
10. Dahlmann, A.; Dorfelt, K.; Eicher, F.; Linz, P.; Kopp, C.; Mossinger, I.; Horn, S.; Buschges-Seraphin, B.; Wabel, P.; Hammon, M.; et al. Magnetic resonance-determined sodium removal from tissue stores in hemodialysis patients. *Kidney Int.* **2015**, *87*, 434–441. [CrossRef]
11. Hammon, M.; Grossmann, S.; Linz, P.; Kopp, C.; Dahlmann, A.; Garlichs, C.; Janka, R.; Cavallaro, A.; Luft, F.C.; Uder, M.; et al. ^{23}Na magnetic resonance imaging of the lower leg of acute heart failure patients during diuretic treatment. *PLoS ONE* **2015**, *10*, e0141336. [CrossRef] [PubMed]
12. Hammon, M.; Grossmann, S.; Linz, P.; Kopp, C.; Dahlmann, A.; Garlichs, C.; Janka, R.; Cavallaro, A.; Luft, F.C.; Uder, M.; et al. 3 Tesla ^{23}Na magnetic resonance imaging during acute kidney injury. *Acad. Radiol.* **2017**, *24*, 1086–1093. [CrossRef] [PubMed]
13. Schneider, M.P.; Raff, U.; Kopp, C.; Scheppach, J.B.; Toncar, S.; Wanner, C.; Schlieper, G.; Saritas, T.; Floege, J.; Schmid, M.; et al. Skin sodium concentration correlates with left ventricular hypertrophy in CKD. *J. Am. Soc. Nephrol.* **2017**, *28*, 1867–1876. [CrossRef] [PubMed]
14. Kromeyer-Hauschild, K.; Wabitsch, M.; Kunze, D.; Geller, F.; Geiß, H.C.; Hesse, V.; von Hippel, A.; Jaeger, U.; Johnsen, D.; Korte, W.; et al. Perzentile für den Body-mass-Index für das Kindes- und Jugendalter unter Heranziehung verschiedener deutscher Stichproben. *Mon. Kinderheilkd.* **2001**, *149*, 807–818. [CrossRef]
15. Flynn, J.T.; Kaelber, D.C.; Baker-Smith, C.M.; Blowey, D.; Carroll, A.E.; Daniels, S.R.; de Ferranti, S.D.; Dionne, J.M.; Falkner, B.; Flinn, S.K.; et al. Clinical practice guideline for screening and management of high blood pressure in children and adolescents. *Pediatrics* **2017**, *140*. [CrossRef] [PubMed]
16. Neuhauser, H.K.; Thamm, M.; Ellert, U.; Hense, H.W.; Rosario, A.S. Blood pressure percentiles by age and height from nonoverweight children and adolescents in Germany. *Pediatrics* **2011**, *127*, e978–e988. [CrossRef]
17. Wang, P.; Deger, M.S.; Kang, H.; Ikizler, T.A.; Titze, J.; Gore, J.C. Sex differences in sodium deposition in human muscle and skin. *Magn. Reason. Imaging* **2017**, *36*, 93–97. [CrossRef]
18. Machnik, A.; Neuhofer, W.; Jantsch, J.; Dahlmann, A.; Tammela, T.; Machura, K.; Park, J.K.; Beck, F.X.; Muller, D.N.; Derer, W.; et al. Macrophages regulate salt-dependent volume and blood pressure by a vascular endothelial growth factor-C-dependent buffering mechanism. *Nat. Med.* **2009**, *15*, 545–552. [CrossRef]
19. Kopp, C.; Linz, P.; Maier, C.; Wabel, P.; Hammon, M.; Nagel, A.M.; Rosenhauer, D.; Horn, S.; Uder, M.; Luft, F.C.; et al. Elevated tissue sodium deposition in patients with type 2 diabetes on hemodialysis detected by ^{23}Na magnetic resonance imaging. *Kidney Int.* **2018**, *93*, 1191–1197. [CrossRef]
20. GenSaltGroup. GenSalt: Rationale, design, methods and baseline characteristics of study participants. *J. Hum. Hypertens.* **2007**, *21*, 639–646. [CrossRef]
21. Kopp, C.; Beyer, C.; Linz, P.; Dahlmann, A.; Hammon, M.; Jantsch, J.; Neubert, P.; Rosenhauer, D.; Muller, D.N.; Cavallaro, A.; et al. Na^+ deposition in the fibrotic skin of systemic sclerosis patients detected by ^{23}Na-magnetic resonance imaging. *Rheumatology* **2017**, *56*, 674. [CrossRef] [PubMed]

22. Crescenzi, R.; Marton, A.; Donahue, P.M.C.; Mahany, H.B.; Lants, S.K.; Wang, P.; Beckman, J.A.; Donahue, M.J.; Titze, J. Tissue sodium content is elevated in the skin and subcutaneous adipose tissue in women with lipedema. *Obesity* **2017**, *26*, 310–317. [CrossRef] [PubMed]
23. WHO. WHO Guidelines Approved by the Guidelines Review Committee. In *Guideline: Sodium Intake for Adults and Children*; World Health Organization: Geneva, Switzerland, 2012.
24. Kurtz, T.W.; DiCarlo, S.E.; Pravenec, M.; Schmidlin, O.; Tanaka, M.; Morris, R.C., Jr. An alternative hypothesis to the widely held view that renal excretion of sodium accounts for resistance to salt-induced hypertension. *Kidney Int.* **2016**, *90*, 965–973. [CrossRef] [PubMed]
25. Rakova, N.; Rakova, N.; Juttner, K.; Dahlmann, A.; Schroder, A.; Linz, P.; Kopp, C.; Rauh, M.; Goller, U.; Beck, L.; et al. Long-term space flight simulation reveals infradian rhythmicity in human Na(+) balance. *Cell Metab.* **2013**, *17*, 125–131. [CrossRef] [PubMed]
26. Wilck, N.; Matus, M.G.; Kearney, S.M.; Olesen, S.W.; Forslund, K.; Bartolomaeus, H.; Haase, S.; Mahler, A.; Balogh, A.; Marko, L.; et al. Salt-responsive gut commensal modulates TH17 axis and disease. *Nature* **2017**, *551*, 585–589. [CrossRef] [PubMed]
27. Freitas, S.R.S. Molecular genetics of salt-sensitivity and hypertension: role of renal epithelial sodium channel genes. *Am. J. Hypertens.* **2017**, *31*, 172–174. [CrossRef]
28. Yatabe, M.S.; Yatabe, J.; Yoneda, M.; Watanabe, T.; Otsuki, M.; Felder, R.A.; Jose, P.A.; Sanada, H. Salt sensitivity is associated with insulin resistance, sympathetic overactivity, and decreased suppression of circulating renin activity in lean patients with essential hypertension. *Am. J. Clin. Nutr.* **2010**, *92*, 77–82. [CrossRef]
29. Elijovich, F.; Weinberger, M.H.; Anderson, C.A.; Appel, L.J.; Bursztyn, M.; Cook, N.R.; Dart, R.A.; Newton-Cheh, C.H.; Sacks, F.M.; Laffer, C.L.; et al. Salt sensitivity of blood pressure: A scientific statement from the American Heart Association. *Hypertension* **2016**, *68*, e7–e46. [CrossRef]
30. Oberleithner, H. Two barriers for sodium in vascular endothelium? *Ann. Med.* **2012**, *44*, S143–S148. [CrossRef]
31. Garofalo, C.; Borrelli, S.; Provenzano, M.; De Stefano, T.; Vita, C.; Chiodini, P.; Minutolo, R.; De Nicola, L.; Conte, G. Dietary salt restriction in chronic kidney disease: A meta-analysis of randomized clinical trials. *Nutrients* **2018**, *10*, 732. [CrossRef]
32. Brands, M.W.; Manhiani, M.M. Sodium-retaining effect of insulin in diabetes. *Am. J. Physiol. Regul. Integr. Comp. Physiol.* **2012**, *303*, R1101–R1109. [CrossRef] [PubMed]
33. Zhou, M.S.; Liu, C.; Tian, R.; Nishiyama, A.; Raij, L. Skeletal muscle insulin resistance in salt-sensitive hypertension: Role of angiotensin II activation of NFkappaB. *Cardiovasc. Diabetol.* **2015**, *14*, 45. [CrossRef] [PubMed]
34. Deger, S.M.; Wang, P.; Fissell, R.; Ellis, C.D.; Booker, C.; Sha, F.; Morse, J.L.; Stewart, T.G.; Gore, J.C.; Siew, E.D.; et al. Tissue sodium accumulation and peripheral insulin sensitivity in maintenance hemodialysis patients. *J. Cachexia Sarcopenia Muscle* **2017**, *8*, 500–507. [CrossRef] [PubMed]
35. Han, S.Y.; Kim, N.H.; Kim, D.H.; Han, K.; Kim, S.M. Relationship between urinary sodium-creatinine ratios and insulin resistance in Korean children and adolescents with obesity. *J. Pediatr. Endocrinol. Metab.* **2018**, *31*, 375–383. [CrossRef]

Lebenslauf

Mein Lebenslauf wird aus datenschutzrechtlichen Gründen in der elektronischen Version meiner Arbeit nicht veröffentlicht.

Publikationsliste

Originalarbeiten in Zeitschriften mit peer-review Verfahren (mit Impact Factor)

- Stoiber, L., **Ghorbani, N.,** Kelm, M., Kuehne, T., Rank, N., Lapinskas, T., Stehning, C., Pieske, B., Falk, V., Gebker, R., Kelle, S. "Validation of simple measures of aortic distensibility based on standard 4-chamber cine CMR: a new approach for clinical studies." Clin Res Cardiol. (2019) – **Impact Factor: 4.907**

- **Ghorbani, N.**, Muthurangu V., Khushnood A., Goubergrits L„ Nordmeyer S., Fernandes J.F., Lee C.B., Runte K., Roth S., Schubert S., Kelle S., Berger F., Kuehne T., Kelm M., "Impact of Valve Morphology, Hypertension and Age on Aortic Wall Properties in Patients with Coarctation: a two-centre cross-sectional study" BMJ Open (2020) – **Impact Factor: 2.376**

- Roth, S., Marko, L., Birukov, A., Hennemuth, A., Kuhnen, P., Jones, A., **Ghorbani, N.**, Linz, P., Muller, D. N., Wiegand, S., Berger, F., Kuehne, T., Kelm, M. "Tissue Sodium Content and Arterial Hypertension in Obese Adolescents." J Clin Med (2019) – **Impact Factor: 5.688**

Publizierte Abstracts und Poster

- **Ghorbani N**, Muthurangu V, Khushnood A, Goubergrits L, Schubert S, Kelle S, Berger F, Kuehne T, Kelm M. "Personalized Effects of Valve Morphology, Blood Pressure Control and Age on Aortic Wall Properties - A two-center study in Congenital Heart Disease". (Abstract und Poster) Leopoldina, Nationale Akademie der Wissenschaften, Symposium 2020 – Mission Innovation, Charité - Campus Mitte, Berlin, 02/2020

Auszeichnungen

- **Posterpreis des Leopoldina-Symposium 2020 – Mission Innovation**
  Leopoldina, Nationale Akademie der Wissenschaften und Klinik für Anästhesiologie der Charité - Universitätsmedizin Berlin (Erster Platz, dotiert mit 3000€)

Danksagung

An dieser Stelle möchte ich mich herzlich bei allen Menschen bedanken, die mich im Laufe meiner Dissertation begleitet und unterstützt haben.

Mein Dank gilt zunächst Herrn Professor Dr. med. Titus Kühne, meinem Doktorvater, der mir diese Arbeit in seinem Institut ermöglichte und mich auf dem Weg zur Promotion jederzeit mit wertvoller Hilfestellung unterstützte.

Mein außerordentlicher Dank gilt darüber hinaus Herrn Dr. Marcus Kelm, der mir als Betreuer unermüdlich zur Seite stand. Durch seine Unterstützung konnte ich meine wissenschaftlichen Kompetenzen weiterentwickeln und die Fertigstellung dieser Promotionsschrift erreichen. Außerdem bedanke ich mich bei Herrn Prof. Dr.-Ing. Leonid Goubergrits für die immer freundliche, interdisziplinäre Beratung in Hinblick auf die angewandte Methodik.

Meinen Mitdoktoranden und Freunden Chong-Bin Lee und Sophie Roth möchte ich für all ihre Unterstützung danken - sie standen mir immer bei. Außerdem danke ich Julius Lehmann und Friedrich Kühn für die immerwährende Unterstützung und Motivation.

Mein größter Dank gebührt meinen Eltern, deren uneingeschränkte Unterstützung diese Promotion und meine bisherige Bildung ermöglicht haben.